UNIVERSITY OF TURIN
DOCTORAL SCHOOL IN LIFE AND HEALTH SCIENCES:
PhD IN NEUROSCIENCE
XXIX

PhD THESIS

"miRNAs and biomimetic scaffolds as potential strategies in spinal cord injury"

Candidate

Matilde Ghibaudi

Tutor

Alessandro Vercelli

TABLE OF CONTENTS

0 ABSTRACT 1

1 CHAPTER 1: INTRODUCTION 2

1.1 SPINAL CORD INJURY INCIDENCE 2

1.2 SCI-PATOPHISIOLOGICAL MECHANISMS 3

1.3 MECHANISMS OF AXON REGENERATION FAILURE AFTER SCI 4

1.4 ANIMAL MODELS 7

1.5 SCI THERAPEUTIC INTERVENTIONS 8

1.5.1 NON-CELLULAR APPROACHES 8

1.5.2 CELLULAR APPROACHES 12

1.6 AIM OF THE THESIS 13

2 CHAPTER 2: miRNAs IN SCI 15

2.1 miRNA BIOGENESIS AND NOMENCLATURE 15

2.2 miRNAs IN CENTRAL AXON REGENERATION 17

2.3 miRNAs IN AXONAL GROWTH NETWORK: PTEN PATHWAY 18

2.4 miRNAs IN AXONAL GROWTH NETWORK: GSK-3β PATHWAY 21

2.5 MiRNAs IN AXONAL GROWTH NETWORK: MAP1B-Rac1 PATHWAY 23

2.6 MiRNAs IN AXONAL GROWTH NETWORK: RhoA-PI3K-AKT PATHWAY 24

2.7 AIM OF THE PROJECT 25

2.8 MATERIALS AND METHODS 26

2.9 RESULTS 35

2.10 DISCUSSION 49

3 CHAPTER 3: BIOMATERALS IN SCI 58

3.1 NATURAL SCAFFOLDS 58

3.2 SYNTHETIC SCAFFOLDS 61

3.3 STEM CELLS 66

3.3.1 NEURAL STEM CELLS AND NEURAL PRECURSORS 66

3.3.2 MESENCHYMAL STEM CELLS 67

3.4 AIM OF THE PROJECT 69

3.5 MATERIALS AND METHODS 69

3.6 RESULTS 76

3.7 DISCUSSION 86

4 CONCLUSIONS AND FUTURE PERSPECTIVES 98

5 ACKNOWLEDGEMENTS 100

6 BIBLIOGRAPHY 101

PERSONAL INFORMATION 123

ABSTRACT

Spinal cord injury (SCI) affects 6 million people worldwide, unfortunately without any available treatment. Despite research advances, the limited regeneration potential of the CNS remains one of the major obstacles. The aim of this work was to investigate the therapeutic potential of i) miRNAs, as inner regulatory system, and ii) biomaterials, as scaffolds for stem cells. We performed both *in vitro* (primary cell cultures) and *in vivo* studies (acute SCI transection mouse model).

Among the miRNAs analyzed, miR-7b-3p was confirmed to be upregulated after SCI both in young and adult mice. In silico functional analysis revealed that this miRNA could be implicated in axon growth and/or neuroprotection, thus prompting us to understand its role in SCI condition. Studying its expression in primary cortical neurons, we noticed that miR-7b-3p level did not increase through time, according to the cell differentiation process. Moreover, its overexpression did not change axon length and the number of dendrites, thus suggesting that its overexpression *in vivo* after SCI could be directly related to the lesion.

Biomimetic polyurethane and chitosan hydrogels were tested with the aim to improve stem cell survival/integration after graft. The most promising results were obtained with chitosan and polyurethane nanofibers. The chitosan hydrogel tested *in vitro* in presence of mesenchymal stem cells (MSCs) resulted highly biocompatible, as shown by different cell survival assays; moreover chitosan did not affect the therapeutic potential of MSCs. When injected in SCI mice, it supports MSC survival more effectively than in standard conditions. Similarly, the nanofiber membrane showed a good biocompatibility for MSC growth *in vitro* and when implanted *in vivo* they perfectly integrated into the host tissue without causing any immune reaction.

These results may lead to identify innovative therapeutic targets/tools for CNS regeneration after SCI.

CHAPTER 1: INTRODUCTION

1.1 SPINAL CORD INJURY INCIDENCE

Spinal cord injury (SCI) is the cause of over 6 million people disability in the world. The incidence rate of SCI is higher in middle age people (from 30 to 65 years), with prevalence for male subjects. The majority of spinal cord lesions are traumatic, mainly caused by motor vehicle accidents, falls and sporting injuries. Despite research advances, SCI remains a devastating condition often resulting in severe and permanent disability that leads to devastating social consequences and huge economic costs (Ahuja et al., 2017; Miller and Herbert, 2016). Current treatments are limited to surgical approaches in order to stabilize the lesion, without any available therapies to restore motor, sensory and autonomic functions. Depending on the injury severity the lesion can result in four different clinical outcomes as defined by the ASIA (American Spinal Injury Association) impairment scale (Figure 1):

- *Quadriplegia*

  Loss of motor and sensory function at the cervical level (forelimb, hindlimb, trunk and pelvic region damage)
- *Paraplegia*

  Thoracic, lumbar and sacral dysfunction with forelimb preservation
- *Tetraparesis*

  Incomplete paralysis of limbs
- *Paraparesis*
- Incomplete paralysis of hindlimbs

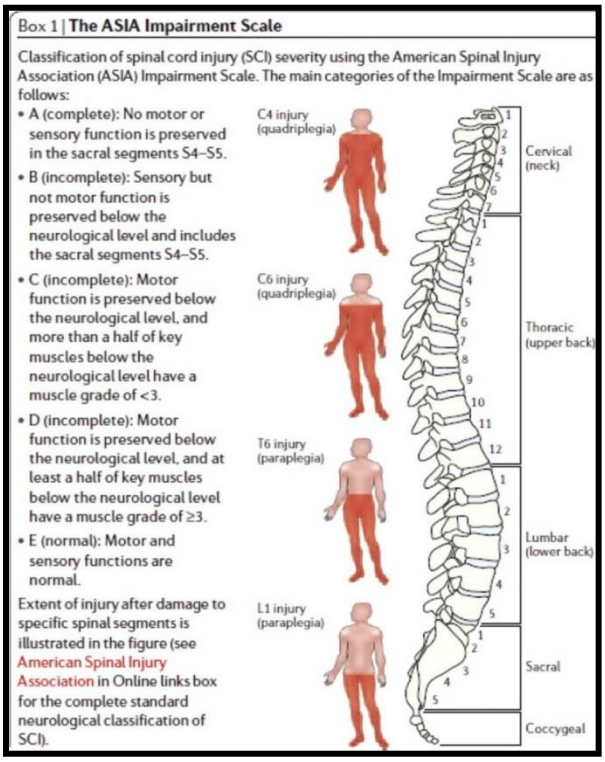

Figure 1: ASIA scale of spinal cord injury (Thuret et al., 2006)

1.2 SCI-PATOPHISIOLOGICAL MECHANISMS

The pathophysiology of SCI (Figure 2) consists of two consequent phases: primary and secondary injury. The primary injury is the direct consequence of the mechanical damage that can lead to permanent or transient neuronal deficits. It primarily affects the grey matter and is characterized by haemorrhage, oedema, hypoxic and ischemic damage. The nervous transmission is then compromised by the consequent demyelination and cell death. Only after three days the damage becomes irreversible also for the white matter. The time course of the secondary injury is characterized by an initial phase (0-2h) characterized by neuronal and glial death associated with hemorrhage and ischemia both rostrally and caudally to the lesion, followed by an acute phase (2h-2 weeks) that consists of an intense inflammation process (microglia, astrocyte, neutrophil and T cell recruitment). In detail, the blood brain barrier (BBB) alteration increases the vessel permeability with inflammatory cytokine extravasation and glial cell recruitment.

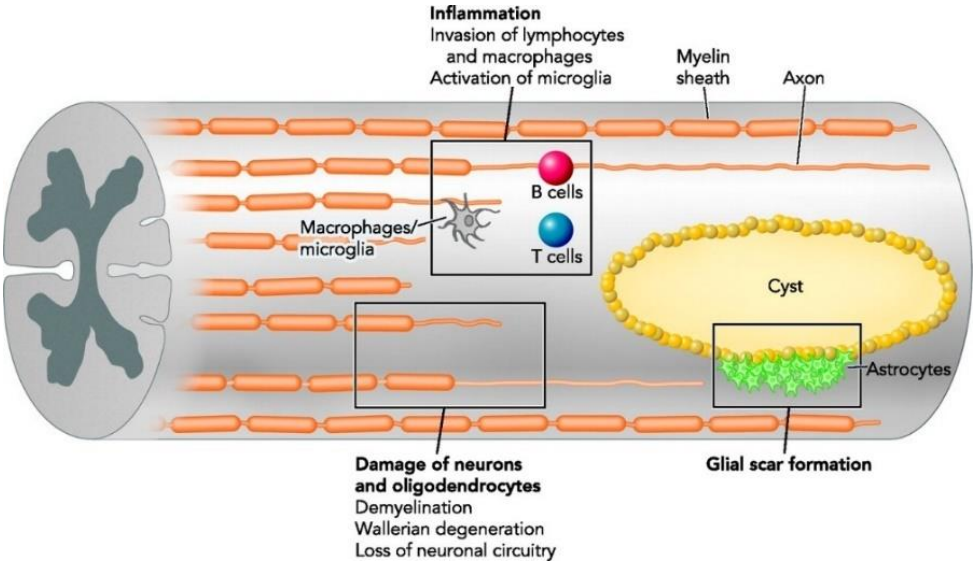

Figure 2: main events of SCI pathophysiology (Tsintou M, Dalamagkas K and Seifalian AM, 2015)

Glial cells, and in particular astrocytes, are the main responsible of the glial scar formation. Therefore, vascular defects and haemorrhage cause excitotoxicity, ionic dysregulation, free radical production and further inflammatory reaction that all together lead to neuron and glial cells death.

Then an intermediate phase (2 weeks-6 months) characterized by glial scar maturation and inefficient attempts of axon sprouting occurs. The astrocytic glial scar has a double role: it restricts the damage, restores the homeostasis, re-establishes the integrity of the BBB and limits further immune cell infiltration. but on the other hand, it is associated with a detrimental function as it acts as a physical barrier for axonal regeneration.

In the last chronic phase (> 6 months) the lesion stabilizes: glial scar continuously forms; Wallerian degeneration (i.e. the axonal fragmentation and degradation due to transection/crush) occurs and

axon fragmentation leads to final deficits and symptoms. Even if therapeutic strategies are generally applied at this stage in order to enhance axon regeneration and promote the re-myelination process, the lesion and the glial scar stabilization generally minimize their efficacy (Vercelli and Boido, 2015).

1.3 MECHANISMS OF AXON REGENERATION FAILURE AFTER SCI

After SCI, the spinal cord has a very limited capability to restore its connectivity. This is due both to a sequence of anatomical changes (including neuron cell death, neuroinflammatory reaction, glial scar formation and myelin inhibitory proteins) that create a growth inhibitory environment, and to the adult physiological inactivation of the growth program by oligodendrocytes (OLs) (Kwon et al., 2004).

More in detail neuron and OL death is the first event occurring by necrosis and later by apoptosis. The Ca^{2+} influx induced by the lesion leads to calpain activation with mitochondria dysfunction and excitotoxicity damage (mediated by N-methyl-D-aspartate receptor). Reactive oxygen and nitrogen species exacerbate the damage causing OL loss that in turn leads to further neural cell death. One of the first apoptotic pathway activated is the JNK cascade, whose specific inhibition prevents caspase 3 cleavage, promotes locomotor recovery and neuroprotection after SCI (Repici et al., 2012). Upstream caspase activation, associated protein with death domain- associated protein with death domain ligand (FAS-FAS-L) mediated cascade plays a critical role in axon degeneration and OL apoptosis: FAS deficient-mice with a SCI compression show improved locomotor recovery, axonal sparing and myelin preservation (Casha et al., 2005; Yu et al., 2009).

The limited regrowth ability of CNS is probably due to the lack of a sustained upregulation of growth factors. However it is known that when BDNF, neurotrophin 3, 4 and ciliary neurotrophic factor are released at the spinal lesion level, they are able to sustain axon growth after 1-2 months from the injury (Bregman et al., 2002). In the same way, it has been demonstrated that the selective downregulation of axon growth inhibitory molecules, such as Ras homolog gene family member A (RhoA), GSK-3β and PTEN, strongly sustains axon regeneration. Synaptogenesis and neurite outgrowth are reached by a RhoA inhibitory treatment in a rat acute SCI model (Devaux et al., 2017); GSK-3β inhibition significantly reduces secondary damage of SCI and ameliorates motor recovery in injured mice (Cuzzocrea et al., 2006); conditional PTEN depletion enhances the regenerative growth of corticospinal tract in association with motor function restoration in adult mice post-SCI (Danilov and Steward, 2015). Other growth inhibitors belong to 1) chemorepulsive

axon guidance molecules, such as the semaphorin family, ephrin, netrin and wingless-related integration site (wnt) known to limit axonal elongation after CNS lesion; 2) chondroitin sulfate proteoglycans (like neurocan, brevican, versican), a class of extracellular matrix (ECM) molecules, strongly upregulated after SCI, that are expressed by astrocytes in the glial scar and therefore limit neuronal plasticity both *in vitro* and *in vivo*; 3) myelin inhibitors such as Nogo-A, myelin-associated glycoprotein (MAG) and oligodendrocyte myelin glycoprotein (OMgp) that have been established to synergistically restrict axon growth after SCI both *in vitro* and *in vivo* (Cafferty et al., 2010).

Neural death and axon regeneration proceed in parallel to a demyelinating process. In detail demyelination is accompanied by oligodendrocytes progenitor cell (OPC) proliferation as demonstrated by the presence of neural/glial antigen 2 positive cells 4 weeks after SCI and increased level of fibroblast growth factor-2 (FGF-2), a mitotic factor that maintains OPC renewal state (McTigue et al., 2001; Mocchetti et al., 1996). However OPC maturation and re-myelination is prevented by the Notch1 expression rostral and caudal to the injury (Chen et al., 2005): indeed, Notch signals, with "a disintegrin and metalloprotease" (ADAM) molecules as downstream effectors, block myelin maturation. Also neural cell adhesion molecule (NCAM), a factor that prevents myelination, increases in dorsal spinal cord, motor neurons and corticospinal tract after SCI transection (Tzeng et al., 2001).

The apoptosis of neurons and OLs is also the result of the inflammatory response. Vessels and blood brain barrier breakdown cause a rapid infiltration of neutrophils and T cells, attracted by an initial release of TNF-α and IL-6 (Habgood et al., 2007; Pineau and Lacroix, 2007). The following increased production of cytokines gives rise to the secondary inflammatory response characterized by macrophage and microglia recruitment. The inflammation molecular mediators (as TNF-α) are generally described to have a dual role, neurotoxic or neuroprotective (Kim et al., 2001; Lavine et al., 1998). A similar function is attributed to microglia that after an injury become activated assuming a typical amoeboid structure: microglia depletion can be neuroprotective, but its controlled activation can also be beneficial. This paradox is explained by the presence of two different classes of cells, proinflammatory M1 and anti-inflammatory M2 microglial cells (Kigerl et al., 2009). 12-24h after SCI both cell types are expressed, but while M1 population persists into the lesion also in the chronic phase, M2 disappears after 1 week. Therefore, the increased ratio M1/M2 assures an efficient cellular debris removal and further inflammatory cell recruitment, but it also prevents regeneration and probably causes the axon retraction (Horn et al., 2008).

Also, astrocytes are activated by injury: these cells form a strong inhibitory scar that works as an anatomical barrier for axonal regeneration, in the ineffective attempt to limit the spread of damage and preserve the healthy tissue. Astrocytes are recruited to the injury site by a molecular cascade

that includes TGF-β, interleukin-1 (IL-1), interferon-γ and FGF-2, and become hypertrophic with an increased production of GFAP (Cregg et al., 2014).

Despite the limited axon regrowth potential of CNS, some regeneration associated genes have been described after central lesion. For example, the transcription factor CREB is induced by SCI and is able to promote axon growth and regeneration when overexpressed (Qiao and Vizzard, 2005; Qiu et al., 2002). The transcription factor ATF3 is known to enhances c-Jun mediated sprouting in response to neural axotomy *in vitro* (Pearson et al., 2003). JAK-STAT pathway is described to control the reestablishment of spinal cord continuity in response to a Xenopus Leaves model of spinal cord injury with a differential pathway activation during regenerative and non-regenerative stages (Tapia et al., 2017). GAP-43 can promote axon growth when upregulated after SCI compression (Curtis et al., 1993; Zhang et al., 2005). The effect of these molecules is proved by the postsynaptic re-connections of regenerating axons and by the spontaneous neuronal plasticity occurring after SCI. Both these phenomena represent adaptive reorganization mechanisms occurring as a consequence of collateral sprouting (damaged and spared axons) to create novel neuronal circuits (Bradbury and McMahon, 2006).

However, the molecules/pathways involved in regeneration cannot completely revert the intrinsic limited axon regrowth and overcome the inhibitory environment that is created after a lesion. Indeed for instance, it is estimated that only 2-10% of corticospinal tracts regenerate after experimental intervention with a total length of 2-3 mm (Bradbury and McMahon, 2006). Therefore, it is evident the importance to find new strategies able to enhance spontaneous plasticity, in order (i) to maintain and promote axon outgrowth and elongation attempts, (ii) to properly direct and reconnect the regenerating axons, and (iii) to restore original neuronal circuitry.

1.4 ANIMAL MODELS

In order to study SCI pathological mechanisms and evaluate therapeutic approaches, several experimental models have been developed, including transection, contusion and compression of spinal cord. It should be considered that all these models produce variable lesions due to a different relevance and anatomical location of the corticospinal tract among species (Figure 3). Indeed in primates the motor control is mainly achieved by CSMNs located in the ventral portion of the spinal cord. On the other hand, in rodents the locomotor behavior is preferentially mediated by rubro- vestibulo- and reticulospinal tracts rather than the corticospinal tract that is located in the dorsal portion of the spinal cord (Watson et al., 2009). The transection model can determine a complete disconnection between sensorimotor cortex and motoneurons under the lesion: it is generally realized at cervical or thoracic level with the aim to evaluate motor control and axonal regeneration. Despite the majority of data derives from studies on SCI cats, the murine model is the most used, whereas primates are rarely employed (Zhang et al., 2014). However, the incomplete lesions are much more frequent in human patients so that this kind of model is generally used to resemble the human pathophysiology. It can be experimentally obtained as the complete injury, but in this case the hemisection only involves a specific spinal region (lateral, ventral, dorsal) with a moderate secondary damage.

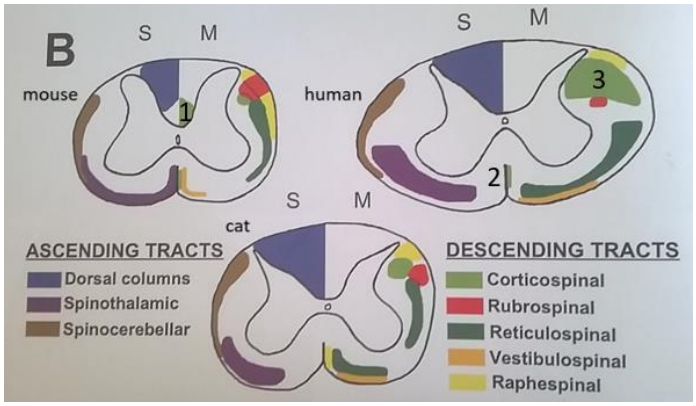

Figure 3: pyramidal and extrapyramidal tracts in mouse, human and cat. The corticospinal tract (CST) in mouse is located dorsally (1, top left in green), while in human there is a lateral and ventral CST (2-3, top right in green; Watson C, Paxinos G and Kayalioglu G, 2009)

Compared to the transection model, the contusion model better resembles what occurs in humans, in terms of histological features and neuropathological progression. However, the damage is very variable depending on the tissue areas lesioned and on the different techniques employed to reproduce SCI. A laminectomy followed by the fall of a weight on the spinal cord was one of the first methods employed (Anderson, 1982). In this case the lesion extension and the initial speed cannot be controlled, so that modern automated systems (impactors) have been developed to reach a more reproducible lesion (Gruner, 1992).

SCI compression can be realized by the application of a weight, swelling balloons or a modified aneurysm clip: this kind of lesion is characterized by a severe secondary damage and a limited involvement of the white matter. This model is particularly suitable for the study of neuronal

regeneration rather than functional recovery. Despite the absence of a standardized protocol, this is the SCI model that better resembles the tissue damage and histopathological events occurring in patients (Bouyer, 2005; Kwon et al., 2002).

1.5 SCI THERAPEUTIC INTERVENTIONS

The complex nature of spinal cord injury prompted researchers to try different strategies in the attempt to restore the lost functions. In order to stimulate axonal regrowth, several therapeutic interventions have been exploited both independently and in combination. Basically, they can be divided in two main classes: non-cellular and cellular approaches.

1.5.1 NON-CELLULAR APPROACHES

Surgery and rehabilitation

The traditional approach for the treatment of SCI patients consists of a prompt surgery intervention in the acute phase, followed by a rehabilitation period and a pharmacological treatment. Despite opposing data about the benefits of the surgical intervention, decompression and stabilization of the vertebral column improve the neurological recovery and minimize the damage especially in acute phase (within 24h after the lesion); (Fehlings & Perrin, 2006). Thereafter paraplegic patients may undergo specific treatments like functional electrical stimulation (FES) and tendon transfer surgery that should be employed to promote motor and sensory recovery. The first one uses an electric stimulus on the damaged nerve/muscle to re-establish its function: this technique allows to strengthen muscle mass and regain upright position. However, FES cannot be employed on denervated muscles and patients need to follow a rehabilitation programme to reach a good result (Sadowsky et al., 2002). Similarly, tendon transfer surgery is a quite safe procedure that allows patient to restore lost movements: it consists in repositioning a tendon of a working muscle at the place of the one of a paralyzed muscle, so that it takes over its functions. As for FES, a rehabilitation period should be associated to this procedure (Bélanger et al., 1996; Sadowsky et al., 2002). The rehabilitation programme has the main goal to increase muscle mass and strength in order to allow patients to walk again independently. One of the methods employed is the partial weight supported walking (PWSW) that combines the use of a tapis roulant (connected to the body weight supported, BWS) with a suspension automatic device. This technique has been demonstrated to improve the life quality and motor functions of 14 patients with an incomplete chronic damage

(Hicks et al., 2005). However, PWSW can only be applied to C and D ASIA impairment scale patients (Becker et al., 2003) and in general it should be carefully considered for each single case as SCI people present a different response to physical exercise that could be detrimental if not properly considered. Moreover, the rehabilitative potential is much higher if combined with a correct pharmacological treatment that should be always employed to obtain the best recovery.

Pharmacological approaches

The pharmacological interventions can be classified in neuroprotective and neuroregenerative drugs.

Methylprednisolone was the first neuroprotective agent and one of the most common drug used for SCI treatment (Bracken et al., 1992). It is described as an anti-inflammatory steroid that inhibits lipid peroxidation and cytokine release, improves vascular perfusion and prevents Ca^{2+} accumulation. Although at least three clinical trials have been performed since 1984, its beneficial effect seems to be inconsistent if compared to the poor neurological improvements and side effects. Therefore, methylprednisolone administration is not recommended anymore for SCI acute treatment.

Other pharmacological agents used in SCI treatment include minocycline, riluzole [both already employed for the treatment of amyotrophic lateral sclerosis (ALS)] and erythropoietin. Minocycline is known to have anti-inflammatory, anti-apoptotic and anti-excitotoxic effect. Moreover, it seems to reduce OL death and lesion volume in a rat SCI model (Stirling et al., 2004). A randomized clinical trial to assess its safety and dose optimization, showed significant ASIA score improvements in patients 1 year after SCI (Casha et al., 2012). Instead, riluzole is a chlorine channel inhibitor, whose action in preclinical SCI animal models reduced damage extension and glutamate release. Its neuroprotective effect is demonstrated by the induced white and grey matter sparing and by the functional locomotor recovery achieved after SCI compression (Azbill et al., 2000; Nógrádi et al., 2007). Finally, since the erythropoietin receptor is known to be upregulated after trauma conditions, the ligand administration has been proposed to have anti-inflammatory and anti-oxidant effect, and to induce neurotrophic factor release after SCI (Okutan et al., 2007; Yazihan et al., 2008).

Nowadays, the list of molecules under investigation is long and includes a variety of modifiers and monoclonal antibodies against ECM components, cyclooxygenase inhibitors, ionic channels inhibitors and neural electrical stimulators.

Moreover, molecules physiologically present in our organism, such as growth factors and microRNAs (miRNAs) can be included in this category as modulators of neural survival, plasticity and regrowth. Growth factors such as BDNF and GDNF have been investigated for their regenerative and re-myelinating capacities (Koda et al., 2004; Namiki et al., 2000; Zhou et al., 2003). A particular efficient approach is the combination of different factors as demonstrated by the axon regrowth and re-myelination induced by BDNF and GDNF administration after thoracic SCI (Blesch and Tuszynski, 2003). However, the limits of this technique are the low efficiency rate and the side effects. Indeed, high amount of growth factors should be administered in order to achieve the correct effect with a site-specific distribution. microRNAs (miRNAs) emerged as new players in SCI condition. Several microarray analyses revealed specific and aberrant miRNA expression patterns depending on the duration and severity of lesion, at different time points (Yunta et al., 2012; Ziu et al., 2014). Consistent with their widespread involvement, many studies described alterations of miRNAs and of their potential target genes correlated with different processes like axon growth, inflammation, oxidation and apoptosis [Figure 4 (Bhalala et al., 2012; Jee et al., 2012; Liu et al., 2009; Nakanishi et al., 2010)]. Therefore, new repairing strategies exploiting miRNAs as powerful inner regulatory system have been proposed trying to re-express downregulated small RNAs or to downregulate detrimental miRNAs activated after SCI.

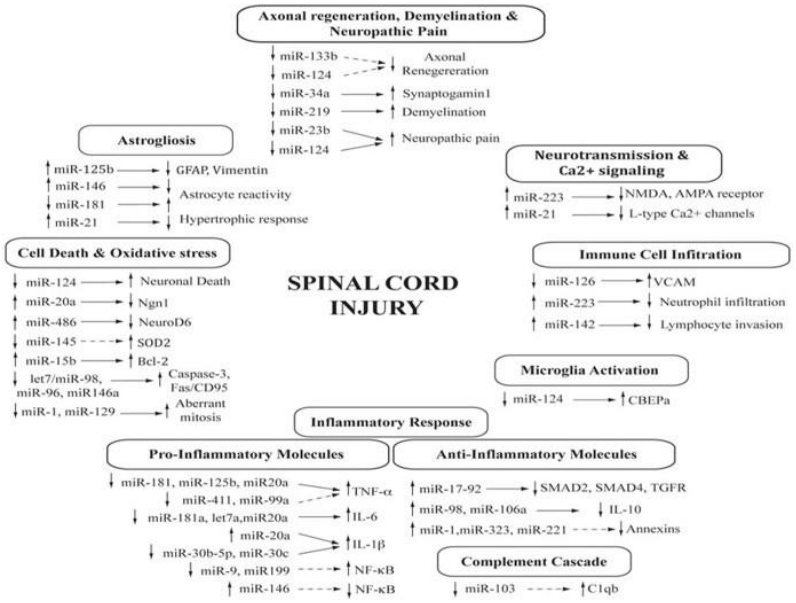

Figure 4: miRNAs involved in the pathophysiological mechanisms of SCI (Nieto Diaz M et al., 2014)

Biomaterials

One of the major limitations of "pharmacological strategies" (including drug, stem cell, growth factor delivery) still remains the administration route, that is often inefficient and highly invasive. Thus, biomaterial scaffolds emerged as valid tools i) to simplify and control the delivery of these agents, but also ii) to promote spinal cord repair exploiting their intrinsic properties. Indeed biomaterials can act both as efficient delivery systems, and as "bridge" to fill the gap created by the lesion.

Different systems are available, each one with its specific advantage. Channels, guidance conduits, macro and nanofibers offer the big potential to mimic the organization and orientation of axons, thus promoting their regrowth in the correct direction. In particular nanofibers present highly porosity and plasticity with the big advantage to be modified in different shapes and topography, a feature that is essential to accurately guide axon elongation through the lesion site (Guo et al., 2014a). On the other hand, hydrogels present the great advantage to be mechanically similar to spinal cord tissue and easily implantable by a simple injection.

Many biomaterials have been already tested *in vitro* and *in vivo* to promote axon regeneration after SCI, in the continue effort to find out both new materials (such as graphene) and new formulations (such as different types of polyurethanes, PUs), in order to improve and increase biomimetic properties (Kim et al., 2014).

Despite biomaterial properties basically depend on the material composition, they should ideally present a variety of features: high porosity to allow an adequate cell density; biocompatibility; biodegradability; non-toxicity; minimal host inflammatory response; elastic properties to well resemble the normal spinal cord minimizing the mechanical damage between the scaffold and the tissue; low manufacturing cost; ease handling at various conformations and modifications.

Moreover, besides representing a structural support, they are rarely used alone as some beneficial effects can also depend by their intrinsic properties. Therefore, the most common employment of biomaterials is in association with cells, neurotrophic factors or other materials, in order to enhance the regenerative and neuroprotective effects.

1.5.2 CELLULAR APPROACHES

Regenerative medicine focused the attention on cell therapy as it is suitable for the multifactorial damage that characterizes SCI. Encouraging results have been obtained with stem cell transplantation both in neurodegenerative disorders, in which one type of cell is involved, and traumatic events such as SCI, in which different cellular population are damaged. It has been hypothesized that the reconstruction of a small portion of neural circuits could be sufficient to promote functional recovery (at least in murine models): therefore the stem cell potential can be exploited also in case of SCI, representing a promising tool also for injured people (Garbossa et al., 2012).

The main sources and cell types used in SCI preclinical and clinical studies are numerous: neural stem cells (NSCs), mesenchymal stem cells (MSCs), embryonic stem cells (ESCs), induced pluripotent stem cells (iPSCs) and olfactory ensheating cells (OECs). Also Schwann cells have been extensively used even if they cannot be properly considered stem cells. Each cell type carries its own pros and cons, in terms of safety security, functional recovery and clinical viability applicability. To be classified as stem cells, they should self-renew (i.e., originate other undifferentiated cells) and differentiate into mature committed cells. On the basis of this last feature, stem cells are divided in totipotent, pluripotent, multipotent and unipotent (Figure 5). Totipotent cells are the only ones that can originate all the cells of the organism, while pluripotent cells have the limitation that placental cells cannot be obtained from them. Multipotent and unipotent stem cells are found in adult in specific cell niches and present a restricted differentiative potential: multipotent cells (such as

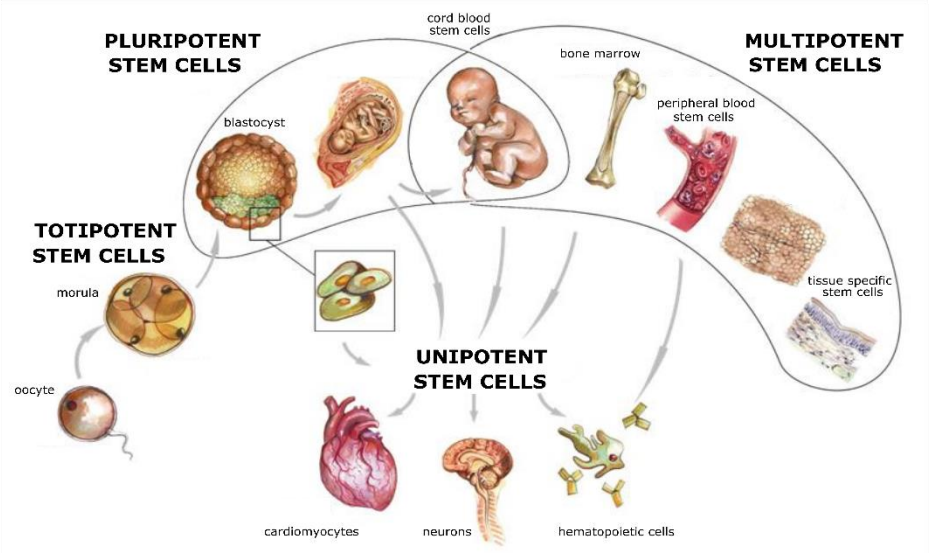

Figure 5: hierarchy of stem cells modified from http://www.smartbank.it/cellule-staminali/staminali-cosa-sono/

MSCs) can originate ectodermic, endodermic and mesodermic lineage cells, while unipotent cells, despite the self-renewal ability, can only differentiate in one cell type.
The exact mechanisms of action of stem cells are still not completely clear, but depending on the cell type may include: replacement of damaged neurons, reorganization of neuronal networks, axon remyelination, neuroprotection, angiogenesis induction and inflammation reduction.
Despite their extraordinary potential, there are also some risks connected to tumorigenesis (in particular for ESCs), possible rejection and unclear mechanisms of action.
Therefore, stem cells present advantages and limits that need to be considered and further investigated before a therapeutic employment.

1.6 AIM OF THE THESIS

In order to test and develop innovative treatments to promote axonal regeneration after SCI, we decided to focus our attention on **miRNAs** and **biomaterials** associated with **stem cells**, since both approaches should assure enormous potential benefits.
miRNAs are still a quite unexplored and unclear field in the panorama of SCI. It is already known that spinal cord trauma can alter miRNA expression thus affecting different pathophysiological processes and influencing the axon regeneration. Despite every year new miRNAs are described to influence axonal regrowth after SCI, we still lack a complete overview of the miRNA network acting after trauma. Moreover, the majority of miRNA studies in the SCI field are generally focused only on the spinal cord, disregarding the cerebral cortex where corticospinal motor neurons (CSMNs, the main cells disconnected after SCI) reside. Studying CSMN miRNA expression after SCI can contribute 1) in better understanding the molecular cascades occurring after trauma, and 2) in identifying new therapeutic targets.
Similarly, the available biomaterials represent an interesting and promising tool in case of SCI, since their structural and chemico-physical properties can efficiently support the axon regeneration. The additional contribution of stem cells (able to replace damaged neurons, reorganize neuronal networks, induce remyelination, promote neuroprotection, reduce neuroinflammation…) can be combined with biomaterials that have not only the great advantage to exert beneficial effects by themselves, but also to protect stem cells from the SCI inhibitory environment.
In a context in which axon regeneration represents the big challenge for SCI repair, we decided to investigate the potentialities offered both by miRNAs and new biomaterial formulations associated with stem cells as suitable and innovative approaches to induce axon regrowth and circuitry reorganization. In particular, the second chapter of the thesis is dedicated to the analysis of miRNA

networks (with specific relevance on axon regeneration pathways) and to the study of CSMN miRNA alterations and functions in an experimental model of SCI. Instead, in the third chapter, we propose an overview of the main biomaterials and stem cells employed in SCI conditions, followed by the description of an experimental approach (*in vitro* and *in vivo*) with polyurethanes or chitosan in association with MSCs and NPs.

CHAPTER 2: miRNAs IN SCI

2.1 miRNA BIOGENESIS AND NOMENCLATURE

MiRNAs are small non-coding RNAs about 20-22 nucleotides-long, which negatively regulate gene expression at post-transcriptional level. They were discovered by Lee and co-workers (1993), who demonstrated that lin-4 "gene" is able to repress the lin-14 gene (Lee et al., 1993). Since then, research on miRNAs expanded rapidly, demonstrating not only how many different physiological roles they play, but also revealing how their aberrant expression is implicated in several diseases. MiRNAs are highly conserved across species: they appeared first in invertebrates as a defense

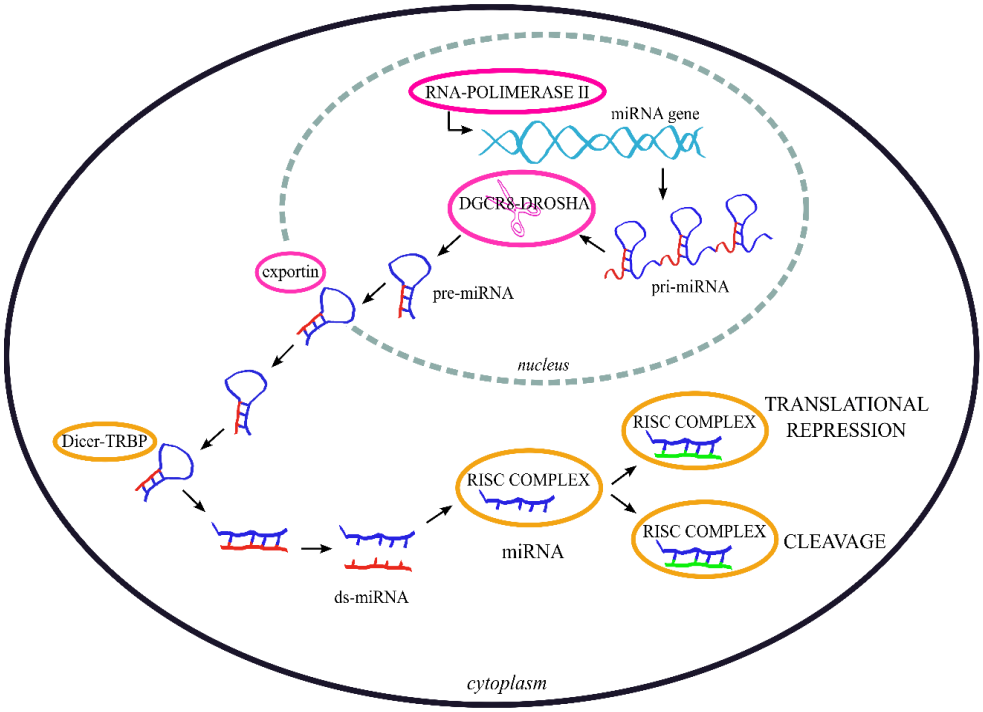

Figure 6: miRNA maturation process (Ghibaudi M et al., 2017)

mechanism against infection, then were conserved through evolution to refine gene expression in more complex organisms (Lee and Ambros, 2001). At present, over 2000 miRNAs have been involved in the regulation of one third of the human genes (Hammond, 2015). The miRNA maturation process (Figure 6) can be divided in two steps (Bartel, 2004). The first one consists of miRNA transcription by the RNA polymerase II into the primary miRNA (pri-miRNA) (Lee et al., 2004): this hairpin loop structure undergoes a process of capping (at 5'end), polyadenylation with

multiple adenosine (poly-A tail) and splicing. Then, DiGeorge Syndrome critical region 8 (DGCR8)-Drosha association (Filippov et al., 2000; Han et al., 2004) is required for the cleavage of the double-stranded pri-miRNA, thus releasing the hairpin and allowing the formation of the precursor miRNA (pre-miRNA) (Ketting et al., 2001; Knight and Bass, 2001).

Both pri- and pre-miRNAs can be modified by RNA-editing, which entails important functional implications related to maturation and target specificity (Blow et al., 2006; Kawahara et al., 2008; Yang et al., 2006). Then the enzyme exportin 5 translocates the generated pre-miRNA from the nucleus to the cytoplasm, where the second step occurs (Kim, 2004). Here, the endonuclease Dicer, in association with trans-activation response RNA-binding protein (TRBP), removes the loop from the 5' and 3' ends producing a double RNA of 21-22 nucleotides. Usually only one strand becomes the real mature miRNA, while the other is degraded (Khvorova et al., 2003). However, recently next generation sequencing experiments demonstrated that occasionally both strands could be expressed. Therefore i) the standard nomenclature system named "5p" the microRNAs derived from the 5' arm, and "3p" those derived from the 3' arm of the hairpin stem loop; ii) they are loaded at the same frequency in the RNA-induced silencing complex (RISC). Additionally, when distinct precursor sequences and genomic loci express identical mature sequences, they are named "1" and "2", as for example miR-121-1 and miR-121-2. However it is also possible to find "miR-121a" and "miR-121b", in which letter suffixes denote closely related mature sequences deriving from two different precursors (Kozomara and Griffiths-Jones, 2014). The selected single strand/double strand(s) is/are incorporated in the RISC that, among many other components, contains the Argonaute (AGO) proteins (Vaucheret et al., 2004) essential for the miRNA orientation and interaction with their targets occurring between 6-8 nucleotides (seed region) at the 5' UTR of the miRNA and the mRNA 3' UTR.

The maturation process described above is the most frequent, but alternative pathways may occur for some miRNA families (Ha and Kim, 2014). Drosha-independent (but still Dicer dependent) pathways have been described for mirtrons (miRNA located in mRNA introns) and miRNAs derived from short hairpin RNAs (Okamura et al., 2007; Xie et al., 2013): in the first case pre-miRNA is generated by splicing, debranching and trimming processes, while in the second the miRNA (for example miR-320) is directly transcribed and transported by exportin 1. Also Dicer-independent biogenesis is possible as in the case of miR-451, that is directly loaded to AGO2 protein to produce the miRNA mature transcript (Cifuentes et al., 2010; Yang et al., 2010b). Finally some miRNAs, like let-7 and miR-105, present a short 3' overhang from Drosha processing that requires terminal uridylyl transferases mono-uridylation in order to be processed by Dicer (Heo et al., 2012).

At the same time, miRNA cleavage/translational repression of the target represents their traditional mechanism of action, but not the only one. Indeed, some miRNAs, during cell quiescence, may directly mediate the upregulation of their targets (Rusk, 2008). The miRNA role in controlling specific target expression can also be extended to a regulation at the nuclear level. Several lines of evidence demonstrated a specific interaction between transcription factors (TFs) such as CREB, REST, FOXO and KLFs, and miRNAs. For instance, STAT3, one of the best known TF, has been demonstrated to regulate axon growth both in PNS and CNS by a strict interplay with miR-14 and miR-15 (Ghibaudi et al., 2017).

The apparently intricated miRNA panorama starts from their biogenesis, reflecting how wide is their role in a great variety of biological processes both in physiological and pathological conditions.

2.2 miRNAs IN CENTRAL AXON REGENERATION

In the last ten years the increasing interest in miRNAs in the nervous system revealed their specific involvement in many aspects of neuronal function and disease, such as neurite growth and neurodegeneration. To underline the potentially big impact of non-coding RNAs in neurodegenerative diseases, the latter ones are often defined as RNA disorders (Johnson et al., 2012). Moreover, taking into account miRNA intrinsic properties to regulate several biological functions, it is not surprising that they are considered one of the major players in the pathogenesis of CNS/PNS injury.

In the CNS context in which sprouting is limited and axon regeneration almost absent, miRNAs represent major players in the maladaptive changes occurring after SCI. As for the PNS, several studies analyzed the global profiling of miRNA expression after SCI obtaining differential expression for a great number of small RNAs (Liu et al., 2009). Indeed they can play either a protective or a detrimental role (Nieto-Diaz et al., 2014; Ning et al., 2014). Some miRNAs acting on different pathways promote functional recovery. For instance, an increased axon density within the lesion site was shown after miR-21 inhibition in astrocytes in a SCI mouse model (Bhalala et al., 2012). Even better, miR-133b is an important determinant for axon regrowth and functional recovery by reducing RhoA protein in an adult zebrafish SCI model (Yu et al., 2011). Considering that some miRNAs are evolutionarily conserved, the ability of let-7 to turn back the clock on regeneration in adult C. Elegans neurons suggests that its potential could also be applied for mammalian axon regrowth (Nix and Bastiani, 2013; Zou et al., 2013). Moreover further evidence

for the regenerative potential of some miRNAs comes from *in vitro* studies, such as the role exerted on embryonic cortical neurons when the miR-17-92 cluster is overexpressed: indeed this cluster acts on PTEN pathway as many other small RNAs, included the miR-29 family (Zhang et al., 2013a; Zou et al., 2015a). It is noteworthy that miR-17-92 and STAT3 are linked in a positive feedback loop in which STAT3 activation is related to an overexpression of this miRNA cluster in retinoblastoma cells *in vitro* (Jo et al., 2014): although such connection has been only confirmed in cancer pathways so far, it could affect also the axon growth pathways, since STAT3 is a crucial TF in neurite outgrowth (Jo et al., 2014). Somewhere in between peripheral and central nervous damage, miR-142-3p seems to be a potential target to enhance central regeneration of primary sensory neurons by inhibiting the adenylyl cyclase 9 molecule (Wang et al., 2015a).

The list of miRNAs with regrowth potential is long in the literature and, despite the encouraging results achieved, we are still far from a full understanding of their mechanisms. The main reason lies in the difficulty to connect every single element to reconstruct a broken system. This is particularly true for miRNAs, since each of them is only a piece of a complex and perfectly functioning puzzle. For this reason it is necessary to re-think of miRNAs not as acting singularly, but as coordinated members of different groups. Indeed miRNA action demonstrates their synergistic role in well-known molecular pathways related to different processes such as axonal growth and regeneration, making possible to identify specific functional miRNA networks. We are going to summarize the main axonal growth networks in which miRNAs are pivotal players (Ghibaudi et al., 2017).

2.3 miRNAs IN AXONAL GROWTH NETWORK: PTEN PATHWAY

miRNAs participate in one of the main molecular cascades regulating axon growth, i.e. the PTEN pathway. Indeed, acting as an inner regulatory system, they represent a promising tool still quite mostly unexplored. As shown in Figure 7, axonal growth is under the control of different growth factors, such as nerve growth factor, that stimulate the conversion of lipid second messenger phosphatidylinositol (4,5) bisphosphate (PIP_2) into phosphatidylinositol (3,4,5) trisphosphate (PIP_3) by PI3K. Then PIP_3 activates AKT through phosphatidylinositol-dependent kinase 1/2 (PDK1/2) recruitment. AKT in turn switches on a large spectrum of downstream effectors. Among them, the mechanistic target of rapamycin (mTOR) synthetizes raw material for axon extension and GSK-3β promotes cytoskeleton reorganization (as shown further in Figure 8). Unfortunately, after an injury, this pathway is inhibited by PTEN that antagonizes PI3K activity, thus resulting in the failure of

axon regeneration (Chadborn et al., 2006; Park et al., 2010; Rodgers and Theibert, 2002). To promote neuronal regeneration, several strategies (molecular deletion, shRNA, antagonists or inhibitors) have been applied at different levels of this cascade. However, until now, none of them can be completely restored the pre-injury condition, due to the complex network of cooperating molecules that orchestrate the different steps of the process. Based on the literature (Li and Sun,

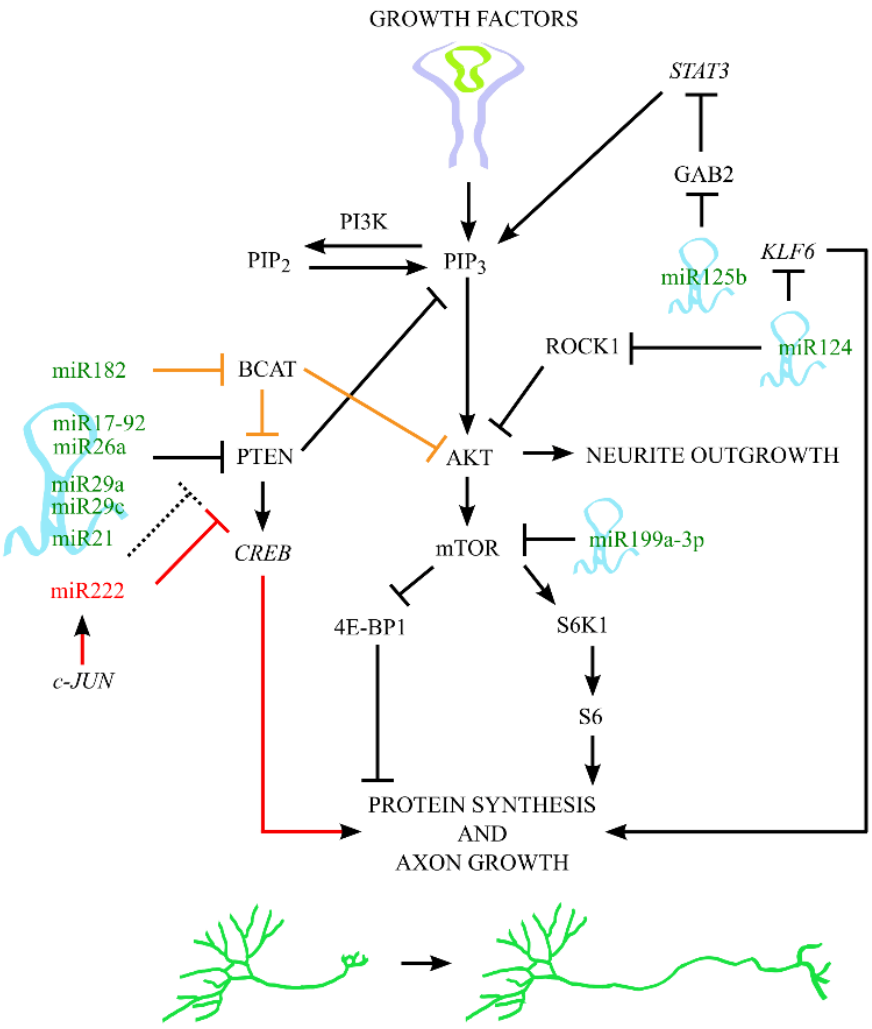

Figure 7: miRNAs in axonal growth network-1, focused on PTEN-AKT-mTOR; continuous lines indicate validated interactions and dotted line identifies a hypothesized interaction; miRNAs in green, red and black colors refer respectively

2013; Zhang et al., 2013a; Zou et al., 2015a; Zou et al., 2015b), we identified a miRNA network acting on the PTEN pathway (Figure 7). miR-17-92 cluster and miR-26a directly repress PTEN expression in primary cortical neurons during development, whereas miR-29a and miR-29c have the same effect on PC12 neural differentiating cell lines. When these miRNAs are overexpressed, PTEN protein levels decrease to 41% (miR-17-92 cluster), 38.3% (miR-26a) 44% (miR-29a), and 54% (miR-29c), validating this molecule as one of their main targets. Further evidence of the effect

of these miRNAs on PTEN is the upregulation of some downstream effectors, such as mTOR and AKT: the downregulation of PTEN is thus associated with the enhancement of axonal outgrowth for miR-17-92 and of neurite outgrowth for miR-29a miR-29c and miR-26a. Indeed the inhibition of miR-17-92 cluster revealed a suppressed axonal growth by 50% during 60 min of *in vitro* observation. miR-21 is involved in decreased expression of PTEN as well. It contributes to explain the mechanism underlying the benefits of docosahexaenoic acid (DHA), a fatty acid promoting functional recovery after SCI. In fact, DHA *in vivo* administration significantly upregulates miR-21 that in turn downregulates PTEN in corticospinal neurons. The decreased PTEN levels are accompanied by an increase in neurite outgrowth of primary cortical neurons *in vitro*, supporting a key role for miR-21 in the enhancement of neuroplasticity after SCI. Similarly *in vivo* a single acute (1-2 days), but not delayed, administration of DHA induces a significant sensorimotor and functional recovery after rat cervical hemisection (Liu et al., 2015). miR-26a and miR-222 have been described to repress PTEN respectively in bupivacaine DRG induced nerve injury, and in adult DRG after sciatic nerve transection models, thus promoting nerve regeneration (Cui et al., 2015; Zhou et al., 2012). Some small RNAs indirectly influence mTOR or AKT in order to reach the same goal. For example, miR-222 has been studied both *in vitro* (PC12 cell line) and *in vivo* (laryngeal nerve injury in rabbit): when activated by BDNF administration, miR-222 acts as a promoter of mTOR upregulation (probably by inhibiting PTEN, dotted line in Figure 7), significantly inducing neurite outgrowth, increasing the number of regenerating fibers, decreasing fibrous connective tissue and restoring nerve conduction velocity. Similarly, when SCI rats undergo cycling exercise to stimulate neuron regenerative potential, the expression of miR-199-3p is reduced and mTOR expression results increased: the raised regenerative neuronal potential observed should be attributed to the synergistic effects of miR-199-3p and miR-21, that are responsible for PTEN mRNA decrease (Liu et al., 2012a; Xie et al., 2015). Moreover, also miR-124 indirectly targets AKT through the repression of rho-associated coiled-coil-containing protein kinase 1 (ROCK1), a protein serine/threonine kinase and the major downstream effector of RhoA GTPase. Gu and coll. determined that the PI3K/AKT signalling acts downstream ROCK1 whose repression by miR-124 can activate AKT. The activated AKT is then able to induce neurite outgrowth and elongation during neural development of neuroblastoma cell line [BE (2) M17] and mouse P19 cells (Gu et al., 2014).

Recently another miRNA emerged as a new regulator of PTEN pathway: indeed the overexpression of miR-182 in cultured murine cortical neurons increases the complexity of the dendritic branches and promote axon outgrowth by inhibiting PTEN and activating AKT signal through a decreased

expression of branched-chain aminotransferase (BCAT2) (Wang et al., 2017b) (orange line Figure 7).

2.4 miRNAs IN AXONAL GROWTH NETWORK: GSK-3β PATHWAY

During development, axon growth is mediated by several pathways that can be reactivated and/or inhibited in the mature nervous system as a consequence of a lesion. Moreover, one single molecule can participate in different pathways and/or be the target of different miRNAs. A paradigmatic example of these intersections is represented by miR-124, previously involved in neurite elongation of M17 cells (neuroblastoma cell line) *in vitro* through ROCK1-PI3K/AKT regulation (Gu et al.,

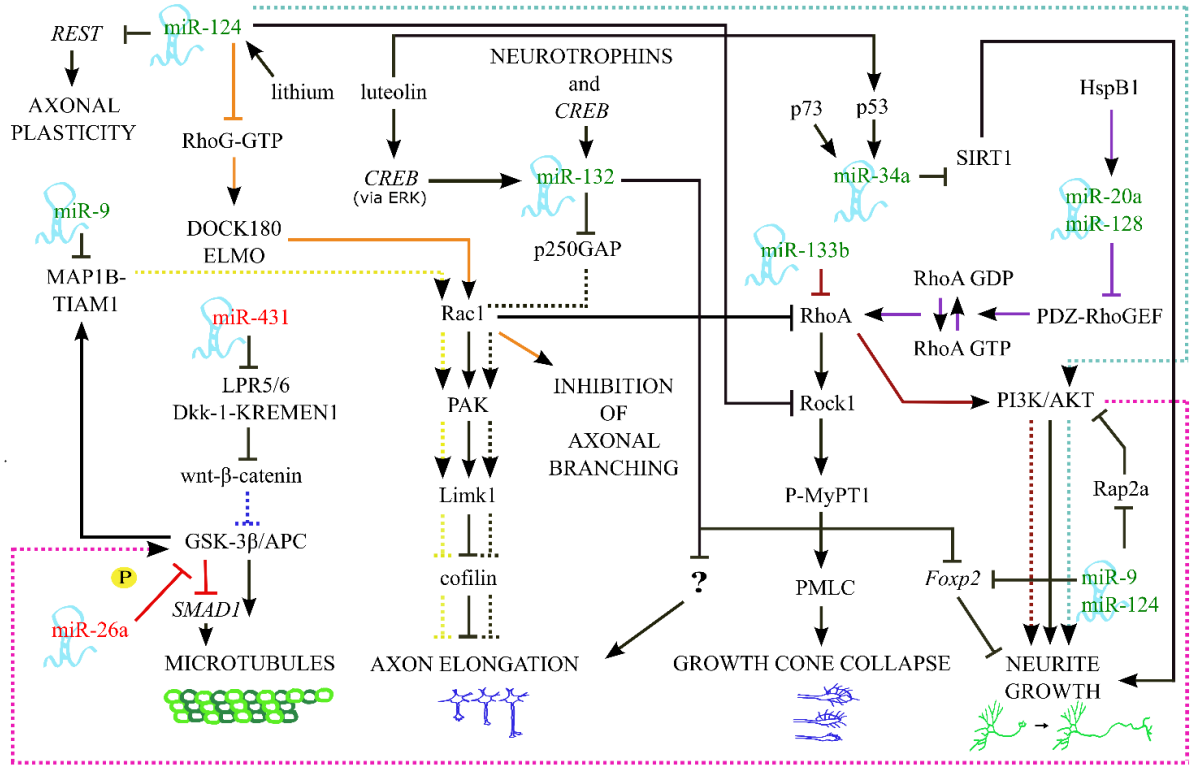

Figure 8: miRNAs in axonal growth network-2 (2.1-2.2), whose core molecules are represented by GSK-3β, Rac1, RhoA and PI3k/AKT; miRNAs in green and red colors refer respectively to CNS and PNS. Continuous lines indicate validated interactions, whereas dotted line hypothesized interactions. TFs are written in italic (Ghibaudi M et al., 2017)

2014). As shown in Figure 8, PI3K/AKT signaling is also linked to axonal microtubule assembly. The inhibition of GSK-3β leads to the dephosphorylation of GSK-3β substrates that regulate the dynamics and stability of axon microtubules (Zhou and Snider, 2006). PI3K-GSK-3β signal represents a key step in the axon specification and growth of hippocampal neurons (Jiang et al.,

2005; Yoshimura et al., 2005), making possible to establish a connection between miR-124 and GSK-3β through PI3K-AKT signal (blue dotted line). Recently, it has been shown that miR-124 operates synergistically with miR-9 to promote neuronal differentiation and dendritic branching of neural stem cells: these miRNAs, repressing their common target (Rap2a protein), elicit the inhibition of Rap2a protein on AKT. AKT in its active form phosphorylates and suppresses GSK-3β thus leading to neuronal development and maturation (Hur and Zhou, 2010). GSK-3β could be also a downstream effector of the wnt-β-catenin cascade, which is activated after SCI and promotes several biological functions including axon remodeling. In the classical pathway, wnt binds to its receptors (Low-density lipoprotein receptor-related protein 5 and frizzled) to signal to the GSK-3β/adenomatous polyposis coli (APC) complex and finally to β-catenin that translocates to the nucleus to elicit a change in the cytoskeleton components. However, wnt inhibitors (like Dickkopf-related protein 1 (Dkk-1) and Kremen 1) are overexpressed early after a SCI or nerve crush, thus inhibiting the cellular processes activated by β-catenin (Fernández-Martos et al., 2011). As illustrated in Figure 8, GSK-3β could be the converging point of two molecular cascades (PI3K-AKT- GSK-3β/APC and wnt-β-catenin-GSK-3β) that probably reach the same effect, i.e. the reorganization of microtubules. Moreover as reported in subsection 4, miR-9 and TLX are involved in a feedback regulatory loop that control neurogenesis: also GSK-3β downregulates TLX together with high IL-1β upregulation thus inhibiting hippocampal neurogenesis. Indeed both GSK-3β, TLX and IL-1β are dysregulated in neurodegenerative and psychiatric disorders suggesting that a complex interaction among all these factors could result in a complete regulation of neurogenesis and axon growth (Green and Nolan, 2012).

Another miRNA can be inserted in the wnt-β-catenin-GSK-3β molecular cascade as a regulatory molecule of the cytoskeleton dynamics. Indeed miR-431 is induced after sciatic nerve crush and is able to stimulate the regeneration of cultured DRG axons silencing Kremen-1, an antagonist of wnt-β-catenin signaling (Wu and Murashov, 2013): Kremen 1 was identified as one of the main targets of miR-431; moreover, the *in vivo* mRNA and protein expression in DRG neurons is reduced in presence of miR-431. The effect of this miRNA consists in a significant increase in axon length (about 30%) after its overexpression, whereas cells treated with a miR-431 inhibitor display a reduction in axon branching by 35%. Similarly, evidence of miRNA action on GSK-3β has been demonstrated by the administration of miR-26a inhibitor after a nerve crush that can impair *in vivo* axon regeneration. The endogenous regulatory effect of miR-26a is mediated again by GSK-3β as demonstrated by *in vitro* and *in vivo* experiments in DRG neurons. However, in this case, GSK-3β has a direct effect on gene expression controlling the TF SMAD1, a TF known to promote axon outgrowth after axotomy (Saijilafu et al., 2013; Zou et al., 2009). GSK-3β regulation of axon

growth is mediated both via controlling microtubules dynamics, at the growth cone level, or via controlling gene expression at the soma level (Jiang et al., 2015). We can finally conclude that a low level of GSK-3β needs to be endogenously maintained by miRNAs in order to support an efficient regeneration process.

2.5 MiRNAs IN AXONAL GROWTH NETWORK: MAP1B-Rac1 PATHWAY

The mitogen-activated protein kinase (MAPK) system is found upstream GSK-3β activation and makes it phosphorylate MAP1B stimulating axon growth (Goold and Gordon-Weeks, 2005): this link has been proved in a context in which NGF partially contributes to axon elongation through MAPK- GSK-3β-MAP1B cascade (Figure 8). MAP1B is also the target of miR-9, a highly conserved miRNA detected in the axon of primary cortical neurons. By acting locally in the axon, this miRNA is able to control axon length both *in vitro* (E17 primary cortical neurons) and *in vivo* (E 14.5 embryos brain) during development. In particular, the axon extension is allowed by preventing the interaction between miR-9 and MAP1B (Dajas-Bailador et al., 2012): the authors attributed this effect to a short stimulation with BDNF and the consequent increase of MAP1B protein level. MAP1B is a fundamental stabilizer of axonal microtubules, and it is highly expressed at the distal tip of the growing axons. Indeed MAP1B deficient mice present a delay in axon outgrowth and a reduced rate of its elongation. Montenegro-Venegas and co-workers (2010) demonstrated the role of this protein in the cross-talk between microtubules and actin filament: when MAP1B is present, T-cell lymphoma invasion and metastasis 2 (TIAM1, a guanine exchange factor) binds to microtubules, activates Rac1 that in turn inhibits cofilin, thus allowing actin polymerization and axon growth (the pathway is briefly illustrated in Figure 8). Considering the miR-9 effect on primary cortical neurons through MAP1B silencing, we can suppose that miR-9 suppresses the axon elongation process acting on this pathway. Moreover one of its first elements (Rac1 GTP, the activated form of Rac1) is a "crossroad" directed to different molecules and signal cascades, and possibly regulated by several miRNAs, like miR-9, miR-124 and miR-132 (Figure 8). Indeed the last one (whose expression is highly induced by neurotrophins and CREB) promotes neurite outgrowth by p250GAP, a Rho family GTPase-activating protein, inhibition during cortical neuron morphogenesis *in vitro* (Vo et al., 2005): its downstream molecules can be pinpointed in Rac1 pathway, involved in actin polymerization (Figure 8, dotted yellow lines). Indeed, the link

miR-132-p250GAP-Rac1-p21-activated kinases (PAK) is involved in the remodeling and maintenance of spine growth and probably in the axon growth (Lai and Ip, 2013).

2.6 MiRNAs IN AXONAL GROWTH NETWORK: RhoA-PI3K-AKT PATHWAY

Another molecule controlled by miRNAs in the axonal growth network is MAP1B. According to the role attributed to MAP1B during axon development (Del Río et al., 2004; DiTella et al., 1996; Montenegro-Venegas et al., 2010), it activates Rac1 pathway that inhibits RhoA, thus avoiding the growth cone collapse (Figure 8). Similarly, miR-133b is a suppressor of RhoA, contributing *in vitro* to neurite outgrowth both in PC12 cell lines and primary cortical neurons (E18; (Lu et al., 2015)). Extracellular signal-regulated kinases and PI3K/AKT are the main effectors of the signaling pathway downstream miR-133-RhoA. As already described above, PI3K/AKT is one of the best known pathway involved in axon growth and is probably linked to GSK-3β, another key player of such process. The role of miR-133 emerges even more significant if we consider the work of Xin and co-workers (2012): neurite outgrowth of primary cultured neurons isolated from post-middle cerebral artery occlusion brain was stimulated by miR-133b-enriched exosomes derived from mesenchymal stromal cells, through RhoA repression. Therefore miR-133 seems to be responsible for axon growth not only during development, but also during brain repair (Xin et al., 2012). In addition, Yu and co-workers (2011) described the essential role of miR-133 after SCI in adult zebrafish. miR-133 is endogenously overexpressed six hours after the lesion, but its inhibition blocks the regeneration process increasing RhoA protein level, thus likely activating the growth cone collapse (Figure 8, brown dotted lines). Indeed the injured adult zebrafish, following miR-133 inhibitor administration, showed a reduced locomotor recovery and a low number of neurons with regenerating axons (Yu et al., 2011). Its beneficial effect has been recently demonstrated also in mammals by the lentiviral injection of miR-133b in an adult injured spinal cord: RhoA has been validated as its direct target, whose downregulation was associated to mice locomotor recovery already at 4 weeks after the lesion (Theis et al., 2016). Finally, the indirect connection among other two miRNAs with RhoA pathway was demonstrated by Sun and co-coworkers (2013), that analyzed the mechanism of action of the heat shock protein B1 (HspB1). HspB1 is able to repress RhoA (thus promoting neurite extension), silencing the Rho GTPase, Rho guanine nucleotide exchange factor 11 (PDZ-RhoGEF), an exchanging factor that promotes the switch between RhoA

GDP (inactive) and GTP active. PDZ-RhoGEF repression is driven by miR-20a and miR-128, whose expression is specifically enhanced by HspB1 [(Sun et al., 2013) violet line, Figure 8]. In fact, inhibitors of miR-20a and miR-128 block the neurite growth of E17 cortical neurons promoted by HspB1, thus confirming the molecular cascade analyzed. Even though the downstream effectors of RhoA are not described here, it can be reasonably supposed a connection with the PI3K/AKT pathway that directly promotes neurite growth (brown dotted line Figure 8). In conclusion, this molecular cascade could be a pivotal pathway not only during development, but also after an injury. Indeed all the molecules described have been found in neurites and growth cones, and are produced in the axonal protein synthesis occurring after injury.

2.7 AIM OF THE PROJECT

The above mentioned miRNA networks have been explored in order to modulate their functions and promote axon regeneration process. However, although the evidence confirms the relevance of miRNAs in regulating the events occurring after SCI, we are still far from a total comprehension of miRNA dysregulation after a CNS lesion. In particular we lack both a global overview of the miRNA system and also a classification of specific cell population miRNAs in order to identify those small RNAs selectively involved in axon regeneration.

Therefore, the aim of this study was to explore additional roles for already known miRNAs and define miRNA clusters specifically involved in axon regeneration after SCI. Unlike the majority of studies focused on lesion site, we deeply analysed the sensorimotor cortex in which CSMNs, the main cells affected by SCI, reside. By realizing a complete spinal transection (C6 level) on C57BL/6J mice, we performed a miRNome profile analysis. We focussed our attention on the acute phase of SCI, in which the lesion is not yet stabilized, and on two different ages in order to compare the young plastic system with the adult one. In this way we also aimed at identifying differences and similarities in miRNA expression changes that could uniquely affect the regeneration process. Indeed, the manipulation of miRNAs could represent a new therapeutic approach for the treatment of SCI.

2.8 MATERIALS AND METHODS

In vivo experiments

Experimental animals

C57BL/6J male mice were purchased from Envigo (Udine, Italia). Animals were maintained under standard conditions with free access on food and water. All experimental procedures on live animals were performed according to the European Activities Communities Council Directive of 86/609/EEC (November 24, 1986) Italian Ministry of Health and University of Turin institutional guidelines on animal welfare, authorization No. 17/2010-B, June 30, 2010 (law 116/92 on Care and Protection of living animals undergoing experimental or other scientific procedures).

CSMN labeling and isolation by FACS

P-10 and P-90 C57BL/6J male mice were used to specifically label CSMN cells. Animals were deeply anaesthetized with 3% isoflurane vaporized in O_2/N_2O 50:50. The cervical spine was exposed, the spinal muscles displaced laterally and 1 µl of Green Latex Microspheres/Red latex Microspheres (GLMs/RLMs; Lumafluor Inc, Durham, NC, USA) was injected at the level of the fourth cervical vertebra (C4) into the dorsal column (n= 5). Control mice did not receive microsphere injection (n= 5).

One week after GLM/RLM injection, the animals were sacrificed by cervical dislocation, the brains dissected and the sensorimotor cortices rapidly isolated: under a dissecting microscope we selectively isolated the layer V using a brain matrix to obtain 1 mm-thick sections, avoiding as much as possible upper and lower layers and the subcortical white matter.

According to postnatal neuron dissociation protocols (Arlotta et al., 2005; Catapano et al., 2004), sensorimotor cortices were dissected in cold dissociation medium (20 mM glucose, 0.8 mM kynurenic acid, 0.05 mM (2*R*)-amino-5-phosphonopentanoate (APV), 50 U/ml penicillin, 0.05 mg/ml streptomycin, 0.09 M Na_2SO_4, 0.03 M K_2SO4, and 0.014 M$MgCl_2$). Then cortices were enzymatically digested in dissociation medium containing 0.16 gm/ l L-cysteine HCl and 11.7 U/ml papain at 37°C for 30 minutes at 37°C for 15 minutes. Papain digestion was then blocked with dissociation medium containing 10 mg/ml ovomucoid and 10 mg/ml bovine serum albumin (BSA) at room temperature (RT). The cells were then mechanically dissociated by gentle trituration in iced OptiMem medium supplemented with 20 mM glucose, 0.4 mM kynurenic acid and 0.025 mM

APV. Some experiments were performed in collaboration with Prof. Tonelli (IIT, Genova, Italia) and cell dissociation was performed by the Neural Tissue Dissociation kit (P) (MACS, Miltenyl Biotec, (Germany) following supplier's instruction.
Microsphere-labeled CSMNs were collected from the cortical cell suspension by fluorescence-activated cell sorting (FACS).

CSMN labeling and isolation by LCM

Another set of P-10 and P-90 C57BL/6J male mice (n=5 each group) was employed to specifically label CSMN cells (GLM/RLM injection), as described before, in order to collect them by laser capture microdissection (LCM). According to Zhang Z et al., 2013 sensorimotor cortices sections were dissected and directly frozen at -80° C (Zhang et al., 2013b). Cross-sections of 16-µm thickness were prepared in the cryostat, transferred to PEN membrane slides (Zeiss) and dry on ice/ethanol mixture. LCM was performed on a PALM microbeam UV laser microdissection system (Zeiss). For this process, a variable number of sections were employed (depending on the GLM/RLM fluorescence) to isolate CSMNs. The collected samples were stored at -80° C before RNA isolation as described later.

SCI mouse model

Postnatal 15 (P-15) and P-90 C57BL/6J male mice were divided into two groups: i) SCI mice, and ii) control mice (SHAM). Briefly, mice were deeply anaesthetized as described before. The cervical spine was exposed, the spinal muscles displaced laterally and the lesion performed as follow: using a 27-gauge1/2 needle, the entire spinal cord was dorsally exposed and transected at C6 level. In the SHAM group, the spinal cord was simply exposed without any damage. Cervical transection damaged spinal tissue, including corticospinal dorsal and ventral tracts where CSMN axons are located (Boido et al., 2009).

Histological analysis

A set of animals (P-15 12h n=14, P-15 3d n=15, P-90 12h n=15, P-90 3d n=13) was employed for the histological analysis of the sensorimotor cortex in order to better characterized the SCI model. Twelve hours and three days after injury (P-15 and P-90 groups) mice were anaesthetized with 3% isoflurane vaporized in O_2/N_2O 50:50 and transcardially perfused with 0.1 M PB, pH 7.4, followed

by 4% PFA in PB. The brain and the spinal cord (C6 level) were dissected and post-fixed for 2h at 4°C in the same fixative solution. Samples were transferred overnight into 30% in 0.1M PB at 4°C, embedded in cryostat medium (killik, Bio-Optica, Milan, Italy), frozen at -70°C in 2-methylbutane and cut on the cryostat (Microm HM 550) in coronal and transverse 50 µm-thick sections for brain and spinal cord respectively. The sections were collected into PBS 1X prior to immunofluorescence reactions and Fluoro-Jade C (Histo-Chem Inc., Jefferson, Arkansas, USA) staining.

Immunofluorescence (IF)

For evaluating astrogliosis and microglia activation, sections were immunolabelled with 1:500 anti-rabbit GFAP (Dako Cytomation, Denmark) and 1:500 anti-rabbit IBA1 (Wako Laboratories Chemicals, Japan) respectively. Briefly, after 30 minutes in PBS-triton 2% and 1h in blocking solution [0.2% Triton X-100 and 10% normal donkey serum (NDS; Sigma-Aldrich, Milan, Italy) in PBS pH 7.4], the sections were incubated with the primary antibodies in the same solution at 4°C overnight. Then the sections were washed in PBS 1X and incubated with the secondary antibody (Jackson Immuno Research Laboratories; 1:200 donkey anti-rabbit cyanine 3-coniugated). Pictures of sensorimotor cortex were taken with Nikon DS-5Mc digital camera on a Nikon Eclipse 80i epifluorescence microscope. Photomicrographs at 40X magnification were corrected for contrast and brightness enhancement with ImageJ. The percentage of GFAP/IBA1 positive area was quantified using ImageJ and analyzed with a non-parametric t-test (Mann-Whitney). Values $p \leq 0.05$ were considered statistically significant.

Fluoro-jade C (FJC) staining

To stain degenerating neurons, sections were treated for FJC staining (Histo-Chem Inc, Jefferson, Arkansas, USA), following supplier's instructions. Brain and spinal cord sections were mounted on 2% gelatin coated slides and dried overnight at RT. The day after sections were immersed in a solution of 1% sodium hydroxide in 80% ethanol for 5 minutes. Then they were rinsed for 2 minutes in 70% ethanol, 2 minutes in distilled water and then incubated in 0.06% potassium permanganate solution in PBS 1X for 10 minutes. Then slides were rinsed 2 minutes in distilled water and transferred for 20 minutes to a 0.0004% solution of FJC dissolved in 0.1% acetic acid. The sections were rinsed in distilled water three times for 1 minute before dry them at 37°C for ~30 minutes. Dried slides were then cleared in xylene for 4 minutes and covered with an anhydrous mounting medium. Pictures of sensorimotor cortex were taken on a Nikon DS-5Mc digital camera

on a Nikon Eclipse 80i epifluorescence microscope. Among the animals used for GFAP and IBA1 analyses, 3 SHAM and 3 SCI mice per group were employed for FJC staining.

Sensorimotor cortex dissection

Due to the technical difficulties in isolating CSMNs, we also isolated the whole sensorimotor cortex, in order to perform the miRNA sequencing. Twelve hours/three days after injury, SHAM (P-15 12h and 3d; P-90 12h and 3d) and SCI (P-15 12h and 3d; P-90 12h and 3d) mice were sacrificed by cervical dislocation, the brains removed and the sensorimotor cortices rapidly isolated and dissected as described in the "CSMN labeling and isolation by FACS" section. The samples were individually collected and stored at -80° C until the total RNA extraction.

Total RNA extraction

According to our laboratory experience (Valsecchi V et al.; Plos One, 2015), mice cortices were homogenized in lysis buffer and total RNA, enriched in miRNAs, was extracted with MirVana extraction Kit following supplier's instruction (Life Technologies, Milan, Italy). The quality and quantity of RNA samples was checked by Nanodrop measurements and the samples were stored at -80° C until the miRNA library preparation.

Small RNA library preparation and sequencing

Small RNA (sRNA) libraries were generated using high definition (HD) adapters (Sorefan et al., 2012; Xu et al., 2015) within a method that reduces ligation bias between sRNAs and adapters (Xu et al, 2015). HD adapters contain four degenerate nucleotides on the ligating ends of 5' and 3' Illumina HiSeq adapters. The pool of sequences present in HD adapters, versus one fixed sequence in standard HiSeq adapters, increases the annealing efficiency between sRNAs and adapters. Increased annealing efficiency leads to a greater amount of sRNAs in the libraries that are sequenced and can be analyzed. Next generation sequencing was performed on the Illumina HiSeq 2500 High Throughput Sequencer at Earlham Institute, Norwich Research Park, UK.

Raw fastq files were converted to fasta format. Reads containing unassigned nucleotides were excluded. The 3' adapter was trimmed using perfect sequence match to the first 8 nucleotides of the 3' HiSeq 2500 adapter (TGGAATTC). The HD signatures (four assigned nucleotides at the ligating

ends) of the reads were also trimmed (Beckers et al., 2017). Reads longer than 17 nt were kept for further analysis. Reads with low sequence complexity, i.e. with an overrepresentation of one nucleotide for more than 60% of the sequence length, were excluded. As part of the quality check the size class distributions for redundant reads, i.e. total reads (with their abundance) and non-redundant reads, i.e. unique reads, were plotted side by side with the complexity which is defined as the ratio of non-redundant to redundant reads (Mohorianu et al., 2011) SRNAs were mapped full length with no gaps or mismatches allowed to the mouse genome (v10) and corresponding annotations using PatMaN (Prüfer et al., 2008). The latest set of mouse miRNAs were downloaded from miRBase (v21) (Kozomara and Griffiths-Jones, 2014). sRNA expression levels were normalised using a scaling approach, reads per total, to a fixed total of 12 million reads per sample (Mortazavi et al., 2008). Differentially expressed reads were identified using both the localisation of maximal expression intervals for the control versus treatment comparisons and pairwise comparisons using offset fold change with an empirically determined offset of 20 (Mohorianu et al., 2011). Evaluation of variability between sequencing libraries was conducted using scatter plots, size-split boxplots of the replicate-to-replicate differential expression, intersection and Jaccard similarity analyses (Mohorianu et al., 2011). The empirical differential expression analysis was confirmed by parametric (t-tests) and non-parametric (Mann-Whiney-U) tests. For the statistical tests we considered $p < 0.05$ as statistically significant. Bioinformatics analysis was conducted using custom-made Perl (5.24.0.1) and R (3.2.2) scripts. MicroRNAs were considered differentially expressed if there was a > 0.5 $\log_2$ fold change between controls and treatments, i.e. more than 1.5 fold change (Figure 9).

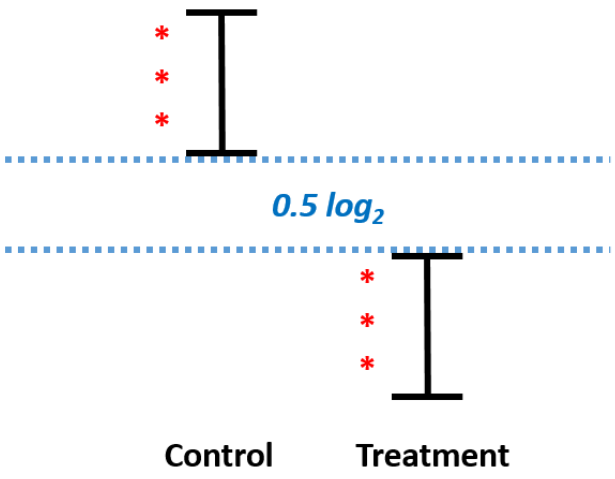

Figure 9: $\log_2$ fold change describes the distance between the control and treatment confidence intervals. > 0.5 $\log_2$ is considered differentially expressed, excluding any background noise

Small RNA libraries were generated by Dr Darrell Green (Norwich Medical School, University of East Anglia), bioinformatics analysis was carried out by Dr Irina Mohorianu (School of Computing Sciences, University of East Anglia) in collaboration with Professor Tamas Dalmay (School of Biological Sciences, University of East Anglia). A total number of 6 mice (3 SHAM and 3 SCI) each group (P-15 12h, P-15 3d, P-90 12h and P-90 3d) was employed for the sequencing experiment.

miRNA functional analysis

The following miRNA functional analysis was performed only on miRNAs with a $\log_2$ offset fold change > 0.5. Different tools have been used: 1) MiRpub (Mullany et al., 2015); database collecting miRNA publications) and PubMed to identify miRNA functions; 2) MiRWalk 2.0 database (Dweep et al., 2011) to check both predicted and validated targets of our set of miRNAs respectively by predicted target module (PTM) and validated target module (VTM); 3) DAVID 6.7 to identify enriched annotation terms (KEGG, Kyoto Encyclopedia of Genes and Genomes pathways and GOBP Gene Ontology biological process) associated with the gene lists generated by miRWalk PTM and VTM; 4) miRNet (Fan et al., 2016), to perform a network analysis of miRNAs; and 5) a miRNA atlas (Fertuzinhos et al., 2014) to verify miRNA expression in mouse neocortex.

Firstly, the presence of miRNAs shared among all the groups was analyzed. Then miRNet tool was employed to identify miRNA neural gene networks within each group or among them.

Secondly, we used miRWalk 2.0 database to identify VTM genes, and MiRpub and PubMed to screen the literature related to the miRNAs of interest. Then identified miRNAs involved in axonal regeneration were validated by RT-PCR as described in the next section prior to further functional analyses. The PTM gene list was analyzed both directly by miRWalk 2.0 (KEGG, GOBP and GOCC p-values ≤ 0.05) or by the miRWalk 2.0 intersection result of 12 different databases. Only the genes predicted at least by 6 databases were considered for the next step. The generated gene list was then uploaded on DAVID 6.7 on the "functional annotation chart" tool to identify KEGG, GOBP and GOCC of a specific miRNA. The degree of enrichment was selected basing on the multiple testing correction techniques Benjamini, considering only the p-values ≤ 0.05 after the statistical correction.

Only miRNAs that overcame sequencing statistical analysis and functional analysis were considered for further studies.

miRNA validation by RT-PCR

A selection of 6 miRNAs (miR-7b-3p, miR-19b-3p, miR-127-5p, miR-381-3p, miR-214-3p, miR-338-5p) resulting from the miRNA sequencing was validated by RT-PCR. Total RNA, enriched in miRNAs, was obtained from 3 SCI and 3 SHAM (sequencing samples) plus 5 SCI and 5 SHAM for the P-15 group, and from 3 SCI and 3 SHAM (sequencing samples) plus 2 SCI and 2 SHAM for the P-90 groups. CDNA was synthesized by 2 ug (Qiagen, Milan, Italy) or 10 ng (Life Technologies) of total RNA using the High Capacity cDNA Reverse transcription kit following supplier's instructions (Qiagen/Life Technologies). Quantitative RT-PCR was performed with SYBR green core reagent kit (Qiagen, for miR-7b-3p) or TaqMan Assay (Life Technologies, for miR-19b-3p, miR-127b-5p, miR-381-3p, miR-214, miR-338-5p) in a Step-One 2000 RT-PCR system. miRNA expression was analyzed using RNAU6 as housekeeping gene. Samples were amplified simultaneously in triplicate in 1 assay run. Changes in miRNA levels were detected as the difference in threshold cycle (ΔCT) between the target gene and the housekeeping gene. The results were analyzed by Mann-Whitney test and presented as normalized values between SHAM and SCI groups.

In vitro experiments

Primary cortical neuron culture

In order to study *in vitro* the miRNAs of interest, we isolated and cultured murine cortical neurons. The cells were obtained from mouse C57BL/6J brain at embryonic day 14.5 (E14.5). Cortices were dissected under the microscope and collected in HBSS 1X (supplemented with 0.7% of HEPES and 1% of P/S/, Invitrogen-Gibco). Then cells were enzymatically dissociated by trypsin-EDTA 0.05% (15 minutes at 37°C) and washed in the same HBSS dissection solution; then DNAse (1000U-Promega, Milan, Italy) was added to the dissection solution, prior to mechanical dissociation by glass Pasteur pipette. Neurons were counted on a Burker chamber and plated at a density of 300,000 cells/dish on Poly-L-Lysine coated coverslips (0.1 mg/ml poly-L-lysine) in MEM 1X medium (supplemented with 20% glucose, 1% of L-glutamine and 10% of horse serum Invitrogen-Gibco) and incubated at 37°C, 5% CO_2 and 95% humidity. After 4 hours MEM 1X-medium was replaced with Neurobasal (supplemented with 2% of B27 and 1% of L-glutamine, Invitrogen-Gibco); coverslips (with paraffin dots) were placed inverted on the cells to create a suitable environment for neuron differentiation. Neurons were cultured for 1-3-7-18 days.

Cell RNA extraction and RT-PCR

To perform a RT-PCR to measure the physiological expression level of miR-7b-3p, the cells were collected after 1-7-18 DIV (total amount of 1,000,000 cells each time point), as follows: the medium was removed and cells were incubated with trypsin-EDTA 0.05% at 37°C. Then the detached cells were centrifuged at 1,000 rpm for 5 minutes, washed with PBS 1X and the pellet was collected at -80°C. RNA was extracted and quantified at Nanodrop, as previously described for *in vivo* experiments. A RNA purification protocol was applied before performing the RT-PCR for miR-7b-3p: a solution of 1/10 volume of NH_4OAC (0.5M), 2.5 volume of cold 100% EtOH and 1 µl of glycogen (Invitrogen) was added for each tube. The samples were incubated at 80°C for 30 minutes and then centrifuged at 12,000 g at 4°C for 20 minutes. The supernatant was removed, the pellet washed with 75% cold EtOH and centrifuged again at 12,000 g at 4°C for 5 minutes. The pellet was resuspended in DEPC water. RNA samples were then collected at -80°C before RT-PCR.

RT-PCR at 1-7-18 DIV was conducted in triplicate (3 different dissections at DIV-1, 2 dissections at DIV-7 and DIV-18). The RT-PCR for miR-7b-3p was performed as previously described for *in vivo* experiments. The expression values (DIV-7 and DIV-18) were normalized with respect to DIV-1, considered as baseline.

Nucleofection

Cortical neurons were electroporated immediately after tissue dissociation and before plating using the rat neuron nucleofector kit (Amaxa, Swiss). In brief, 500,000 cells were centrifuged for 5 minutes at 1,000 rpm. After that, supernatant was removed and neurons were resuspended in 100 µl of Nucleofector solution. Then, 5 nmol of miR-7b-3p-mimic (Invitrogen)/10^6 cells or mimic negative control (Invitrogen) were added to the suspension (Buller et al., 2010). Then neurons were electroporated with the Amaxa program O-003. Finally, neurons were plated on poly-L-lysinate coverslip (see "Primary cortical neuron isolation and culture" section) at a final concentration of 300,000 cells/coverslip.

Three days after nucleofection, cortical neurons grown on coverslips were fixed with 4% PFA for 15 minutes and rinsed three times in PBS 1X. Permeabilization was carried out with 0.1%TritonX-100/PBS 1X for 5 minutes and non-specific binding sites were blocked by 5% BSA/PBS for 30 minutes. The following primary antibodies were incubated for 1 hour: 1:200 monoclonal mouse anti-SMI-312 (Biolegend, San Diego, California) and 1:1000 monoclonal rabbit anti-α-tubulin III

(Abcam). After washing in PBS 1X, primary antibodies were detected with anti-rabbit or anti-mouse cyanine 3-coniugated secondary antibodies, and Phalloidin TRITC (Sigma-Aldrich) 546 (1:1000) for 30 minutes. Once mounted, the samples were examined and images acquired using an Olympus Fluoview 300 confocal laser scanning microscope (CLSM). To check miR-7b-3p overexpression, a RT-PCR was performed on samples at 3 DIV after nucleofection. The statistical analysis was performed by a non-parametric t-test (Mann-Whitney).

Morphometric analysis

The images acquired at CLSM were then analysed with ImageJ software. Differentiated cells were defined as those bearing at least one neurite longer than twice the cell body. For each time point (experiment conducted in triplicate) at least 30 axons were measured. The same cells were also analysed for the number of dendrites emerging from the cell body. Both measures were expressed as the total mean length for cell electroporated with mimic negative control and antagomir-miR-7b-3p. Graphpad Prism software was employed for the t-test. Values $p \leq 0.05$ were considered statistically significant. Four different dissections (2 NC and 2 MIMIC-7) were performed for the nucleofection experiment.

2.9 RESULTS

In vivo results

CSMN labelling and collection by FACS

To set up the procedure of CSMN labelling in the sensorimotor cortex, both GLMs and RLMs were injected into the dorsal tract of the spinal cord at C4 level in uninjured mice (Figure 10 A). As retrograde tracers, GLMs and RLMs were able to move from the spinal cord to the sensorimotor cortex specifically labelling only the CSMN cell body. One week after GLM and RLM injection, brains/sensorimotor cortices were dissected both by P-17 and P-97 animals (sensory cortex –SC- and motor cortex –MC- in Figure 10 B). Both green- and red-positive CSMNs were visible in the layer V of sensorimotor cortex (Figure 10 C). No other cortical layers were labelled, suggesting the

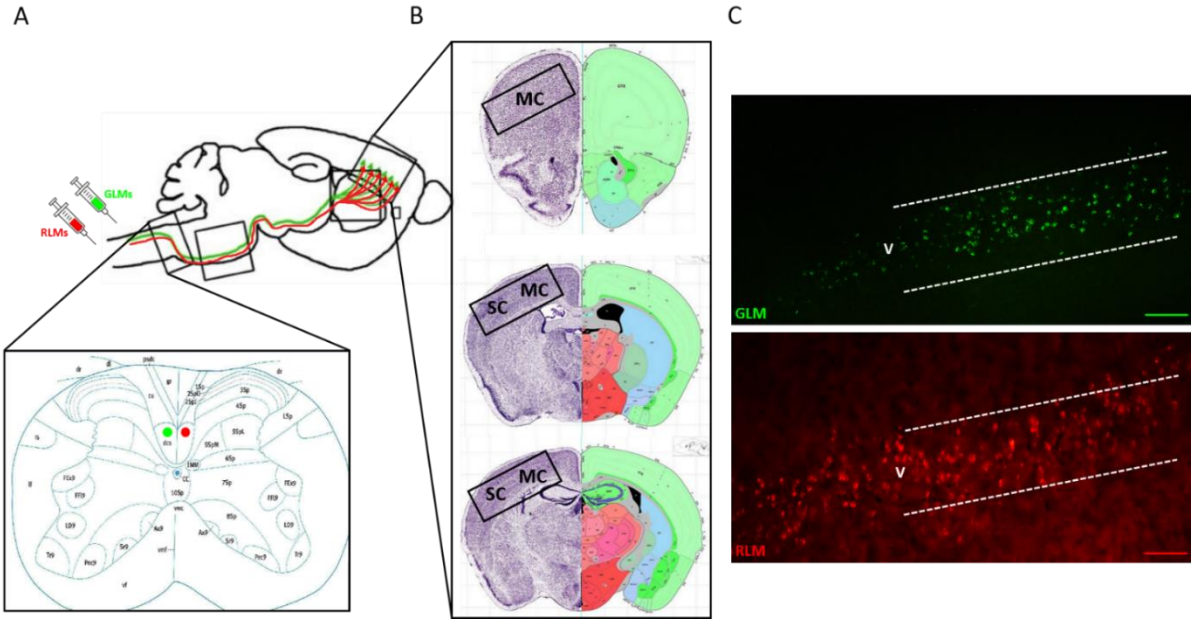

Figure 10: CSMN labelling. A) GLMs and RLMs were injected into the dorsal tract of the spinal cord (green and red dots) where corticospinal tract is located (drawing modified from Jara JH et al., 2014). B-C) Labelled CSMNs were visible in layer V of sensory and motor cortex (SC and MC). Pictures refer to P-90 mice cortex. Scale bar: 100µm

accuracy and specificity of the injection. The labelled cells were then sorted by FACS. Despite several cell dissociation protocols have been tested, the number of positive cells sorted was always very low [0.4% for P-17 pups (Figure 11 B) and 0.2% for P-97 mice (Figure 11 C)]. Similar results were obtained by the LCM employment. Although we were able to easy collect the labelled CSMNs, it was not possible to extract a sufficient amount of RNA for the next experiment. These results suggest that these strategies could not be considered a valid method to specifically collect

CSMNs. Therefore, we decided to proceed with a more general approach isolating the entire sensorimotor cortex, where CSMNs are located, to perform the miRNA profile.

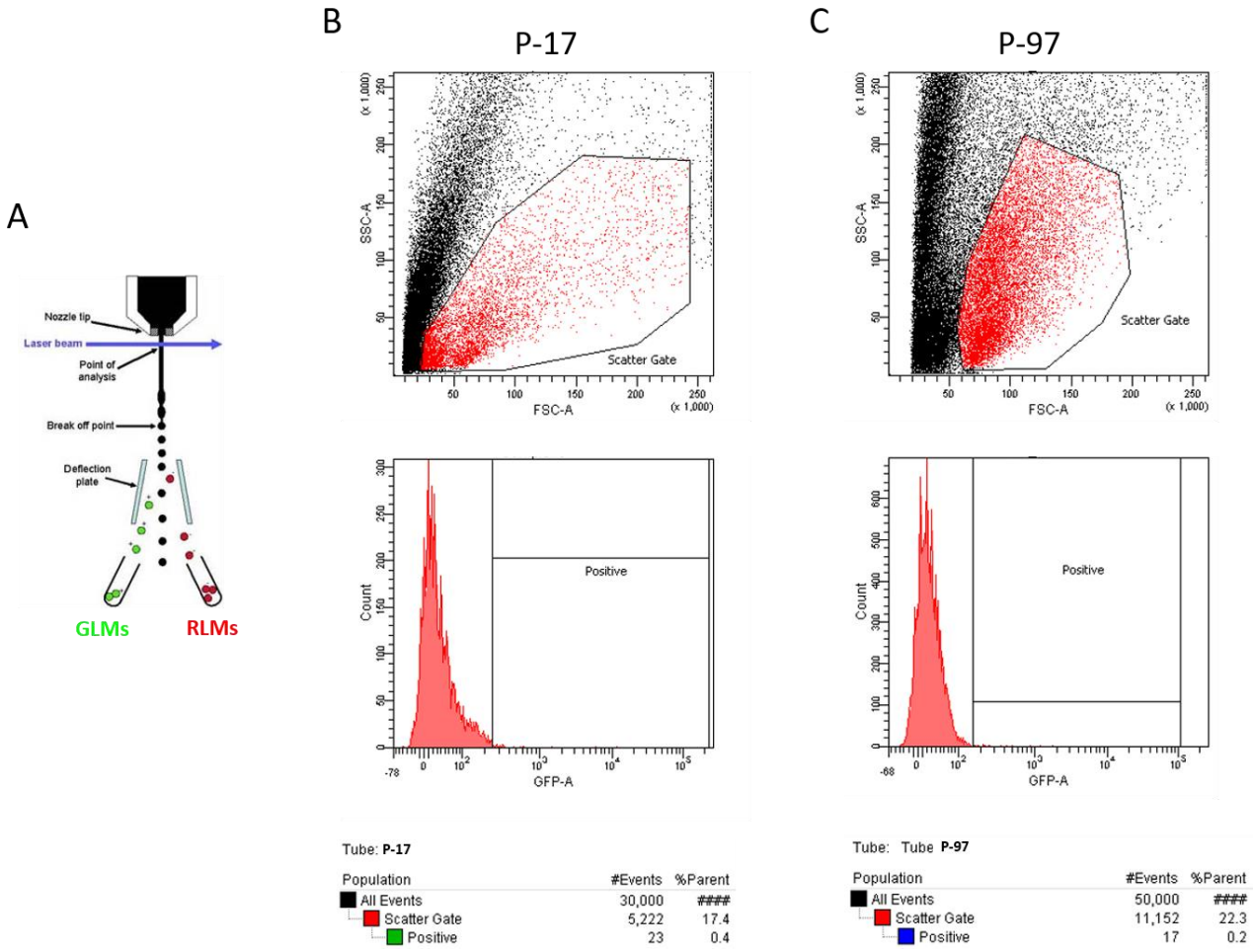

Figure 11: CSMN collection by FACS. A) Scheme of FACS sorting. B-C) FACS scatter plots showing debris in black and selected live cells in red. The number of GLM- and RLM-positive CSMNs is 0.4% and 0.2% at P-17 and P-97 respectively. FACS plots refer to 5 CTRL mice vs 5 injected mice. A) Image from http://www.abcam.com/protocols/fluorescence-activated-cell-sorting-of-live-cells

SCI characterization model

To characterize the transection SCI model employed for this study, we analysed the inflammatory reaction and the presence of degenerating cells in motor and sensory cortex 12h and 3d post SCI both in young and adult groups.

Since it is known that after SCI an intensive immune response is activated at the lesion site, we decided to evaluate the inflammatory reaction also at cortical level by measuring macrophage activation (IBA-1 positivity). As shown in Figure 12 in the P15 group the SCI sensory motor cortex presented an increased macrophage activation both at 12h (16.82%) and 3d (19.16%) after the lesion, compared to the sham group (6.69% at 12h and 6.79% at 3d). Moreover, in both cases, the morphology of macrophages appeared different in comparison to controls: indeed P-15 SCI mice were predominantly characterized by both ramified and amoeboid cells (magnification boxes A-B-C-D). The same pattern of macrophage activation was also present in both adult groups, although the density of IBA-1-immunopositive profiles was unchanged compared to the sham animals. Unexpectedly, in adult mice, any sign of astrogliosis (GFAP reactivity) was observed.

Altogether these results suggest that the spinal cord lesion can trigger an inflammatory response also at cortical level.

To detect the presence of suffering cells, we employed the FJC staining. We did not detect suffering cells in both motor and sensory cortex (data not shown) of P-15 and P-90 SCI mice compared to the SHAM groups (Figure 13 A-B). As positive control, we employed the spinal cord of the same SCI mice, where several suffering cells were visible at the lesion site (Figure 13 A-B SC-SCI). These results indicate that the lesion model does not activate a cell death pathway at the cortical level.

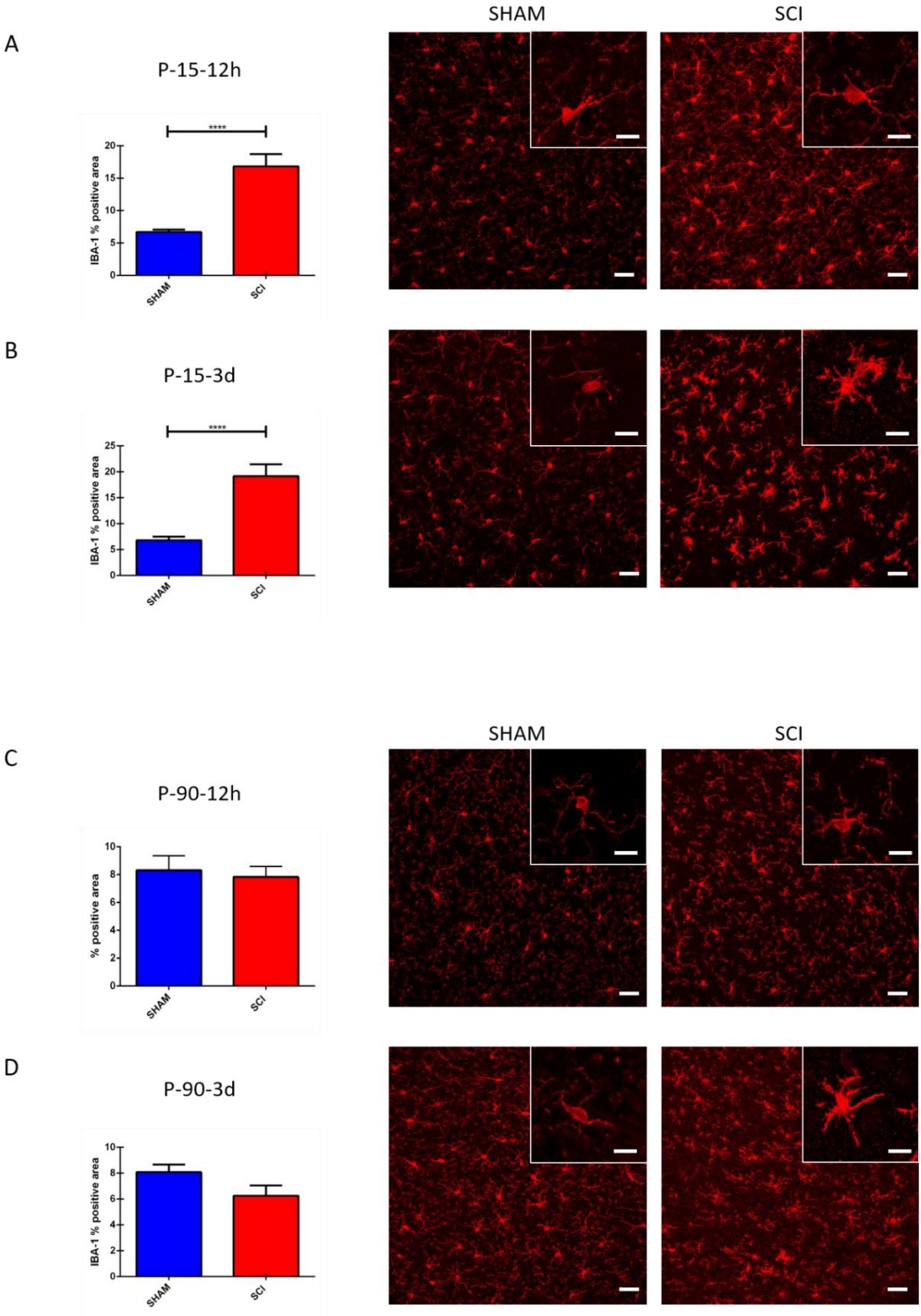

*Figure 12: A-B) IBA-1 increased expression in P-15 groups C-D) IBA-1 increased expression P-90 groups. Data are shown as % positive area of IBA-1 ± SEM. **** p < 0.0001; *** p < 0.001; ** p < 0.01. Scale bars: A,B,C,D 50 µ, A,B,C,D magnification boxes 10µm*

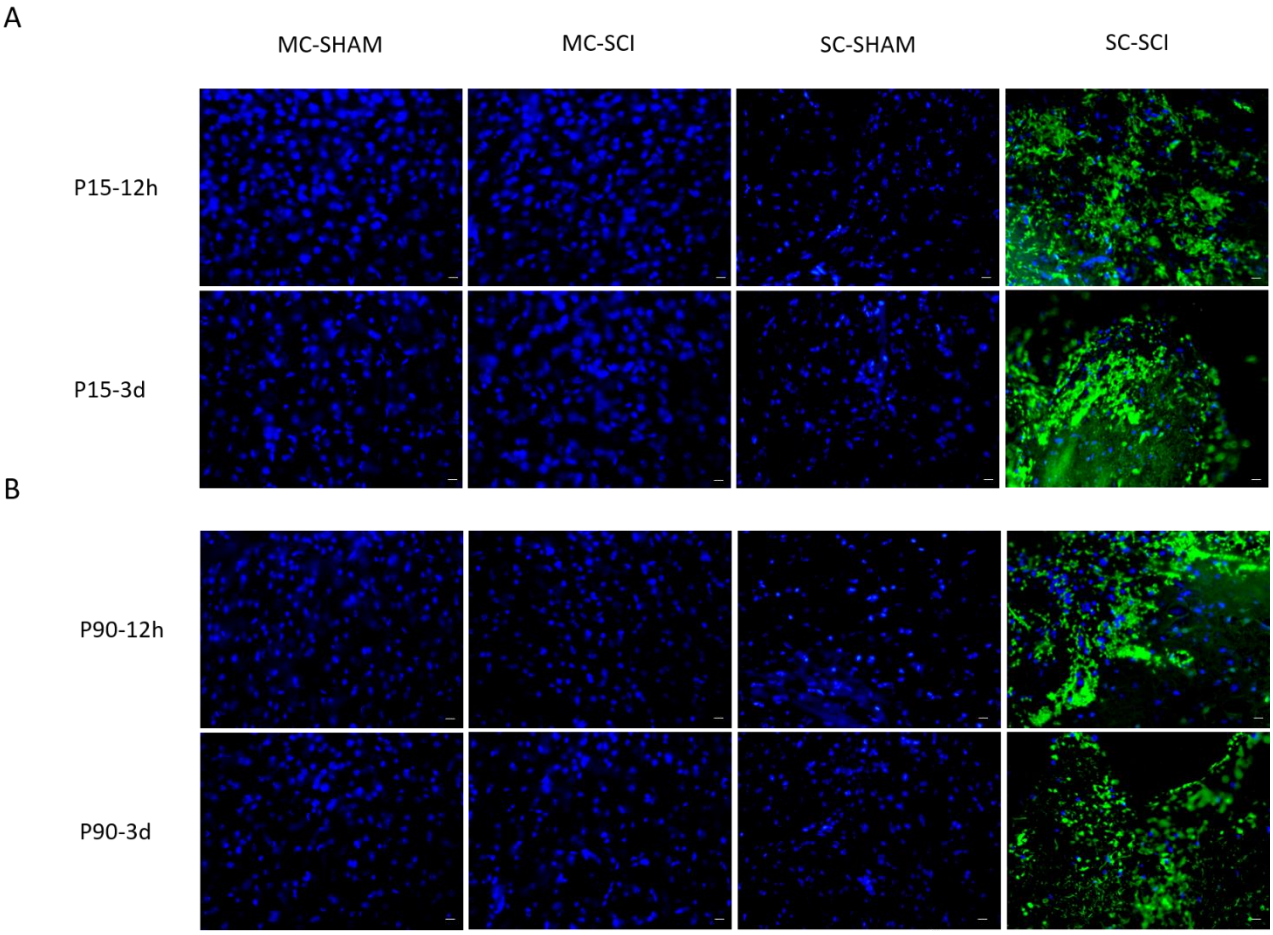

Figure 13: FJ-C staining in MC and spinal cord of SCI mice (SC-SCI). A-B) Both P-15 and P-90 groups do not present any suffering cells into the motor cortex, whereas they are visible in the spinal cord of SCI mice at the lesion site (green labelling in SC-SCI). Scale bar: 10 µm

miRNA sequencing profile

To evaluate miRNA differential expression after SCI, a complete transection of the spinal cord was performed in P-15 and P-90 mice and the miRNA library and sequencing of the sensorimotor cortex carried out 12h and 3d after SCI. Figure 14 shows the list of miRNAs predicted to be differentially expressed between SHAM and SCI mice by the sequencing analysis (log_2 fold change > 0.5). For each group at each time point, different miRNAs were found to be potentially upregulated (orange) or downregulated (green), with the exception of P-15-12h (A) and P-90-12h (F) in which only one miRNA was detected. In two groups (P-15-3d UP, and P-15-12h UP and DOWN) the same miRNA name apparently appears more than ones because it referred to slightly different (1-2 nucleotides at the end of the sequence) annotated sequences. In these cases, the sequence with the higher number of reads was took into consideration.

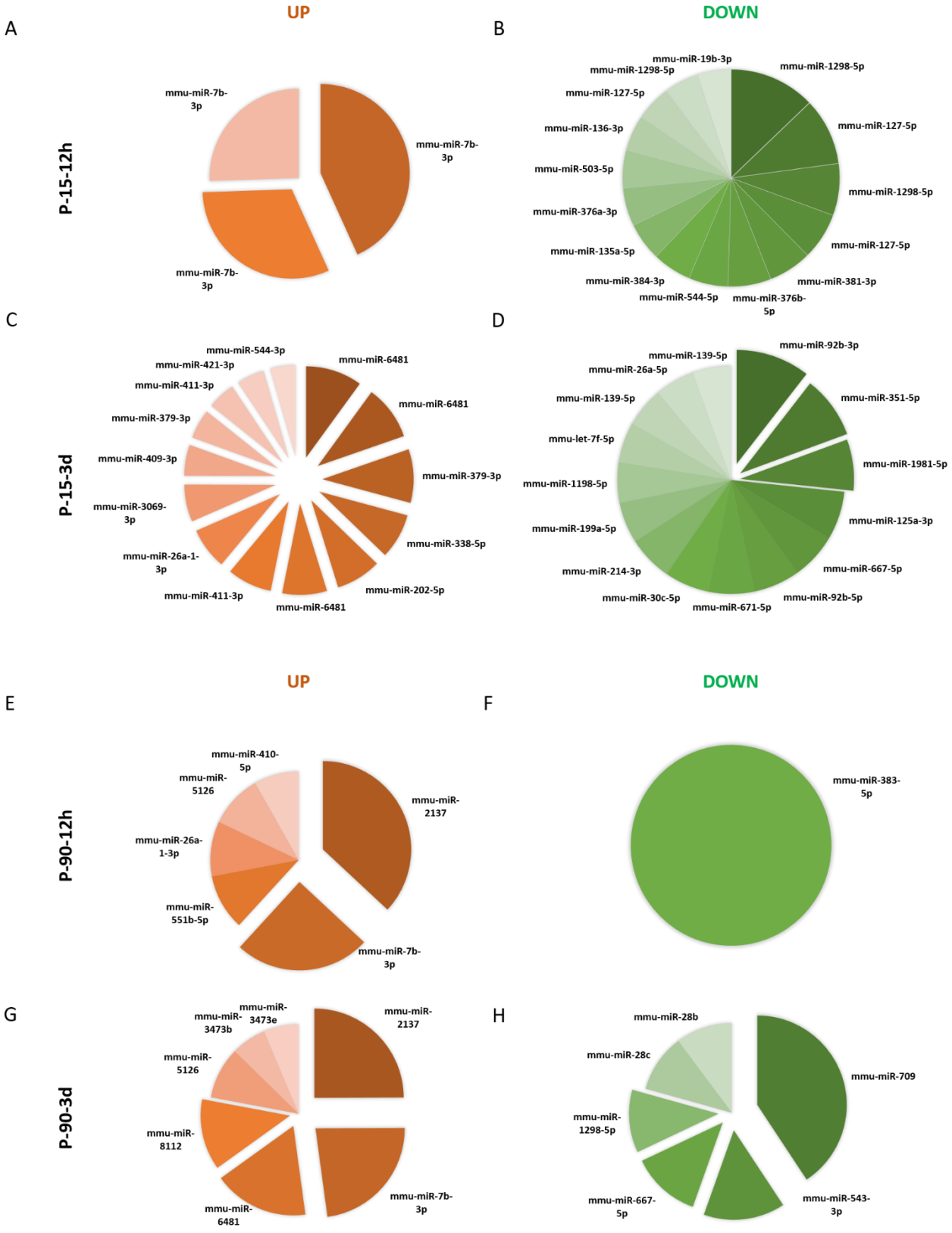

Figure 14: miRNA sequencing profile. A-D) miRNAs predicted by sequencing in P-15-12h and P-15-3d groups. E-H) miRNAs predicted by sequencing in P-90-12h and P-90-3d groups. The miRNA lists in the pie charts is referred only to those miRNAs with a log_2 fold change > 0.5 (the amplitude of each pie chart clove)

miRNA functional analysis-1

In order to understand possible functional connections among the miRNAs differentially expressed by the sequencing, first of all, we analysed miRNA intersection within each group or among them. As shown by Venn diagram (Figure 15 A), four different miRNAs were shared between two groups (miR-5126, miR-1298-5p, miR-6481 and miR-26a-1-3p), whereas miR-7b-3p was shared among three groups: indeed it was found in both adult and in P-15-12h groups. These results suggest that these small RNAs could exert functions related to the injury independently from the age of animals.

A

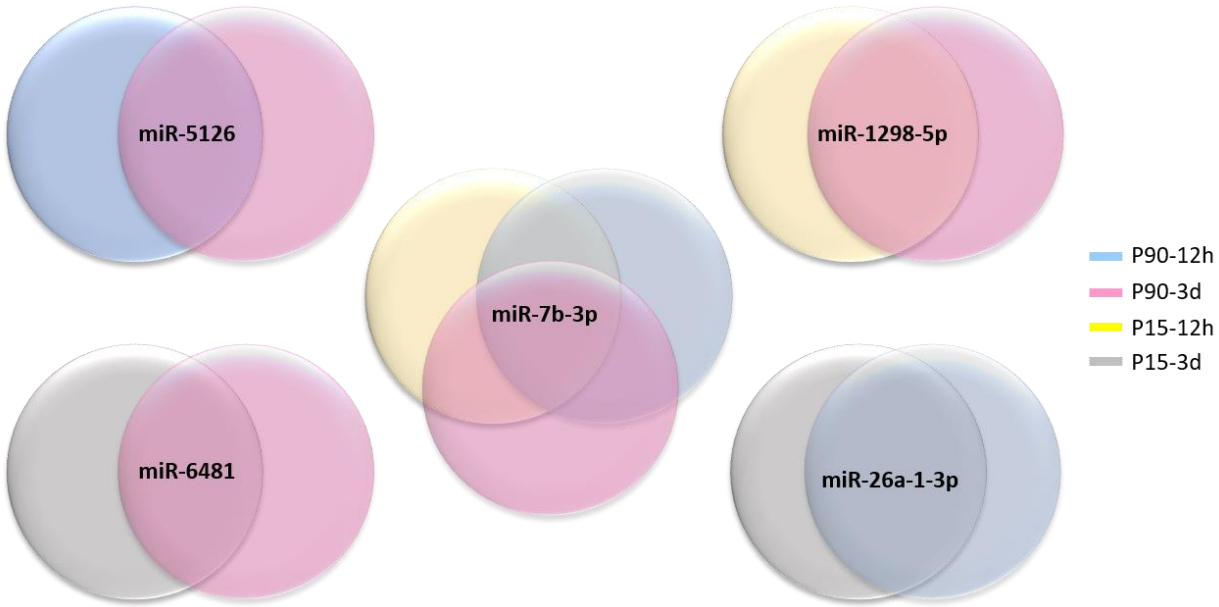

Figure 15: A) miRNA Venn diagram. Four miRNAs are shared between two groups (miR-5126, miR-1298-5p, miR-6481 and mir-26a-1-3p), while miR-7b-3p is the only one found in both adult and P-15-12h groups

Secondly, for each group we tried to identify functional networks specific for neural KEGG, GOBP or GOCC enriched annotation terms (Figure 16 A). miRNet tool generated three different networks for P-15-12h, P-15-3d and P-90-3d, but none of them with a significant p-value, indicating apparently independent function among miRNAs of the same group.

A

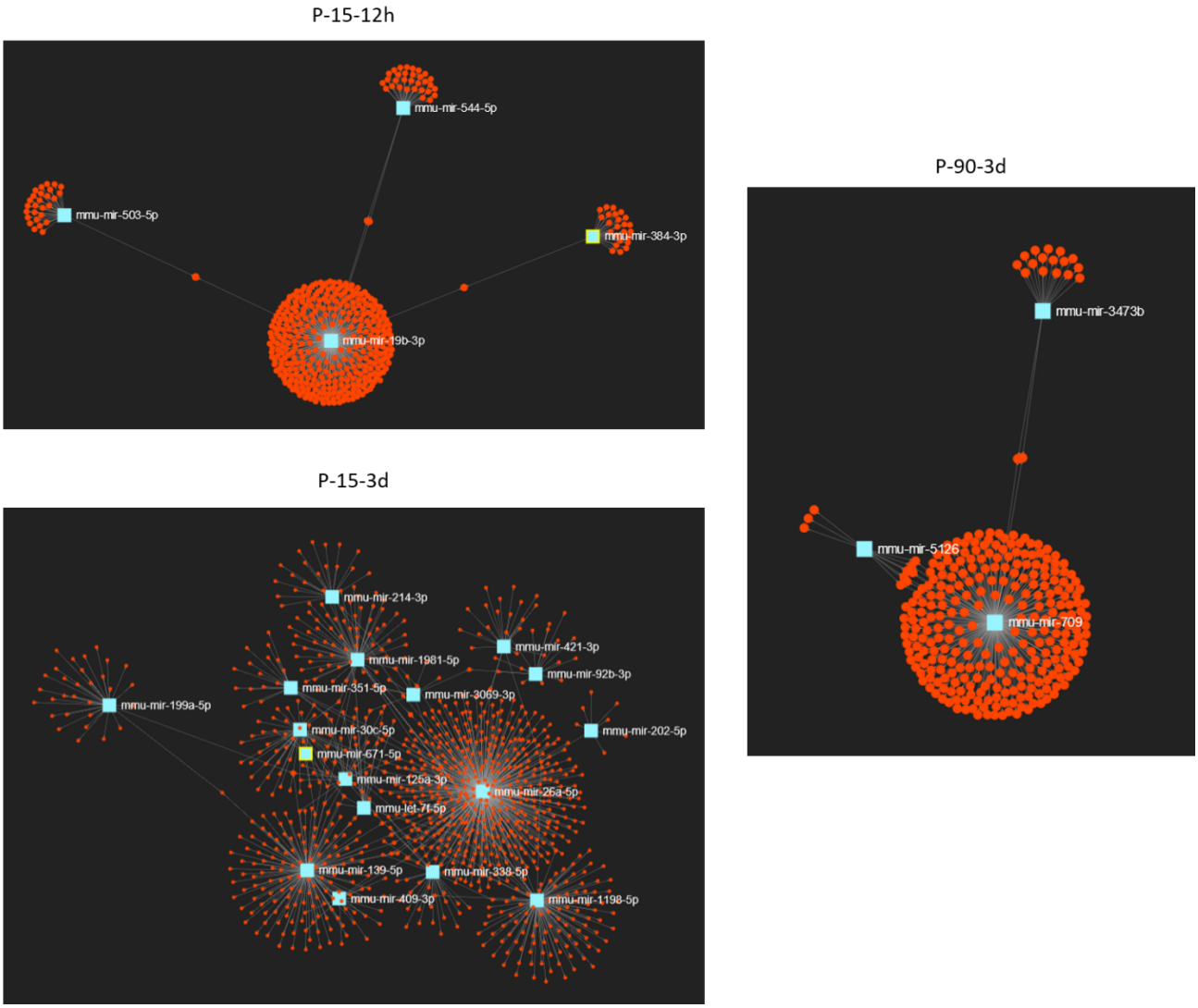

Figure 16: A) miRNA networks generated by miRNet algorithm for KEGG, GOBP and GOCC, p-value not significant

miRNA functional analysis-2

For understanding the role of miRNAs predicted to be differentially expressed by the sequencing, we screened the literature using both Pubmed and miRpub, a specific database collecting miRNA publications. In particular we focused the attention on those miRNAs that could be related to neurite/axon outgrowth during development and following a lesion, or specifically related to SCI. Six miRNAs (mir-7b-3p, miR-338-5p, miR-19b-3p, miR-127-5p, miR-381-3p and miR-214-3p), with a $\log_2$ fold change ≥ 0.5, have been selected (Table 1), since apparently connected with neurite/axon outgrowth; moreover only three miRNAs (miR-7b-3p, miR-127-5p and miR-214-3p) were already known in SCI field. However, the functions listed in Table 1 often refer to different members of the same miRNA family, suggesting that

miRNA roles reported could be different. Validated target genes reported in miRWalk database were found for all of these miRNAs with the exclusion of miR-7b-3p. Since miRNA sequencing is only a prediction, miRNAs in Table 1 were further analysed by RT-PCR to confirm their differential expression in SCI compared to SHAM condition.

Table 1: miRNA functional analysis by miRpub, PubMed and miRWalk. In the second column, log_2 fold change is reported for each miRNA. Abbreviations: OL=oligodendrocytes, PD=Parkinson's disease, AD=Alzheimer's disease, NP=neural precursors, ALS=amyotrophic lateral sclerosis. In orange miR-7b-3p and miR-338-5p predicted to be upregulated; in green miRNAs predicted to be downregulated

	Log_2 FOLD CHANGE	EXPERIMENTAL GROUP (S)	FUNCTIONS	REFERENCES	miRWalk VALIDATED TARGET (S)
miR-7b-3p	0.67 1.52 1.89	P-15-12h P-90-12h P-90-3d	• Cerebral cortex development • Neurite outgrowth • Synaptic formation • OL specification • PD, Schizophrenia and SCI pathogenesis	• Chen H et al., 2010 • Pollock A et al., 2014 • Liu J et al., 2012 • Zhao X et al., 2012 • Doxakis E et al., 2010 • Beveridge NJ et al., 20120 • Liu NK et al., 2009	No validated targets
miR-338-5p	0.89	P-15-3d	• Cortical placement and polarity • Neuronal outgrowth • Ischemic stroke and ALS marker • OL differentiation	• Kos A et al., 2017 • Kos A et al., 2017 • Peng G et al., 2015 and De Felice B et al., 2014 • Zhao X et al., 2010	36 validated targets
miR-19b-3p	0.50	P-15-12h	• NP specification • Age associated • Axonal-neurite outgrowth • PD and ALS pathogenesis • OL regulation	• Barca-Mayo O and De Pietro Tonelli D, 2014 • Hackl M et al., 2010 • Zhang Yi et al., 2013 and Kye MJ et al., 2011 • Hu X et al., 2015 • Wang Y and Yang GY, 2013	298 validated targets
miR-127-5p	1	P-15-12h	• Regulator of inflammation in SCI • Neurite outgrowth • Memory function	• Liu Nk et al., 2009 • He QQ et al., 2016 • Chen Z et al., 2015	1 validated target
miR-381-3p	0.65	P-15-12h	• Neuroplasticity network • Regulation of dendritic outgrowth • Synapse formation/maturation	• Tapocik JD et al., 2013 • Favre G et al., 2012 • Wu H et al., 2010	1 validated target
miR-214-3p	0.58	P-15-3d	• Early neurogenesis • Dendritic development • PD and AD pathigenesis • Downregulated in PNI • Neurite outgrowth • Neuronal apoptosis in SCI	• Mellios N et al., 2017 • Irie K ey al., 2016 • Dong H et al., 2016 and Mallick B and Ghosh Z, 2011 • Zhang HY et al., 2011 • Chen H et al., 2010 • Liu J and Wu Y, 2017	24 validated targets

miRNA validation by RT-PCR

The RT-PCR analysis revealed that all the miRNAs predicted to be downregulated by the sequencing (i.e. miR-19b-3p, miR-127-5p, miR-381-3p and miR-214-3p) and miR-338-5p predicted to be upregulated were no differentially expressed between SHAM and SCI group (Figure 17 A). On the other hand, a significant upregulation of 2.28 ± 0.37, 2.57 ± 0.85, and 9.8 ± 3.01 times was observed for miR-7b-3p in SCI P-15-12h, P-90-12h and P-90-3d respectively (Figure 17 B) compared to controls, as predicted by the sequencing. Although it was not predicted by the sequencing, we decided to evaluate miR-7b-3p expression also in P-15-3d group: by RT-PCR analysis, we found that its expression level was 6.16 ± 2.02 times higher in SCI mice compared to SHAM group (Figure 17 B). This result suggests that miR-7b-3p could exert a specific role connected to SCI condition independently of animal age and time after lesion.

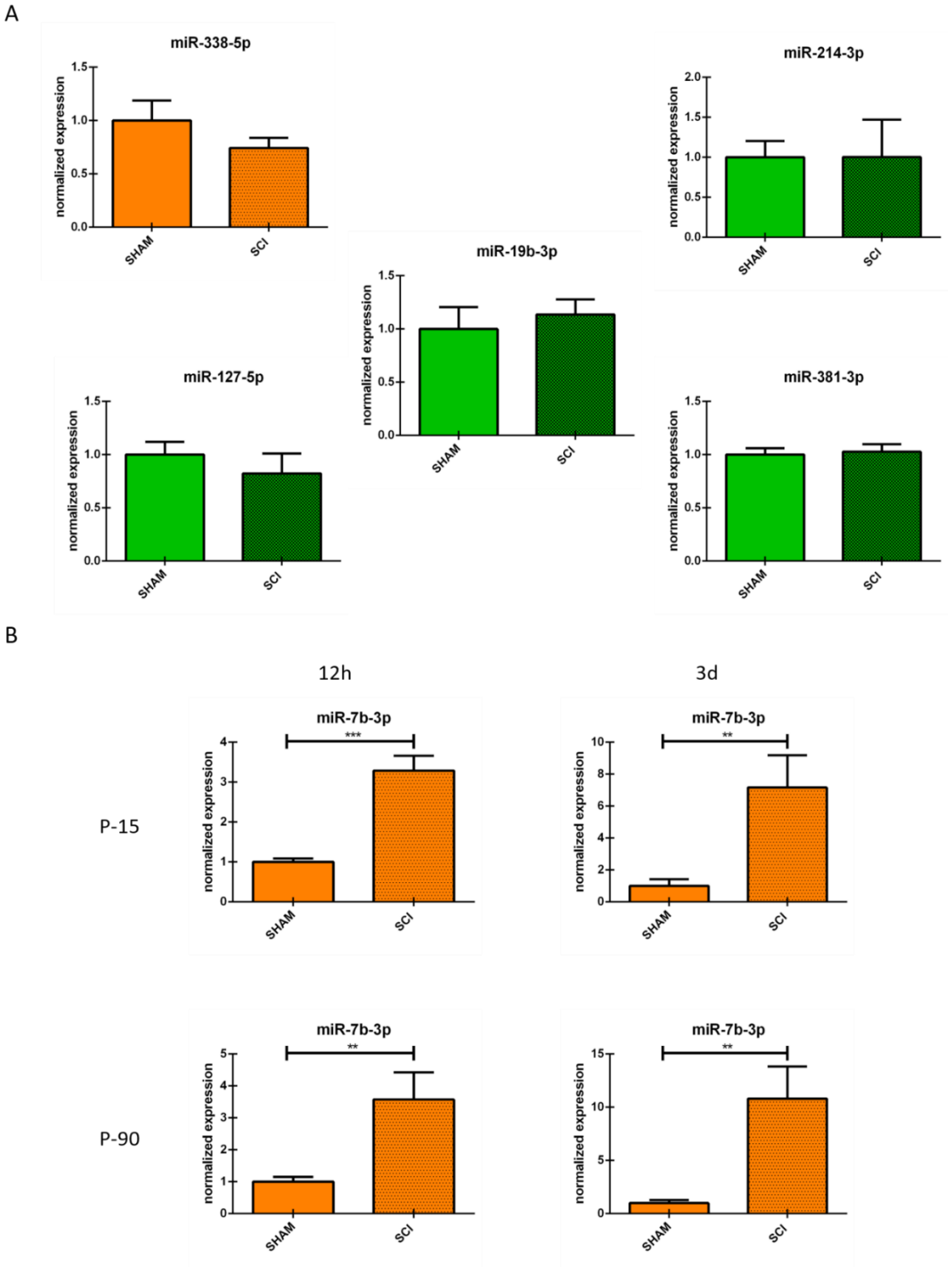

*Figure 17: A) The downregulation of 5 miRNAs predicted by the sequencing was not confirmed by RT-PCR; B) miR-7b-3p upregulation in all SCI groups was confirmed by RT-PCR. The graphs express miRNA normalized relative expression values ± SEM (*** p < 0.001; ** p < 0.01)*

MiR-7b-3p physiological expression and its putative function

We decided to focus the attention on miR-7b-3p in order to understand its function in SCI. Consistently with the literature, we decided to first evaluate if miR-7b-3p could be related to the axon growth during cortical neuron development, a function that could be reactivated after SCI. Therefore, we used an *in vitro* system to mimic three different time points, DIV-1-7-18, corresponding to the undifferentiated neuron stage, dendritogenesis beginning stage, and mature neuron stage respectively (Figure 18 A). As shown in Figure 18 B miR-7b-3p expression is quite constant during time with a slight increase at DIV-18, further suggesting its specific reactivation only after SCI.

Since no validated targets are known for this miRNA, we performed a functional analysis based on putative targets predicted by 1) miRWalk algorithm or 2) miRWalk intersection among 12 different databases. We considered only genes predicted by at least 6 databases for DAVID 6.7 upload. In the first case, different KEGG and GOBP neuronal related functions (mainly connected to axon cytoskeleton, neural development and apoptosis) showed a significant p-value (Figure 18 C "KEGG-miRWalk" and "GOBP-miRWalk"). In the second case, only two KEGG neuronal functions (axon guidance and regulation of actin cytoskeleton) reached statistical significance (Figure 18 C-"KEGG-DAVID") suggesting that miR-7b-3p could be related to these functions.

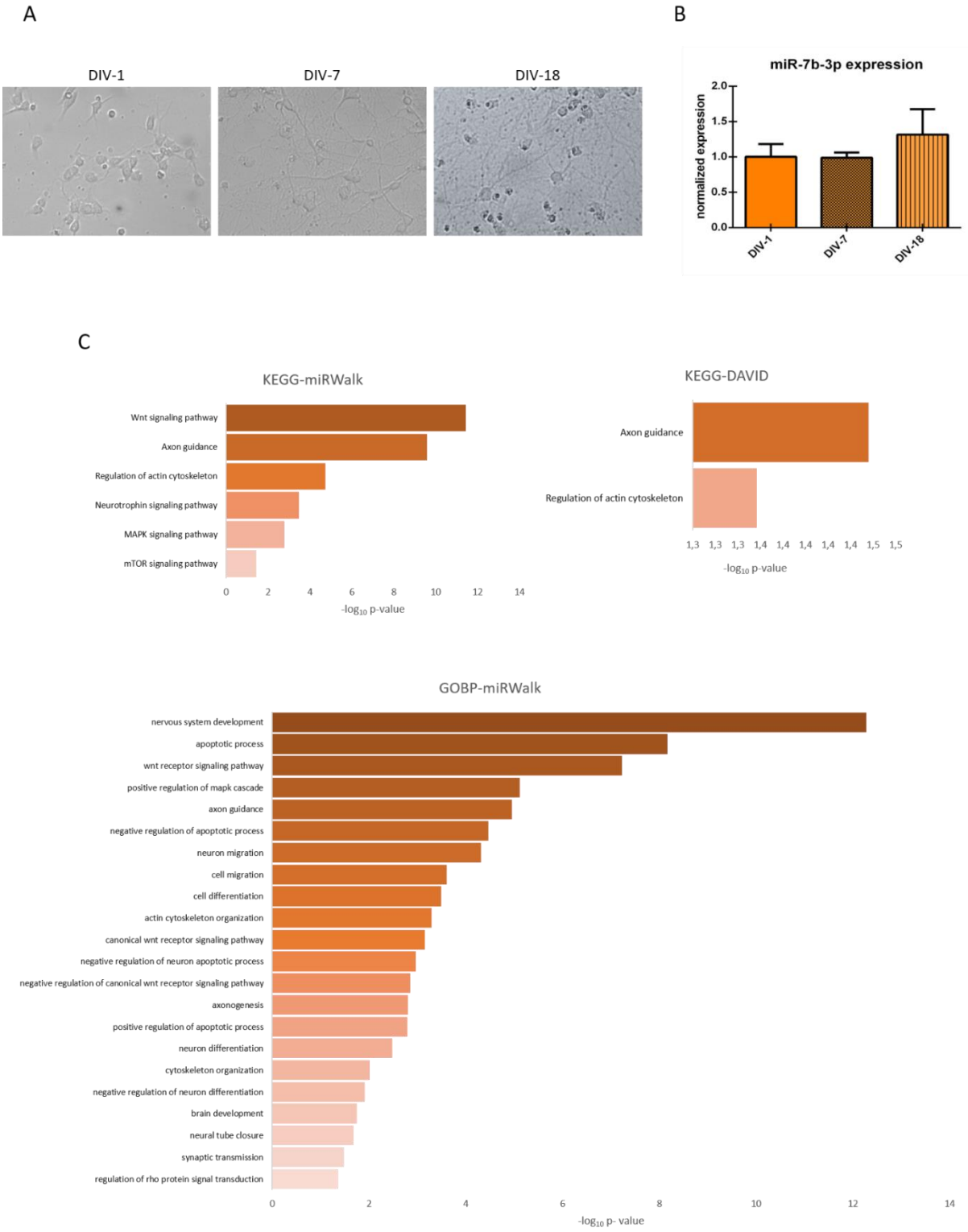

Figure 18: miR-7b-3p expression and functional analysis. A) developing in vitro cortical neurons, DIV-1 undifferentiated neuron stage, DIV-7 dendritogenesis stage, and DIV-18 mature neuron stage; B) miR-7b-3p expression at DIV-1-7-18 presented as normalized relative expression value compared to DIV-1; C) enriched annotation terms with a significant p-value analysed by miRWalk and DAVID 6.7 (values expressed as -log$_{10}$ p-value)

miR-7b-3p role during cortical development

To further analyse miR-7b-3p function, we studied the morphological phenotype of cortical neurons that overexpressed this miRNA. As shown in Figure 19 A cells transfected with miR-7b-3p mimic showed an upregulation of 3.05 compared to the negative control transfected cells. However, miR-7b-3p overexpression did not change the axon length and the number of dendrites as shown by comparable results in Figure 19 A and B. These results suggest that miR-7b-3p is not involved in axon and dendrite growth during cortical development.

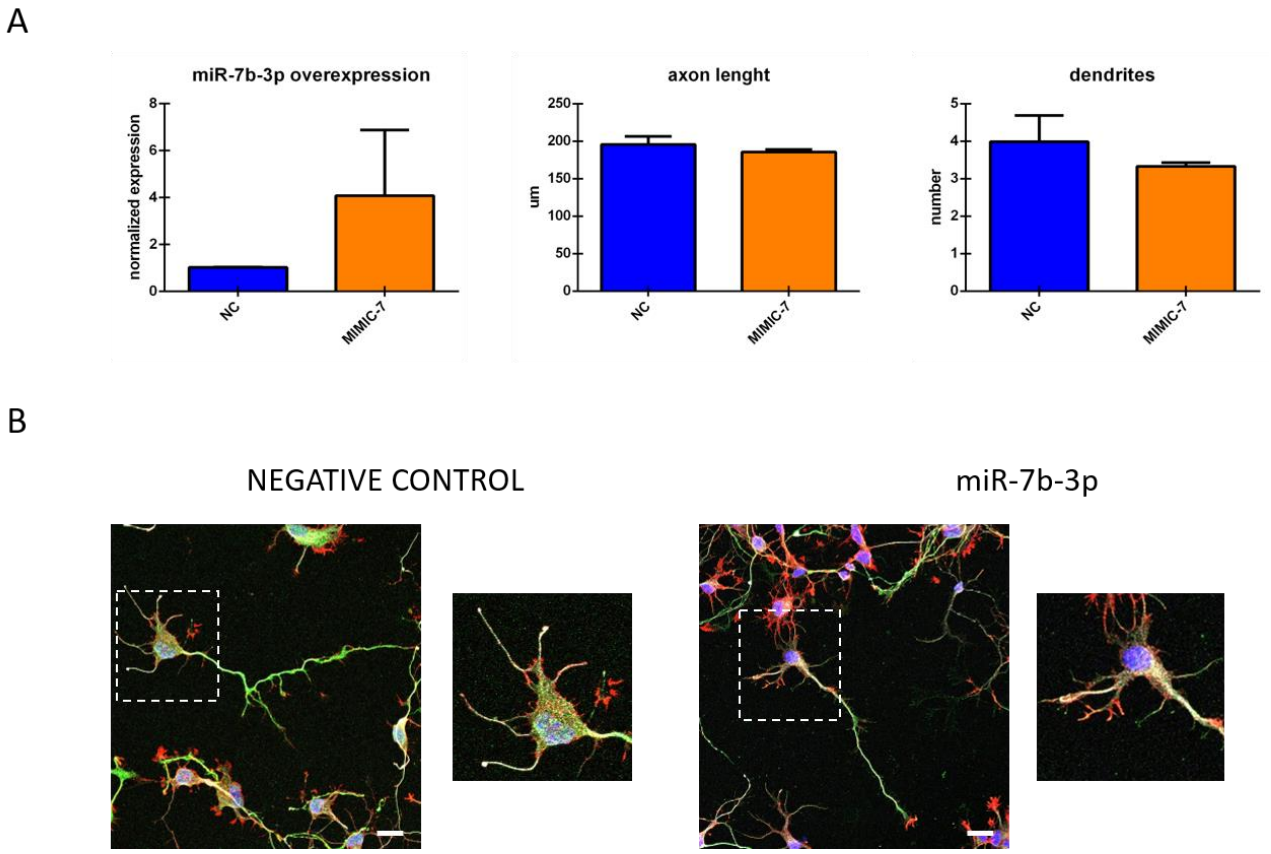

Figure 19: miR-7b-3p overexpression: A, miR-7b-3p overexpression and measurement of axon length and number of dendrites. B, comparable axon length and number of dendrites in NC (negative control) and mimic-7b-3p electroporated cells. Scale bars: B, 20 µm

2.10 DISCUSSION

We have investigated the miRNA profile in SCI condition in order to identify specific miRNAs involved in the axon regeneration process. In particular we focused on the sensorimotor cortex of young and adult mice, for evaluating the expression changes in the CSMNs, the main cells affected by SCI. Due to the low efficiency of single CSMN collection, we decided to perform a next generation sequencing of the entire sensorimotor cortex to evaluate miRNA dysregulation both at 12h and 3d after SCI. The only miRNA (mir-7b-3p) significantly upregulated after SCI in all the evaluated conditions was further analysed for better understanding its role after injury and eventually for therapeutically targeting it.

Labelling and collecting CSMNs by FACS

In the last years, the big challenge of axon regeneration failure after SCI encouraged the investigation of miRNAs as powerful inner regulatory system. Indeed, miRNA dysregulation after SCI is one of the most interesting and still poor understood mechanism involved in axon regeneration. In SCI several microarray analysis already revealed specific and aberrant miRNA expression patterns (Ziu M et al.,2013 and Yunta M et al., 2012) (Liu et al., 2009). However, the majority of these works have focused their analysis on the spinal cord tissue where different types of cells and fibers are present, and have associated miRNA function to different molecular cascades and mechanisms activated by SCI (Nieto-Diaz M et al., 2014). Among them, the miRNA role in axonal regeneration is still far to be elucidated. The current strategies (employing shRNA, antibodies, antagonists and knockout system) are only partially functioning, likely due to unknown upstream and downstream pathways and to the complexity of a convergent system in which the regrowth is likely regulated by several miRNAs. Known miRNAs involved in axon regeneration are still a few number, with only predicted targets. Moreover, single-cell miRNA profile analyses are generally carried out by microarray for a specific set of miRNAs: however, in this way a global view of the entire miRNA profile is lost and a possible enrichment in miRNAs not yet annotated is not possible.

Here we proposed a different approach, namely a miRNA profile generated from CSMNs located in the layer V of sensorimotor cortex. Indeed, CSMNs are the main cells affected by SCI whose axon transection is responsible of the sensorimotor deficits. The identification of specific CSMN-miRNAs firstly transcribed and maturated in the cell body (cortical layer V) and then transported to the spinal cord could precociously reveal essential miRNAs able to selectively regulate the axon

regeneration process. Therefore, in order to analyse the miRNA profile of the CSMNs, we tried to specifically label and collect these cells from the sensorimotor cortex. Since there are no markers to selectively label CSMNs (Arlotta et al., 2005), we employed GLMs and RLMs, retrograde tracers particularly suitable for their intrinsic properties. Indeed they do not diffuse far from the injection site (at spinal cord level), assuring the selective labelling of the cell of interest, and they run quite fast reaching the CSMN cell body (Vercelli et al., 2000) in one week. As also shown by other authors, GLMs and RLMs were found in the layer V of sensorimotor cortex when injected in the dorsal tract of the spinal cord (where CSMN axons are located), confirming the efficacy of this labelling technique (Arlotta et al., 2005; Catapano et al., 2004). However, despite the labelling success, we were not able to collect a sufficient amount of CSMNs by FACS due to several technical problems. First of all, a very small number of CSMNs were GLM/RLM-positive: indeed, although only 10 cortices were employed, we estimated that the minimum number of animals necessary to guarantee a sufficient cell collection was too high (around 50) to proceed with this technique. Moreover CSMNs are fragile cells, and the dissection/dissociation protocols could have considerably affected the cell viability and so the final amount of cells. Finally, it should be considered that cortical cells reside in an tangled network of different neural cells, ECM and myelin both at P-17 and, even more, at P-97. Therefore, different strategies like myelin removal during the dissection step or specific neuronal dissociation kit to obtain more purified samples have been employed. However, probably due to the compactness of tissue structure, a huge amount of myelin debris was always present. Altogether these technical issues probably justified the extremely low percentage of positive sorted cell, i.e. 0.2% at P-97 and 0.4% at P17.

Labelling and collecting CSMNs by LCM

We also considered another technique to reach the same goal: the employment of the laser capture microdissection (LCM) as a valid alternative to the FACS cell sorting. The LCM method allows the isolation of specific cells by the help of a laser under the direct microscope visualization of the region of interest. This approach has been successfully employed both in single-cell RNA-seq and miRNA profile analysis (Roncon et al., 2015; Zhang et al., 2013b). The main difference is that very low RNA quantities such as 17-20 ng of RNA extracted from 1500-2000 motoneurons by LCM are sufficient to perform a single-cell RNA profile. However, since miRNAs are very short RNA sequences, a sample of at least 500 ng of total RNA is generally required for a miRNA profile sequencing experiment (Zhang et al., 2013b). Therefore, considering the small number of GLM-

positive sections (3 each animal; also depending on the GLM/RLM injection efficiency), again an excessive number of animals should be employed to theoretically reach the RNA amount required.
A promising strategy that could solve the problem related to the number of CSMN labelled cells is the employment of a EGFP-CSMN transgenic mouse line. UCHL1-eGFP mice express the Enhanced Green Fluorescent Protein under the control of the *Uchl1* promoter specifically labeling CSMNs. However, the use of such transgenic mouse line would not overcome the intrinsic cell fragility and the low number of cells obtained by the dissection-dissociation protocol (Yasvoina et al., 2013). Therefore, it is evident that the optimization of the dissociation protocol from postnatal brain tissue is an essential requirement for a successful CSMN miRNA sequencing profile.

SCI model

Consistently with the negative results obtained by a single-cell approach, we evaluated an alternative solution, collecting the whole layer V of the sensorimotor cortex In order to evaluate the altered expression of miRNAs after SCI, we chose a transection model to completely disconnect the sensorimotor cortex and the spinal cord. This type of lesion is quite infrequent in humans where the majority of SCI cases are caused by a spinal cord compression: however, the transection model is recognized as the most suitable one to study the axon regeneration process (LJ, 2005) and so the best model to investigate miRNAs selectively involved in this mechanism.
Moreover, it should be noticed that while in primates the motor control is mainly regulated by CSMNs, in rodents the extra-pyramidal tracts play a consistent role that is not comparable to the humans. Such a difference needs to be considered in the interpretation of the results here obtained.
With regard to the SCI groups, we decided to investigate both adult and young mice at two different time points, 12h and 3d after SCI. At P-90 the nervous system is considered completely mature and less plastic compared to P-15 when neuronal networks are still arranging. Therefore, the comparison between these two different systems could also highlight differences in miRNAs age-related. On the other hand, despite cortical tissue from younger mice could be easily dissociated, we also chose P-90 age, considering that SCI mainly occurs in adult people. Moreover, the time points considered are specifically connected to the acute phase of SCI when the lesion is not yet stabilized and a therapeutic intervention could be more efficacious.

Neural apoptosis and inflammation

In order to better understand the miRNA expression profile following injury, we firstly characterized possible changes in the sensorimotor cortex of the SCI mouse model here employed in terms of apoptosis and inflammatory reaction. Indeed at the spinal cord level a consistent motor neuron degeneration and an increased neuroinflammation have been extensively described (Dumont et al., 2001). At the cortical level, we did not reveal any sign of suffering cells both in sensory and motor cortex of SCI mice. The survival of cortical motor neurons axotomized is quite controversial in literature: some authors report the presence of apoptotic neurons in the primary motor cortex (Hains et al., 2003; Lee, 2004), while others did not observe any change in the number of pyramidal neurons (Brock et al., 2010; Nielson et al., 2010; Wannier et al., 2005). The absence of apoptotic neurons at cortical level can be explained by the fact that longer is the distance between the cell body and the axon, more unlikely is the activation of the apoptotic process. Moreover, spared collaterals rostral to the injury site, trophic factors released by other cortical cells and new connections forming after SCI may support CSMN survival (Nielson et al., 2010).

Despite the absence of degenerating CSMNs, it was possible to observe an increased microglia activation (IBA-1 positivity) in the sensorimotor cortex of SCI mice, in particular in the P15 groups. Notably, in all the groups analyzed, we also observed an evident alteration of the cell morphology: indeed both ramified and amoeboid macrophages were present in SCI cortex and absent in the control mice. At the spinal cord level microglia activation is described to have both a beneficial and a detrimental role, partly protecting motor neurons but also impeding the regeneration of their axons (Gensel and Zhang, 2015). Therefore, consistently with this idea and with a well-known cortical reorganization occurring after SCI (Freund et al., 2012; Oudega and Perez, 2012), the observed microglia activation at cortical level, could reflect a double role of these cells, maybe partly protecting CSMNs cells and partly impeding their regeneration.

miRNA sequencing profile of the SCI sensorimotor cortex

By isolating the whole sensorimotor cortices, we obtained a sufficient amount of RNA to perform the following analysis. In collaboration with the group of Prof. Dalmay (Univ. of East Anglia; Norwich, UK), we performed the library construction with a recently developed technique (Sorefan K et al., Silence, 2012 and Xu P et al., Methods Next Generation Seq, 2015). This new method employs high definition (HD) adapters with degenerate tags at their end that, binding to 5’ and 3’ miRNA extremities, allowing the formation of stable secondary structures for more sequences and a

reduction of RNA ligase-dependent sequence bias. In this way sequencing bias in biological samples can be reduced and the representation of low abundance miRNAs can increase, allowing the identification of previously unknown miRNAs. The library was sequenced by The Genome Analysis Centre (Norwich, UK) on a Hiseq 2500 machine. The data were then analysed by the Dalmay group in order to identify miRNA up- and downregulation in SHAM and SCI condition. The same group performed the bioinformatic analysis with the UEA Small RNA Workbench software, especially developed for miRNA data analysis from High-throughput sequencing devices.
For all the groups considered, the sequencing has generated a list of miRNAs potentially dysregulated in SCI cortex. First of all, some miRNAs (such as miR-7b-3p) were reported more than once in the same group (Figure 14): this repetition is due to the fact that slightly different sequences have been attributed to the same miRNA name. Therefore, we chose the sequence with the more abundant number of reads as the most valid one, like in the case of miR-7b-3p.

miRNA functional analysis and validation

Since miRNAs are emerging as a complex network of interacting components known to potentially regulate all the molecular pathways (Ghibaudi et al., 2017; Pons-Espinal et al., 2017), we evaluated the presence of a functional miRNA network after the lesion with particular relevance to those genes related to neuronal functions. However, miRNet did not reveal any significant interaction, suggesting that there is no a direct link among miRNAs of the same group. Indeed, even if some neuronal genes were shared among miRNAs, the interaction was not statistically significant. However, it is known that a miRNA network can be considered as a convergence on targets and pathways, but also as a convergence on functions (Barca-Mayo and De Pietri Tonelli, 2014) (Ghibaudi et al., 2017). Therefore, we selected a list of miRNAs that, based on the literature and on validated targets, were potentially implicated in axon growth and regeneration. Indeed, these miRNAs could be related to an axon regeneration programme and so reactivated after injury. Consistently with this idea, among the miRNAs predicted to be up/downregulated, we validated mir-7b-3p, miR-338-5p, miR-19b-3p, miR-127-5p, miR-381-3p and miR-214-3p by RT-PCR. Only miR-7b-3p, the only one miRNA predicted to be up-regulated in 3 SCI groups (P-1512h and P-90 12h-3d), was confirmed to be overexpressed in all SCI conditions with respect to the SHAM groups.
Such a discrepancy between sequencing results and RT-PCR could be explained in different ways. First of all, a sequencing experiment is only a prediction that is generally considered reliable only when validated by RT-PCR/western blot. Moreover, it is known that cluster of genes/proteins

implicated in neuronal plasticity are downregulated one day after SCI followed by a coordinated recovery after one-two weeks (Di Giovanni et al., 2005). Therefore, a miRNA network could be activated in a subsequent period compared to the time points (12h and 3d) here analysed. However, already one week after SCI the glial scar is completely formed thus stabilizing the lesion and rendering any therapeutic interventions less efficacious: for this reason and for our therapeutic purposes, the identification of miRNAs in the first phase after injury represents the best time point in order to eventually target them and modulate their dysregulated action.

It should be also considered that among all the miRNAs with a high/low $\log_2$ fold change value, we selected a pool of small RNAs that could be directly linked to an axon regeneration programme. In this way, we excluded some miRNAs whose sequencing values could have also reflected a real up/downregulation and whose role is beyond the purpose of this thesis.

Although miRNA mechanism of action should be considered in a network system, here we propose to understand the role of one of its component, miR-7b-3p, whose function need to be integrated in a more complex view.

miR-7b-3p

The focus on miR-7b-3p derives on the consistent literature describing miR-7 function both in normal brain and neurological diseases. Indeed, miR-7b-3p belongs to the evolutionary conserved miR-7 family that counts multiple miR-7 genes. In particular in human, there are three different independently regulated miR-7 genes, suggesting its important function during the course of evolution. miR-7 role has been described during development and normal function of different organs (pancreas, heart, skin) with a particular enrichment profile in brain (Horsham et al., 2015). However, its implication in neuronal development and differentiation is still quite controversial. A miR-7 increased expression seems to occur spontaneously during mouse cortical neuron differentiation and postnatal cortical development *in vitro* (Chen et al., 2010). Moreover when miR-7 is overexpressed in cortical neurons *in vitro*, it decreased neurite outgrowth (Chen et al., 2010), suggesting its possible functional involvement in axon growth during development. To confirm this hypothesis, miR-7 depletion in embryonic cortex resulted in reduced neurogenesis and microcephaly (Pollock et al., 2014), confirming its important role during development. On the other hand, some authors did not report any change in miR-7 expression during development and in one case a significant downregulation was observed in human neural stem cells (de Chevigny et al., 2012; Stevanato and Sinden, 2014).

miR-7b-3p functions during development

Consistently with these evaluations, the role of miR-7b-3p upregulation that we observed after SCI required further investigations, especially considering that no validated targets are known for this miRNA: we hypothesized that miR-7b-3p increased expression after SCI could represent an attempt in reactivating a ”quiescent” embryonic molecular program aimed at sustain axonal regeneration.

Firstly, it should be noticed that, although different members of the same family are generally described to have similar functions, none of the miR-7 members described in literature present the same sequence of miR-7b-3p. Moreover, since the functional analysis on the predicted targets conducted both by miRWalk and DAVID 6.7 revealed an enrichment in genes associated with neural development, axon guidance and cytoskeletal regulation, we decided to firstly evaluate this hypothesis. Indeed, it is known that the injured adult CNS re-expresses genes and activates pathways that are observed during development (Emery et al., 2003).

However, in our experiments, miR-7b-3p *in vitro* expression at DIV-1, -7 and -18 (the *in vitro* time points resembling the main neuronal developmental steps) did not increase during time, even if a slight tendency is visible. Indeed, it should be considered that the measure of miR-7b-3p expression has been performed with respect to DIV-1 and not to a control condition.

Also miR-7b-3p overexpression in primary cortical neurons *in vitro* did not affect neither axon length nor the number of dendrites. These results indicate that miR-7b-3p is not involved in neural cortical development, thus suggesting that its overexpression *in vivo* after SCI could be directly related to the lesion.

Indeed, we evaluated the miR-7b-3p expression *in vitro* on “healthy” neurons that were not subjected to any injury and so they were not forced to a rearrangement of gene expression as probably required to increase the level of miR-7b-3p after a trauma. Despite the dissection procedure consists in the detachment of cortical cells from their anatomical position, this does not imply damage to axons and dendrites: this is evident considering that primary hippocampal and cortical neuron cultures have been historically employed to in vitro study and reproduce the developmental processes of axon and dendrite formation in the brain cortex (Dotti et al., 1988; Sakakibara and Hatanaka, 2015). Moreover, the laser axotomy technique directly applied on primary cortical neurons has been recently employed to study the intrinsic regenerative ability of CNS axons (Koseki et al., 2017): this means that a laser axotomy procedure is fundamental to produce a specific damage to the axons of cortical neurons harvested by a primary dissection.

For these reasons, we intend now to verify our hypothesis (miR-7b-3p elevated level after a trauma) using an *in vitro* model of axotomy. This could definitely clarify the miR-7b-3p function in case of pathological conditions, since evidence from the literature is still lacking.

miR-7b-3p functions after SCI

Mir-7 functions are described only in Parkinson's disease and Schizophrenia: in the first case, it seems to reduce the level of α-synuclein in transfected cortical neurons thus suggesting a potential neuroprotective effect for miR-7 (Doxakis, 2010); similarly, miR-7 overexpression in blood samples of schizophrenia patients has been associated with low level of SHANK3 protein and the consequent alteration of neuronal morphology and function (Zhang et al., 2015).
With regard to miR-7 in SCI condition, also in this case its role is quite unexplored and still poorly understood. Indeed contrary to what we observed, a miRNA microarray on the spinal cord tissue of SCI contusive rats revealed a downregulation of miR-7a until 7 days after the lesion (Liu et al., 2009), without giving an explanation for its function. However, another member of the same family, miR-7-1, has been described to potentiate the effect of the estrogen receptor agonists thus promoting a functional neuroprotection of motor neurons *in vitro* (Chakrabarti et al., 2014): the authors described a potentiation of the anti-apoptotic effect and an inhibition of pro-apoptotic genes, a functional class that we observed to be enriched in miR-7b-3p functional analysis. To further confirm this hypothesis, Pollock A and coll. demonstrated that miR-7 upregulation silenced the activity of apoptotic specific apoptotic genes, thus reverting the neurogenesis impairment and the macrocephalic phenotype connected to miR-7 depletion (Pollock et al., 2014).
Therefore, consistently with the absence of neuronal death we observed at cortical level, it could be hypothesized that the increased level of miR-7b-3p after SCI is related to a neuroprotective effect linked to a downregulation of apoptotic genes. To investigate this hypothesis, we will test whether miR-7b-3p overexpression can protect primary cortical neurons from apoptosis. In this case the validation of the targets related to apoptosis will clarify miR-7b-3p mechanism of action in this process.

In conclusion, we reported that miR-7b-3p is strongly upregulated in both young and adult SCI sensorimotor cortices at all the time points analysed compared to the SHAM groups. However, mir-7b-3p normal expression during cortical development remained stable and its overexpression did not change the axon length and the number of dendrites, thus indicating that it does not play an

essential role during development. Moreover, this result suggests that miR-7b-3p upregulation is directly related to the SCI condition as also suggested by the functional analysis of its targets. Therefore, starting from the putative targets and on the neuroprotective role of other miR-7 members, further analyses are required to elucidate miR-7b-3p functions after SCI both related to axon growth and apoptosis.

CHAPTER 3: BIOMATERALS IN SCI

Biomaterial scaffolds can be divided in two main classes each of them with its specific properties: natural and synthetic scaffolds.

3.1 NATURAL SCAFFOLDS

Natural scaffolds present high biocompatibility and functionality compared to the synthetic scaffolds that in turn exhibit a great mechanical strength and flexibility in manipulation. As listed in Table 2, eight natural compounds, mainly made of carbohydrates or proteins, are generally used as scaffolds for animal SCI models.

- *Alginate*: it is a linear polysaccharide commercially available, extracted from brown algae or derived by bacterial biosynthesis. In particular it is an anionic polymer composed of (1→4) linked β-D-mannuronic acid and α-L- glucuronic acid residues that has been extensively used for different biomedical applications due to its favourable properties of biocompatibility, bio-resorption, low toxicity, relatively low cost and ease of gelation by the addition of divalent cations. Alginate can be used in the formulation of microcapsules and hydrogels to fill the damage spinal cord or as a vehicle for drugs, growth factors and cells. Indeed, alginate sponge or hydrogels have been employed to physically directing regenerating axons functioning as a bridge also in combination with growth factors or stem cells (Kim M, Park SR, 2014; Lee and Mooney, 2012) (Ansorena et al., 2013; Hosseini et al., 2016). However, some alginate disadvantages derive from its high degradation rate, cytotoxicity and immunogenicity.

- *Agarose:* as alginate, it is a linear polysaccharide derived from red algae but also a thermal gelling hydrogel. The structure of agarose consists of alternating units of β-d-galactopyranose and 3,6-anhydro-α-l-galactopyranose with different chemical composition. Changes in temperature allow agarose aqueous solution to reversely transit from solid to gel, the most prevalent conformation (Gasperini et al., 2014). Tubular agarose scaffolds have been employed to exploit both the possibility to release growth factor to the lesion site but also to guide the damaged axons towards a correct regenerative direction. This is the case of neurotrophin-3 (NT-3), BDNF and chondroitinase ABC delivery trough agarose scaffolds

into SCI rats supporting long-tract axon regeneration and functional recovery (Gao et al., 2013; Gros et al., 2010; Lee et al., 2010). Agarose hydrogels can be filled with different type of cells to improve their viability and delivery rate, also modulating the inflammatory response *in vivo* (Caron et al., 2016). However, agarose itself does not provide adhesion substrate for cells, so that supplementary adhesion molecules should be added to the scaffold. Moreover, its poor biodegradability limits the spontaneous repair process *in vivo* requiring specific modification before the injection.

- *Collagen:* this is one of the main component of the ECM in mammals that represents 25-30% of the total protein in human. In the uninjured spinal cord collagen is associated with proteins like fibronectin and laminin to form the perineuronal net, while in chronic SCI it is secreted from cells near and inside the injury. Due to its physiological presence in mammal cells, it has specific binding sites for cell adhesion thus supporting proliferation, migration and differentiation but also high mechanical strength typical to that of our tissue. In addition, is easy accessible, inexpensive and biocompatible and ca be employed in tubular, hydrogel or sponge configuration. For these reasons is one of the most used natural biomaterials initially proposed for the delivery of NGF, NT-3 and BDNF after SCI (Houweling et al., 1998a; Houweling et al., 1998b). Collagen can also support axonal growth and can be further functionalized to extend its regenerative ability. Several collagen configurations can be developed to support this capacity like for example artificial collagen filaments able to promote 3 mm axon extension in a complete transection rat model (Suzuki et al., 2015).

- *Hyaluronic acid:* as a natural polysaccharide of repeated units in linear structure (glucuronic acid and N acetylglucosamine) belonging to the glycosaminoglycan of the ECM, it is found in all tissues. Known to enhance peripheral nerve regeneration *in vivo*, it is suitable for different medical applications due to the fact that it is biodegradable, biocompatible, non-toxic and immunologically and chemically inherent. Among its features HA can strongly adhere to the host tissue and bridge the lesion but also prevent the inflammatory reaction: smaller lesion size, decrease inflammatory cells and scarring tissue and increased motor function have been observed in BDNF-HA hydrogel and in a HA hydrogel alone implantation in a spinal cord lesion rat (Kushchayev et al., 2016). However, cells do not show good adhesion on HA, so that surface modifications need to be applied to improve its efficacy. Another disadvantage of this compound consists of a high degradation rate and

weak mechanical property. For this reason, in some cases it is fused with other polymers to overcome its limits (Li et al., 2013a; Wen et al., 2016).

- *Fibrin:* it is a fibrous protein responsible of clotting blood that after injury is bound by cells helping them to perform different biological activities. In SCI studies, it has been widely used thanks to its biomimetic property, rapid absorption and feasibility to form aggregate gel *in vivo*. A fibrin scaffold loaded with growth factors and NSCs has been demonstrated to support long distance axon growth, synapses formation with host cells and functional recovery in a severe rat SCI model (Lu et al., 2012).

- *Chitosan:* it is a soluble product prepared by N-deacetylation of chitin, a family member of linear polysaccharides made of β (1→4) linked N-acetyl D-glucosamine and D-glucosamine units. Chitin can be extracted by three main sources: the exoskeleton of arthropods, shellfish, marine crustaceans and the cell wall of fungi. Chitosan is employed in several biomedical applications such as implantable orthopaedic and periodontal systems, wound-healing agents and engineering scaffolds for tissue repair. Its wide diffusion is due to its high biodegradability and biocompatibility, low toxicity and cost, and to its specific interaction with various biomolecules (ECM components or growth factors) thanks to the abundance of amino groups. *In vitro* and *in vivo* studies have demonstrated that it has biomimetic effects by itself in the peripheral nervous system where it promotes neural growth, cell adhesion and differentiation (Gnavi et al., 2013). Moreover, by acting as a bridge, it can fill the cavity of sciatic nerve injury, improving axon growth and functional recovery (Patel et al., 2006; Rosales-Cortés et al., 2003). However residual proteins derived by chitosan production can lead to some allergy and hypersensitivity phenomena (Gnavi et al., 2013).

  Thanks to its promising properties, its employment has been extended also to SCI preclinical studies. Chitosan channels and hydrogels were shown to prolong NSC survival, create a tissue bridge after complete spinal cord transection (Nomura et al., 2008), promote spinal tissue regeneration and glial scar reduction (Chedly et al., 2017a). Indeed, chitosan is known to increase the survival, differentiation and host neuron maintenance of NSCs, MSCs and radial glial cells when implanted in a lesion spinal cord (Gnavi et al., 2013).

  Recently, new chitosan membranes that combine chitosan properties with ECM like structures of nanofibers, have been developed in a modified formulation to enhance biocompatibility, thus better supporting cell function (Tonda-Turo et al., 2017a). Therefore,

new chitosan formulations are continuously produced to find the correct balance among all its properties.

Table 2: the main natural biomaterials used in SCI (modified by Kim m et al., 2014)

Natural biomaterials		Application for spinal cord repair	References
Agarose /Alginate	Encapsulation	Microencapsulation of hMSC or ChABC.	Barminko et al., 2011
	Tubular	Induction of long-tract axons with MSCs and NT-3 or BDNF.	Stokols et al., 2006; Gros et al., 2010; Lee et al., 2010
	Hydrogel	Local delivery of BDNF.	Jain et al., 2006
Chitosan	Tubular	Extra and intramedullary tissue bridge conduits with neural stem/progenitor cells or MSCs.	Nomura et al., 2008; Bozkurt et al., 2010; Chen et al., 2011
	Sponge	Laminin-incorporated nerve conduits.	Cheng et al., 2007
Collagen	Tubular	Using a collagen scaffold containing a collagen binding BDNF and an EGFR neutralizing Ab.	Liu et al., 2001; Spilker et al., 2001; Han et al., 2010
	Sponge	Transplantation of MSCs, Human ESC-derived neural precursor cells and olfactory ensheathing cells	Yoshii et al., 2004; Hatami et al., 2009; Deumens et al., 2013
	Hydrogel	Alignment of astrocytes in 3D collagen gel and axon stretch-growth technology.	Iwata et al., 2006; East et al., 2010
Fibrin	Hydrogel	Controlled release of NT-3 and PDGF from scaffolds containing NPCs. Transplantation of human umbilical MSCs and human BMSCs.	Itosaka et al., 2009; Johnson et al., 2010a-c; Zurita et al., 2010; Liu et al., 2013
Fibronectin	Hydrogel	Neurotrophin/drug delivery	Phillips et al., 2004
Hyaluronic acid	Hydrogel	Modified with nogo-66 receptor Ab and Poly-L-lysine or matrix metalloproteinase-sensitive.	Park et al., 2010; Wei et al., 2010; Khaing et al., 2011; Li et al., 2013

3.2 SYNTHETIC SCAFFOLDS

The main synthetic polymers used in SCI are essentially seven, listed in Table 3. They present two advantages compared to the natural scaffolds: i) they can be easily modified to obtain new mechanical and chemical properties; ii) they can be combined in different proportions to realize new biomaterials with unique features. However, as artificial materials the risk of immune reaction is higher than with natural scaffolds, so that their employment is limited.

- *Poly-lactic-co-glycolic acid (PLGA)*: it is one of the most commonly used biomaterials for diagnosis and medical applications thanks to its physicochemical properties. It is a biodegradable and biocompatible polymer that consists of two different monomers, the cyclic dimer of glycolic acid and lactic acid. Different PLGA can result from the polymerization process depending on the ratio of the two components: the higher glycolic

acid percentage, the lower degradation rate is required. The monomers released by its physiological degradation are non-toxic but can influence bending, swelling, deformation and permeability. Initially hydrogels and nerve conduits made of PLGA were used as delivery system in SCI, then also microsphere and nanoparticles were introduced to vehicle drugs (Goraltchouk et al., 2006; Yang et al., 2005). PLGA scaffolds have also been investigated as a method to deliver stem cells (NSCs and MSCs) with optimal results in terms of regeneration and functional behaviour. A combinatorial effect of PLGA scaffold and OECs to treat SCI has been shown by Wang C and co-workers, assuring greater locomotor recovery, axon myelination and neuron protection after SCI compared to PLGA alone (Wang et al., 2017a). However, one negative aspect that should be consider before clinical application is that PLGA degradation decreases pH environment with potential risks for the host tissue.

- *Poly-β-hydroxibutirate (PHB*): it is a bio-polyester of high molecular weight, present in short chains of monomer units in the plasma membranes of bacteria, in plant tissue and mitochondria, microsomes and membranes of animal cells. It is water insoluble and resistant to hydrolytic degradation and slowly converted in non-toxic metabolites, ultra-violet resistant and with a good oxygen permeability. These properties together with biocompatibility render PHB tubular conduit scaffolds useful to promote attachment, proliferation and survival of SCs supporting axonal regeneration (Novikova et al., 2008). However, its scarce mechanical properties do not make it the first choice for neural regeneration. For this reason, PHB modifications are employed to improve its properties for tissue engineering (Ribeiro-Samy et al., 2013).

- *Poly (2*-hydroxyethyl methacrylate)-pHEMA: it consists of cross-linked hydrophilic polymers that swelling in water form an hydrogel solution. pHEMA is the main component of contact lens thanks to its biocompatibility and physical properties that makes it ideal for medical applications. It is non-biodegradable thus avoiding the release of intermediate toxic products and it has low interfacial tension with biological fluids. The hydrogel formulation, with or without modifications, brings pHEMA closer to spinal cord tissue mechanical properties thus explaining its employment in SCI studies. Chemical modifications render pHEMA flexible and easy to manipulate: pHEMA hydrogel tubular devices modified with methyl methacrylate have been employed to better resemble softness and flexibility of spinal cord tissue revealing less scar formation and brainstem motor nuclei axon regeneration in a

rat transected spinal cord (Tsai et al., 2004). However it should be considered that host reaction has been reported in a spinal cord injury model where the scaffold was rejected and did not integrate in the spinal cord after 28 days post injury (Li et al., 2013b).

- *Poly-ε-caprolactone (PCL)*: it is a biodegradable, bioresorbable and biocompatible aliphatic polyester commonly used for the fabrication of polyurethanes (PUs). It is prepared by a process of polymerization and can be mixed with starch to increase its biodegradability. Despite several PCL devices have been approved for medical applications, it received great attention for its potential employment as implantable biomaterial. Indeed, in physiological conditions PCL degradation by hydrolysis of its ester is an easy and slow process that renders this biomaterial suitable for long-lasting implantable devices. Therefore, PCL itself has been for example used to stabilize a rat lesion spinal cord with good results in terms of motor recovery (Silva et al., 2013). The potential of this polyester is that it can be designed in several architectures (cylinder, tubes, channels, open-path conduits and nanofibers). The biocompatibility of PCL nanofibers have been successfully tested to create an artificial scaffold that could mimic the ECM and support the nervous system regeneration (Raspa et al., 2016). Moreover, PCL membrane have been used to vehicle drugs that reduce SCI reactive astrogliosis and improve functional recovery; PCL scaffolds embedded with NSCs, human endometrial stem cells and neurotrophic factors (such as NT-3 and crocin) revealed their ability to restore the continuity of damaged axons and improved locomotor recovery after SCI (Hwang et al., 2011; Terraf et al., 2017; Wang et al., 2015b).

- Poly-lactic acid (PLA): like PLC, it is a bioactive and biodegradable aliphatic polyester that derives from corn starch, cassava roots or sugarcane. Although extensively used, PLA is structurally unstable and fragmenting but hydrogels, nanofibers, conduits, sponges or channels have been shown to support axon extension after SCI. However, PLA alone had only modest effects so that it was combined with trophic factors, cells or other materials, showing contrasting results (Hurtado et al., 2011; Oudega et al., 2001; Patist et al., 2004). Therefore, the scientific community agree that further investigations are needed before a successful and safe employment of PLA in SCI.

- *Polyethylene glycol (PEG)*: it is a water-soluble, biodegradable and flexible polyether compound with different applications in medicine (laxative, medication, drug excipient). It is generally considered biologically inert and safe even if it potentially contains toxic

impurities. It is available in different geometries (membranes, fibers, hydrogels, channels) and it has been widely investigated in SCI where is known to have multiple beneficial properties: it counteracts nerve fiber degeneration, decreases oxidative stress, reduces cell death, and reduces inflammatory response (Kong et al., 2017; Luo and Shi, 2004). It should be considered that PEG alone does not completely mimic spinal cord structure with a relatively inefficient biocompatibility. Moreover, some adverse effects derived from its implantation and low drug loading capacity have been reported so that PEG conjugation with other materials is preferred in case of drug delivery (Bakshi et al., 2006; Grous et al., 2013).

PEG is also used as an adjuvant to produce other biomaterial scaffolds. This is the case of an high biocompatible hydrogel produced by the PEG cross-linking between thiol-functionalized hyaluronic acid and thiol-functionalized gelatin to optimize cell adhesive and mechanical property in order to support transplanted OPC growth and re-myelination of injured spinal cord (Li et al., 2013a). PUs are a class of organic polymers that can be also produced starting from PEG combined with different materials and are now emerging as new biomaterials in SCI thanks to their versatile and easily manipulating structure. In SCI the PU poly(ethylene glycol)-poly(serinol hexamethylene urethane) has been employed to transplant bone marrow stromal cells increasing cell survival and locomotor recovery of SCI rats (Ritfeld et al., 2014). 3D-PU nanofiber structures are also emerging as *in vitro* cell culture system to support neuronal growth/network (neurons are able to extend their process as a function of nanofiber diameter) and as efficient support *in vivo* to guide axon regeneration after SCI (Puschmann et al., 2014).

Table 3: the main synthetic scaffolds used in SCI (modified by Kim M et al., 2014)

Synthetic biomaterials		Application for spinal cord repair	References
PCL	Tubular	3d plotting and printing, a rapid prototyping technology, was used in scaffold fabrication. In addition, SCI treated with SAP, BDNF and ChABC.	Silva et al., 2010, 2013; Gelain et al., 2011; Donoghue et al., 2013
	Sponge	Transplantation of genetically modified NSCs to secrete NT-3.	Hwang et al., 2011
PHB	Sponge	PHB-HV-based 3D scaffold	Ribeiro-Samy et al., 2013
	Sheet	Transplantation of Schwann cells on PHB with laminin coating.	Novikova et al., 2008
PLA	Sponge	Microporous scaffolds seeded with genetically modified Schwann cells.	Hurtado et al., 2006, 2011; Cai et al., 2007
PLGA	Tubular	Transplantation of NT-3 gene-modified Schwann cells and TrkC gene-modified MSC. Local gene delivery or NT-3 delivery.	De Laporte et al., 2009; He et al., 2009; Krych et al., 2009; Fan et al., 2011
	Sponge	Transplantation of NSCs, Schwann cells and/or MSCs. Evaluation of PLGA seeded with human NSCs in the African green monkey or in canine.	Rooney et al., 2008a,b; Chen et al., 2009; De Laporte et al., 2009; Olson et al., 2009; Rauch et al., 2009; Yang et al., 2009; Pritchard et al., 2010; Du et al., 2013
	Film	NSCs seeded on micropatterned films or Scavenger-releasing films.	Yucel et al., 2010
	Hydrogel	NT-3 delivery	Stanwick et al., 2012
PEG	Hydrogel	Local delivery BDNF or FGF2 with or without cells.	Kang et al., 2010; Conova et al., 2011; Kouhzaei et al., 2013; Li et al., 2013; Shi, 2013
PHEMA	Hydrogel	Scaffolds used for cell adhesion, axonal growth and angiogenesis.	Hejcl et al., 2009, 2013; Ruzicka et al., 2013; Valdes-Sanchez et al., 2013

Therefore it is evident that all the biomaterials described, despite their intrinsic beneficial properties, are rarely used alone in SCI conditions. The reason for this choice resides in the fact that even the most suitable scaffold has some limits that may be overcome by conjugation/association with different molecules/materials. On the other hand, stem cell repair is one of the most studied strategy in SCI thanks to their great potential. However, therapeutic applicability of stem cells is often ineffective due to the unfavourable microenvironment of SCI. For these reasons, we decided to combined the two most relevant approaches available today, in order to reinforce their individual potentiality to reach a valid therapeutic strategy.

3.3 STEM CELLS

Two different stem cells have been used in this study, in combination with biomaterials: neural precursors and mesenchymal stem cells.

3.3.1 NEURAL STEM CELLS AND NEURAL PRECURSORS

NSCs are multipotent stem cells already committed to neural lineage that can be collected from different embryonic and adult CNS areas. Niches of NSCs reside in sub-ventricular zone (Uchida et al., 2000), dentate gyrus of hippocampus (Palmer et al., 1997), central canal of the spinal cord (Mayer-Proschel et al., 1997) and in the optic nerve (Shi et al., 1998). NSCs can be rapidly expanded *in vitro* as neurospheres, cell agglomerates of neural progenitors, stem cells and differentiated cells (Ahmed, 2009). As committed cells to the neuronal fate, NSCs are suitable for neuroregenerative therapy: indeed, it has been demonstrated they can differentiate in interneurons (Scheffler et al., 2005), pyramidal and cortical neurons (Corti et al., 2005; Englund et al., 2002), astrocytes (Eriksson et al., 2003), oligodendrocytes and endothelial cells (Wurmser et al., 2004; Yandava et al., 1999).

NSC mechanisms of action are different. When grafted into a rat SCI model, NSCs collected from embryonic and adult tissue promote functional recovery through neuroprotective and neuroregenerative effects due to GDNF and NGF secretion (Hofstetter et al., 2005; Parr et al., 2008). NSCs from adult mouse brain transplanted into a rat lesioned spinal cord promote oligodendrocyte differentiation and the re-myelination of the damaged axons (Karimi-Abdolrezaee et al., 2006). Moreover it has been demonstrated that these cells can integrate into the lesion site, differentiate in neural like phenotype and create a permissive environment for regeneration through immunomodulatory and excitotoxic protection action (Abematsu et al., 2010; Ziv et al., 2006). Neural precursors (NPs) have been also employed in SCI as more committed to neural lineage than NSCs. NPC ability to integrate and restore synaptic connectivity after SCI has been demonstrated for the first time in a graft of neuronal and glial restricted precursors in a model of cervical SCI. Six weeks after the transplantation sensory axons regeneration and functional excitatory synaptic connections across the injury have been observed (Bonner et al., 2011). NPs transplanted in a lesioned spinal cord migrate into the injury site and partially differentiate into neurons (rarely in astrocytes and oligodendrocytes), leading to a significant functional recovery (M Boido,et al., 2014; Marina Boido et al., 2009; Marina Boido, Garbossa, & Vercelli, 2011). Therefore, NPs integrate into the lesion, surrounding the injury and laying along the damaged axons in the ventral and dorsal

part of the spinal cord. Compared to other types of neural stem cells, NPs can easier differentiate as they are committed towards a more mature phenotype, they are less responsive to inhibitory signals and less predisposed to neoplastic formation than ESCs (Coutts and Keirstead, 2008).

Despite the wide range of preclinical and clinical studies, none of them have reached all three phases of clinical trials. The main reasons reside in the inconsistency of therapeutic efficacy (that is based on rodent models) and in the possibility to obtain donor cells in a reliable and safe way. Further analyses are needed to better understand their mechanism and optimize their employment.

3.3.2 MESENCHYMAL STEM CELLS

MSCs have been described for the first time with the name of "colony forming unit fibroblasts" as they are a resident bone marrow cell population with a fusiform and fibroblast morphology (Friedenstein et al., 1976). They are adult multipotent stem cells able to differentiate in different lineage of mesodermal origin such as bone, adipose and cartilaginous tissue (Pittenger et al., 1999). MSCs can be found in different compartments like bone marrow (the most common source), blood, umbilical cord, amniotic liquid, placenta, adipose tissue, synovial membranes, liver, lungs and spleen (in 't Anker et al., 2003). Currently it is difficult to identify these cells, since they express a variety of markers, none of which mutually exclusive for MSCs (da Silva Meirelles et al., 2006).

MSCs represent a valid alternative to ESCs, since their use does not imply ethical concerns. Moreover, bone marrow collection is an easy and standardized procedure, and their high proliferative potential allows the ex vivo expansion to obtain an adequate cell number for transplantation; additionally, MSCs can migrate into the lesion site and do not present immunogenicity problems (Coutts and Keirstead, 2008; Mothe and Tator, 2012).

MSC graft has been demonstrated a valid approach for different neurodegenerative diseases like ischemia, Huntington's disease, ALS, multiple sclerosis and Parkinson's disease (Chen et al., 2003; Lescaudron et al., 2003; Li et al., 2001; Mandalfino et al., 2000; Mazzini et al., 2008; Vercelli et al., 2008).However, despite the functional recovery achieved, MSC mechanism of action is still not completely understood. Several hypotheses can explain how these cells exert a beneficial role after SCI.

The main MSC mechanism of action concerns their ability in releasing growth (as BDNF, VEGF or HGF) and anti-inflammatory factors, cytokines and microvesicles (mainly containing microRNA, mRNA, lipids and proteins). They exert a neurogenic, angiogenic, neuroprotective, synaptogenic and healing inhibition role (Awad et al., 2015; Hu et al., 2013). Indeed MSCs can exert a

neuroprotective role thanks to their ability in creating a permissive environment to promote fiber regrowth.

MSCs can also deliver immunomodulatory molecules that arrest T lymphocyte cell cycle, and inhibit pro-inflammatory agents like IL-1 and TNF-α thus reducing macrophage activation (Han et al., 2015; Ortiz et al., 2007; Ribeiro et al., 2015; Urdzíková et al., 2014). In particular MSCs seem to be able to reprogram pro-inflammatory M1 to anti-inflammatory M2 macrophages, thus regulating the immune response after SCI. Motor recovery and a partial regeneration have been attributed to this MSC function (Himes et al., 2006; Nakajima et al., 2012).

A permissive microenvironment is also assured by angiogenic factors released by MSCs, determining increased vascularity and oedema reduction (Hofstetter et al., 2002), production of fibronectin, adhesion molecules and neural growth factors, and glial cyst inhibition (King et al., 2006). Such effects can explain the reduced lesion volume, astrogliosis, microglia activation with sprouting promotion and improved functional outcome that we observed in a mouse model of SCI compression after MSC transplantation (Boido et al., 2014a; Boido et al., 2014b).

MSCs can also form cellular bridges across the lesion site, infiltrate it to preserve the tissue and support lesioned fiber regrowth (Ankeny et al., 2004; Bakshi et al., 2006; Wu et al., 2003), as demonstrated in a rat model of thoracic contusion (Ohta et al., 2004).

Finally, a transdifferentiation mechanism has been also hypothesized: indeed some authors described *in vitro* a neural-like morphology for MSCs expressing long processes and neural markers like nestin, NeuN and GFAP (Sanchez-Ramos et al., 2000). The most probable hypothesis is a process of cell fusion rather than transdifferentiation. (Crain et al., 2005; Terada et al., 2002).

Due to the above described characteristics, MSCs have been also tested in some clinical trials. MSC transplantation in complete SCI patients is safe, feasible and well-tolerated (Hur et al., 2016; Mendonça et al., 2014). In particular sensitive and motor improvements were achieved in more than 50% of 12 patients with chronic SCI that received MSC graft (Vaquero et al., 2016). However, discrepancies are present in literature about the current clinical application of these cells. Indeed, labelled MSC injected into a chronic cervical SCI patient were not any more visible after 2 weeks and 1 month with magnetic resonance, reflecting the absence of neurological improvements (Chotivichit et al., 2015).

In conclusion, neural precursor cells and mesenchymal stem cells are generally considered the most promising types of stem cells: the first as they are already committed to the neural lineage, the second as favourable in terms of ethic concern, safety and beneficial effect.

3.4 AIM OF THE PROJECT

In this project, we combined the benefits of two different methods: 1) biomaterials for their intrinsic properties, and 2) stem cells for their neuroprotective and neuroregenerative functions.
Here we analysed innovative biomaterials, provided by the team of Politecnico of Torino, to investigate their therapeutic potentiality in case of SCI. We tested both *in vitro* and *in vivo* the biocompatibility of the scaffolds embedded with different type of cells (NSCs, MSCs and SH-SY5Y): we evaluated cell survival, differentiation, rejection, and neuroprotective action.
In particular we employed three new biomaterial formulations (Tonda-Turo et al., 2017b; Zuber et al., 2015): 1) a thermosensitive solution of inj-bioPUs characterized by solid-gel transition, spinal cord like elasticity and a chemical functionalization that makes it resemble the ECM components; 2) a new PU formulation to synthesize low immunological nanofibers with high surface area to volume ratio suitable for cell attachment; 3) a new chitosan hydrogel suitable for cell injection and localization characterized by high permeability and physiological pH to create a proper environment for cell survival and mechanical properties similar to those of the spinal cord.

3.5 MATERIALS AND METHODS

In vitro experiments

Experimental animals

C57BL/6J male mice for experimental procedures were purchased from Envigo (Udine, Italia), while BCF1 mice that express enhanced green fluorescent protein (EGFP) under the β-actin promoter were obtained by Dr. M. Okabe (Osaka University, Suita, Japan). Animals were maintained under standard conditions with free access on food and water. All experimental procedures on live animals were performed according to the European Activities Communities Council Directive of 86/609/EEC (November 24, 1986) Italian Ministry of Health and University of Turin institutional guidelines on animal welfare authorization No. 17/2010-B, June 30, 2010 (law 116/92 on Care and Protection of living animals undergoing experimental or other scientific procedures). The number of animals and suffering caused were kept to a minimum.

Biomaterial production

All biomaterials were realized in DIMEAS laboratory of Politecnico of Torino, thanks to the collaboration with Dr. Tonda-Turo C. and Prof. Ciardelli G.

Injectable-bioPUs – Inj-bioPUs were prepared following the instructions of Boffito et al., 2016 (Boffito et al., 2016). It was employed a two-step procedure based on the condensation reaction among an amphiphilic polyethylene glycol (PEG)-based macrodiol, an aliphatic diisocyanate (hexamethylene diisocyanate - HDI) and an aliphatic diamine/diol chain extender having a protected ammine group (N-Boc serinol- PCT/IT2013/000196). Two different PEG-based macrodiols were tested, one with and one without free amine groups. Indeed to enhance inj-bioPU bioactivity the first one was prepared adding ECM derived peptides. The free amine groups (IKVAV/YIGSR) along PU macromolecular chains were obtained by reaction of de-protection of chain-extender functional groups and, then, ECM derived peptides were coupled to the PU-amino groups through carbodiimide/hydroxysuccinimide (EDC/NHS)-mediated chemistry.

The hydrogels obtained presented the following features: sol (solution) to gel transition at physiological temperature (reversible process), ~ 100 KPa elastic modulus comparable with spinal cord and a degradation rate within 30-40 days.

Chitosan (CS) - Medical Grade CS (Mw 200 – 400 kDa, deacetylation degree ≥ 92.6 %) was purchased by Kraeber GmbH & Co (Ellerbek, Germany). CS was mixed with 0.5 M acetic acid at RT by continuous stirring obtaining a 2.5% solution (weight/volume). The disodium salt hydrate β-glycerophosphate was then added in a ratio 70/30 (weight/weight) in order to produce a thermosensitive hydrogel (in solution at 10°C and gel at > 25°C) at physiological pH with low viscosity in the solid form.

Nanofiber membranes – they were synthetized following the procedure described by Tonda-Turo C et al., 2016 (Tonda-Turo et al., 2016). The synthesis consisted of a two-step procedure using poly (ε-caprolactone) diol (PCL) as macrodiol, anhydrous 1,2-dichloroethane (DCE) as solvent, 1,4-diisocyanatobutane as diisocyanate and N-Boc serinol as chain extender. Aligned and random nanofibers of 2.8 ± 0.6 μm were obtained by the electrospinning technique using a static 21 G needle and a rotating drum with an angular speed of 2,000 rpm. Then a functionalization step was

performed: to enhance cellular adhesion IKVAV (Ile-Lys-Val-Ala-Val) peptide was covalently cross-linked to the membrane surface.

Cell culture

MSCs - Murine MSCs were collected and expanded *in vitro* before *in vivo* transplantation. Two months old C57BL/6J or EGFP-positive mice were anesthetized with 3% isoflurane vaporized in O_2/N_2O 50:50 and sacrificed by cervical dislocation. Tibias and femurs were extracted, muscles and connective tissues removed and then cells were aspirated from bone marrow through a 22-gauge needle. Cells were centrifuge 5 minutes at 1000 rpm in Minimum Essential Eagle Alpha Modification medium (Sigma-Aldrich), supplemented with 100 U/ml penicillin (Invitrogen-Gibco), 100 µg /ml streptomycin (Invitrogen-Gibco) and 2 mM of glutamine (Invitrogen-Gibco). Polystyrene dishes of 19.5 cm^2 (BD Biosciences, Milan, Italy) coated with fetal bovine serum (FBS, Sigma-Aldrich) were used to plate 700,000 cells/cm^2. MSCs were grown in Minimum Essential Eagle Alpha Modification medium (Sigma-Aldrich) containing 10% of FBS in a 37°C incubator with 95% of humidity and 5% of CO_2. After four days, the medium was replaced to remove floating cells and then replenished every 2-3 days. Ten days after plating, adherent cells were detached by trypsinization (tripsin, Invitrogen) and CD11b positive granulocytic cells removed by bead sorting: briefly, microbeads conjugated to monoclonal rat anti-mouse/human CD11b antibody (Miltenyi Biotec GmbH, Gladbach, Germany) were incubated with cells and loaded onto a MACS column (Miltenyi Biotec GmbH). CD11b-negative cells were retrieved and re-plated in their medium as described above.

NPs - C57BL/6J or EGFP-positive E12 embryos were removed and placed in a petri dish filled with cold saline solution. Under a dissecting microscope, caudal neural tubes (10 lower somites) were dissected removing the surrounding connective tissue and cells dissociated with a Pasteur pipette. Cells were centrifuged at 1,000 rpm, resuspended and counted on a Burker chamber after incubation in 0.4% trypan blue in PBS 1X.

SH-SY5Y - SH-SY5Y neuroblastoma cell line was kindly gifted by Prof. Spillantini in Cambridge. The cells were cultured in Roswell Park Memorial institute (RPMI) 1640 medium (Gibco, Invitrogen) with 2 mM of glutamine (Invitrogen-Gibco) [supplemented with 10% FBS, 100 U/ml penicillin (Invitrogen-Gibco) and 100 µg /ml streptomycin (Invitrogen-Gibco)].

Analysis of cell viability in biomaterials

Inj-bioPUs and CS

For testing the cell viability in presence of biomaterials, MSCs, NPs and SH-SY5Ycells were plated inside or near the hydrogels at a final concentration of 20,000 cells in 100 µl of inj-bioPU hydrogel and in CS hydrogel, and incubated at 37°C with 95% of humidity and 5% of CO_2. Control cells were cultured in the same conditions and plated at the same concentrations.

Nanofiber membranes

SH-SY5Y and MSCs were plated at a final concentration of 20,000/well on the nanofiber membrane positioned on 24 multiwell plates. They were incubated at 37°C with 95% of humidity and 5% of CO_2.

In vitro preliminary examination

In vitro experiments were conducted after 1-2-5-7 days *in vitro*. Prior to immunofluorescence and immunocytochemistry, cells were washed with PBS 1X, fixed in PFA 4% for 20 minutes at RT and washed twice. The cells were examined using an inverted microscope (Nikon Eclipse TE 2000-U). As an alternative, we embedded the whole hydrogel drop (gel + cells) in the cryostat medium (killik, Bio-Optica, Milan, Italy) and we cut the samples into 50 µm-thick sections to better visualize cells into the gel.

Immunofluorescence and immunocytochemistry

For immunofluorescence after 10 minutes in PBS-triton 0.25% and 30 minutes in blocking solution (0.25% PBS-triton and 10% normal donkey serum (NDS; Sigma-Aldrich)-pH 7.4), NPs were incubated with 1:200 monoclonal mouse anti-nestin (Chemicon). Then the cells were washed in PBS 1X and incubated with the secondary antibody for 1h at RT (Jackson Immuno Research Laboratories; donkey anti-mouse1:200 cyanine 3-coniugated).

For immunocytochemistry, MSCs and SH-SY5Y placed on nanofibers were washed in PBS 1X, and processed for Nissl staining: the samples were placed in 0.1% Cresyl violet acetate for 10 minutes, dehydrated in an ascending series of ethanol, rapidly cleared in xylene and cover-slipped

with Eukitt (Bioptica, Milan, Italy). Cells were counted at DIV1-2-5 and two-way ANOVA was performed (significance at $p \leq 0.05$) on GraphPad Prism software.
Pictures were taken on a Nikon Eclipse BOi light and epifluorescence microscope equipped with a Nikon DS-Fi1 digital camera (nanofiber pictures). Photomicrographs were corrected for brightness and contrast with Photoshop CS2 software.

The cell viability was verified by trypan blue staining (MSCs, NPs and SH-SY5Y in inj-bioPUs), morphological observation (MSCs, NPs and SH-SY5Y near and inside CS) and cell counting (SH-SY5Y and MSCs on nanofiber membrane). Pictures were taken on a Nikon Eclipse E800 light and epifluorescence microscope equipped with a Nikon Coolpix 995 digital camera (nanofiber pictures).

Survival assays and cell counting

MSC survival inside CS hydrogel was tested both by counting alive cells and by two cytotoxicity assays: calcein-acetoxymethylester (AM) assay and 3-(4,5-dimethylthiazol-2-yl)-2,5-diphenyltetrazolium bromide (MTT) assay.

Calcein assay - This is an assay to determine cell viability in live cells. MSCs were plated on 24 multiwell plate at a final concentration of 20,000 per well. The experiment was conducted in triplicate for two different conditions: MSCs grown inside CS or MSCs grown alone as positive control. After 1, 5 and 7 days, the medium was removed and cells washed once with PBS 1X at pH 7.4. Afterwards 100 µl of calcein solution 2.5 µM was added and the plate incubated 30 minutes at 37°C. The cells were then fixed in PFA 4% for 20 minutes and cell fluorescence was checked on a Nikon Eclipse BOi epifluorescence microscope equipped with a Nikon DS-Fi1 digital camera (nanofiber pictures). For this experiment, non-EGFP positive cells were employed.

MTT assay - MSCs were culture in their medium in a 96 multiwell plate at a final concentration of 6,000 cell per well. When they reached the confluence, the culture medium was removed and substituted with: 1) MSC medium; 2) MSC medium + CS (48h contact-0.1g CS/ml); 3) MSC medium + 30% DMSO. MSC medium was used as positive control (CTRL+), whereas MSC medium + 30% DMSO was employed to induce cell death as negative control (CTRL-). After an incubation of 24h hours, the supernatant was collected and the MTT assay performed as follow. A volume of 100 µl of MTT solution (Sigma-Aldrich, 5mg/ml in PBS) was added and the plate incubated for 3h. Then, the MTT solution was discarded and 100 µl of DMSO were added and

mixed to dissolve the formazan crystals. Absorbance was measured at 570 nm wavelength on a Multiskan EX (Life Technology). Six samples for each of the three conditions were analyzed. Cell viability was calculated as a percentage value compared to CTRL+. Graphpad Prism software was employed for a T-test. Values $p \leq 0.05$ were considered statistically significant.

Microvesicles (MVs) collection and analysis

In order to verify whether the presence of CS could alter the therapeutic efficacy of MSCs, we evaluated their MV secretion. MSCs were cultured as described above and MVcollection performed as described by Rad F et al., 2016 (Rad et al., 2016). Samples of three conditions (MSCs cultured in normal medium, MSCs cultured into CS, and CS alone) underwent three consequent centrifugations with supernatant collection and transfection on new tubes: 1) 400 g for 10 minutes; 2) 2,000 g for 20 minutes; and 3) 10,000g for 70 minutes at 4°C. The pellet was washed with PBS 1X and then centrifuged again at the same high speed to remove proteins. The pellet containing MVs was stored at -80°C prior to dynamic light scattering.

The MV release was evaluated by dynamic light scattering (DLS; Zetasizer Nano S90, Malvern Instruments, Worcestershire, UK). MV size was calculated as the mean value of three measurements. The result graphically shown the size distribution of MVs as intensity plots.

2', 7'-Dichlorodihydrofluorescin diacetate (DCFH-DA) assay

The antioxidant ability of MSCs was tested by DCFH-DA assay. Briefly, MSCs were cultured for three days in a 24 multiwell plate at the concentration 20,000/well, inside CS or alone; in additional wells we also put CS alone. SHSY-5Y cells were plated in a 24 multiwell plate at the concentration 7,000/well. After 3 days, half of SHSY-5Y medium was replaced with fresh medium and half of supernatant collected from: 1) MSC alone; 2) CS alone; 3) MSCs + CS. SH-SY5Y cultured in their specific medium were used as CTRL+. To induce an oxidative stress, after 24h 400 µM of H_2O_2 was added into some wells and incubated at 37°C for 1h (the other wells were used as controls). The DCFH-DA assay was used to detect oxidative reactive species: the supernatant was removed and substituted with 100 µM of DCFH-DA solution for 1h at 37°C. Then, once removed the solution, repeated freeze-thaw cycles were performed to lyse the cells, before reading the plate on a Multiskan EX (Thermo Scientific) at a 485 nm. The experiment was performed once in triplicate. The results were analyzed by one-way ANOVA and expressed as relative fluorescent units (RFU).

In vivo experiments

Surgery and cell-biomaterial implantation

In order to verify the implantation feasibility of CS and nanofibers, some animals underwent surgery (n=3 for CS, n=2 for nanofibers). Three months-old C57BL/6J mice were deeply anaesthetized with 3% isoflurane vaporized in O_2/N_2O 50:50. The thoracic spine was exposed, the spinal muscles displaced laterally and a complete spinal cord transection was performed using a 27-gauge1/2 needle at T13 level. Immediately after the injury, the animals received directly into the lesion cavity either 1) a solution of 10 µl of EGFP+ MSCs or NPs and CS (150,000 cells-culture medium 3 µl + CS hydrogel 7 µl; outer tip micropipette diameter 100 µm); or 2) a square-sized aligned nanofiber membrane of 140-170 µm.

Histological examination

One week after the lesion and cell-biomaterial injection, mice were deeply anaesthetized with 3% isoflurane vaporized in O_2/N_2O 50:50 and transcardially perfused with 0.1 M PB, pH 7.4, followed by 4% PFA in the same PB. The spinal cord (T10-L2 segment) was dissected and post-fixed for 2h at 4°C in the same perfusion fixative. Samples were transferred overnight into 30% in 0.1M PB at 4°C, embedded in cryostat medium (killik, Bio-Optica, Milan, Italy) and cut on the cryostat (Microm HM 550) in longitudinal 50 µm sections. For immunofluorescence, spinal cord sections were immunoreacted as follows. After 30 minutes in PBS-triton 2% and 1h in blocking solution [0.2% Triton X-100 and 10% normal donkey serum (NDS; Sigma-Aldrich) in PBS pH 7.4], the sections were incubated with the following primary antibodies in the same solution at 4°C overnight: 1:500 polyclonal rabbit anti-GFAP (Dako Cytomation) and 1:200 monoclonal mouse anti-MAP2 (Chemicon, Milan, Italy). Then the sections were washed in PBS 1X and incubated with the secondary antibody for 2h at RT (Jackson Immuno Research Laboratories; donkey anti-rabbit/mouse 1:200 cyanine 3-coniugated).

For immunohistochemistry, spinal cord sections were mounted on 2% gelatin coated slides and processed for Nissl staining as described above.
Pictures were taken on a Nikon Eclipse E800 light and epifluorescence microscope equipped with a Nikon Coolpix 995 digital camera (nanofiber pictures) and on Olympus Fluoview 300 confocal

laser scanning microscope (MSCs + CS pictures). Photomicrographs were corrected for brightness and contrast with Photoshop CS2 software.

3.6 RESULTS

The biocompatibility of three new biomaterial scaffolds embedded with MSCs, NPs and SH-SY5Y cells was analysed *in vitro* and *in vivo* in terms of cells survival, differentiation, rejection, and neuroprotective action.

In vitro results

Cell survival on inj-bioPU hydrogels

Two different inj-bioPUs were prepared with (PEG)-based macrodiol as main component with or without the cross-linking of free amine groups (ECM peptides) to enhance the hydrogel bioactivity. To test PU biocompatibility, MSCs, NPs and SH-SY5Y were grown either inside or near the hydrogels. One, two, five and seven days after plating, none of the cell types was found alive inside the hydrogels: indeed only dead cells and debris were visible (Figure 20 A). When plated close to the hydrogels, some surviving cells were observed during the first hours (Figure 20 B) with a rapid decrease over time in cell viability. Only data on MSC survival near and inside inj-bioPU hydrogel with ECM peptides are shown in Figure 20. The same results were obtained for each time point with both the hydrogels tested for all cell types considered, suggesting possible inj-bioPUs toxicity. Considering the unsuccessful results obtained, we decided to test another hydrogel with the same cell types.

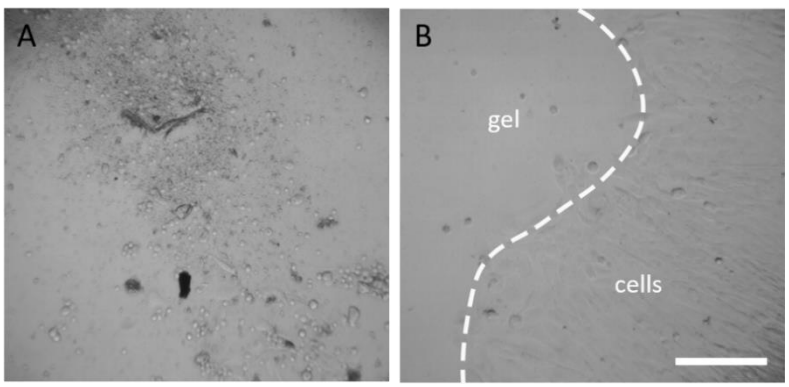

Figure 20: MSCs and inj-bioPUs in vitro. A) the image shows dead cells and cellular debris inside inj-bioPU hydrogel with ECM peptides; B) live MSCs are visible close to the hydrogel 3 hours after the culture. Scale bar: 150 µm

Cell survival and morphology on CS

The biocompatibility of an innovative formulation of CS hydrogel was tested: in collaboration with the Politecnico of Torino, by adding β-glicerolophosphate we obtained a thermosensitive hydrogel at physiological pH that could be used to embed stem cells.

SH-SY5Y cells, MSCs and NPs were grown both inside and near the CS hydrogel. SH-SY5Y cell line was firstly tested as more resistant compared to MSCs and NPs. Surviving SH-SY5Y cells were found both inside and near the hydrogel at 1, 2, 5 and 7 DIV as demonstrated by immunocytochemistry (DAPI- and Nestin-positivity; Figure 21 A-B-F-G). Moreover several SHSY-5Y cells underwent mitoses near the hydrogel (white arrow in Figure 21 A), indicating that the optimal culture condition in the presence of CS allowed cell proliferation. It is possible that mitoses were also present inside the hydrogel, but due to its turbidity we were not able to clearly visualize them.

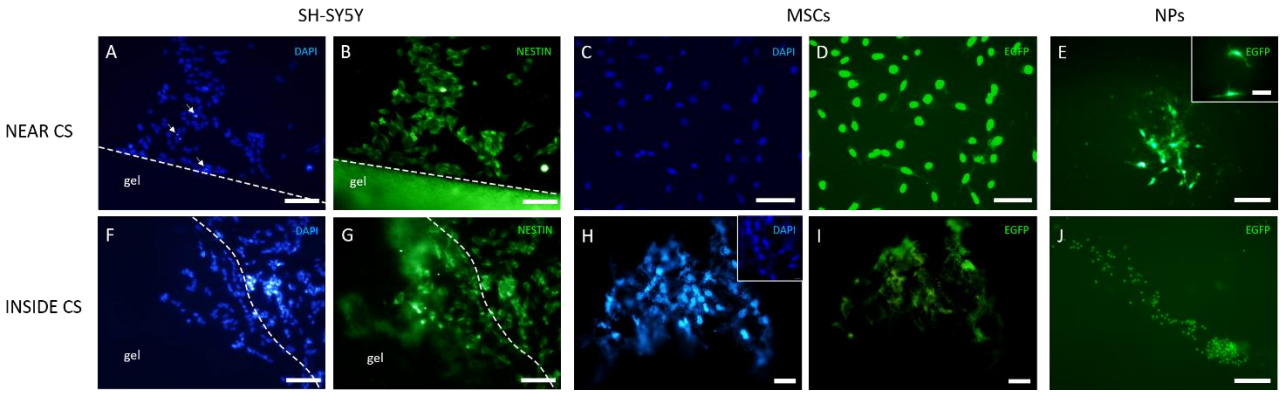

Figure 21: cells grown on CS in vitro. SH-SY5Y DAPI nuclei (A and F) with mitotic cells (white arrows in A) and cell cytoskeleton labelled by nestin (B and G) are visible both near and inside CS hydrogel. MSC DAPI nuclei (C-H) and fibroblast-like morphology (D-I) show live cells near and inside CS (DAPI nuclei in I magnification). NPs can be distinguished near CS, exhibiting the typical neuronal phenotype with elongated processes (magnification box on the right top E), and inside chitosan (J). Scale bars: A,B,F,G 100 µm; C,D 100 µm; H,I 30 µm; E, 100 µm, J, 200 µm and magnification box in E, 10µm

For MSC culture, EGFP-positive cells were used in order to easily identify them without immunofluorescence reactions. MSCs were able to grow both inside and near the hydrogel until 7 days as demonstrated by EGFP and DAPI positivity (Figure 21 C-D-H-I). MSCs showed their typical fibroblast-like morphology (Figure 21 D and I) suggesting CS as biocompatible material for MSC growth. Moreover the number of MSCs plated inside CS hydrogel was slightly higher compared to the control as shown in Figure 22.

Finally also some EGFP-positive NPs were visible both inside and close to the hydrogel (Figure 21 E-J), although their number appeared significantly lower than SH-SY5Y cells and MSCs: this could

be due to an excessive stress for NPs related to the whole procedure (isolation, dissociation and hydrogel embedding). As expected, NPs were able to emit some short processes that could be distinguished when cells were cultured near CS (magnification box on E).

In all cases, when the cells were plated inside the gel, their identification and morphological recognition was much more difficult because of the hydrogel turbidity. For this reason, the pictures were taken in the thinnest hydrogel part (F-G-I-J) or after hydrogel cutting in sections by cryostat (Figure 21 H). All images in Figure 21 refer to cells at DIV 7.

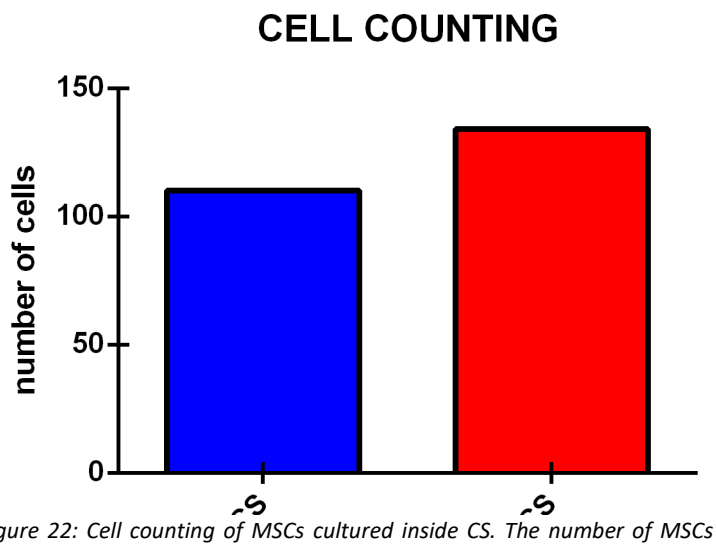

Figure 22: Cell counting of MSCs cultured inside CS. The number of MSCs grown in presence of CS is comparable to the one grown in in normal condition (NO CS)

Calcein-AM assay to assess MSC survival with CS

Based on the preliminary encouraging results, we further evaluated MSC survival in presence of CS by calcein-AM assay. In detail, MSCs cells were plated into the CS hydrogel and compared to MSCs grown in normal medium (positive control). The nonfluorescent calcein-AM probe penetrates cell membranes and is then cleaved by intracellular esterase releasing the hydrophilic fluorescent dye. Only live cells, in which the enzymatic reaction takes place, are fluorescent. As shown in Figure 23, compared to normal conditions (A), MSCs showed a similar survival in presence of CS (B-C).

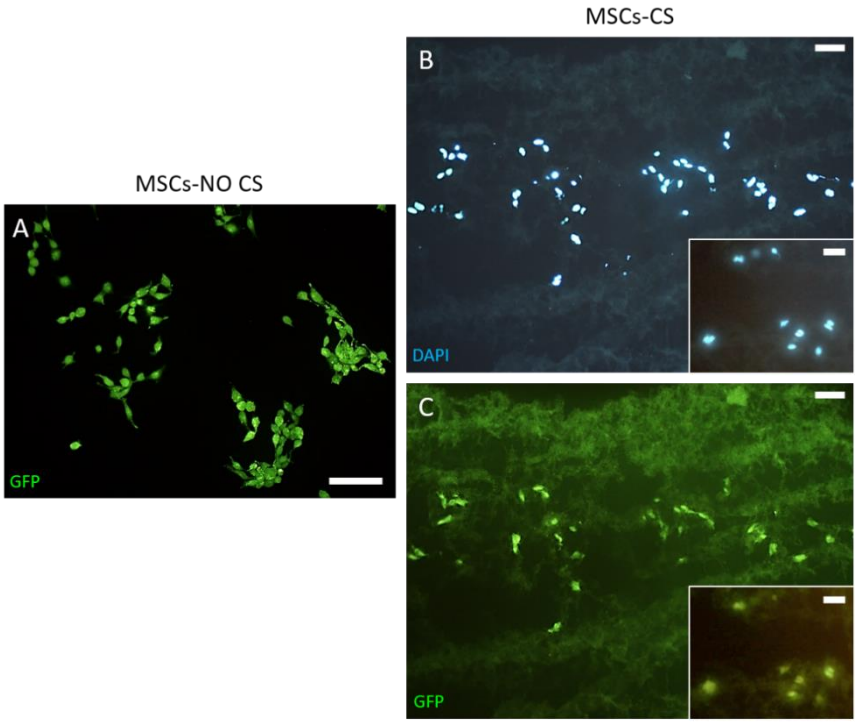

Figure 23: Calcein-AM assay. Live fluorescent MSCs were detected both in normal medium, without CS (A) and in the presence of CS hydrogel (B-C). Scale bar: A, 50 µm; B,C 50 µm and magnification boxes B, C 50 µm

MTT assay to asses MSC survival with CS

To further confirm the previous data concerning chitosan biocompatibility, the MTT assay was performed comparing three different MSC culture conditions: cells grown in 1) MSC medium (CTRL+); 2) MSC medium + CS; 3) MSC medium + 30% DMSO (CTRL-). Only in live cells specific enzymes reduced the MTT dye to formazan crystals that make the solution of purple colour. As indicated in Figure 24 A, both CTRL+ and MSC medium + CS conditions allowed the release of MTT dye at a comparable percentage (100% CTRL+ and 101.77% MSC medium + CS in Figure 24 B), while no signal of live cells was measured for CTRL- (Figure 24 A). Both calcein-AM and MTT assays demonstrated that CS is a valid biomaterial for MSC growth *in vitro*.

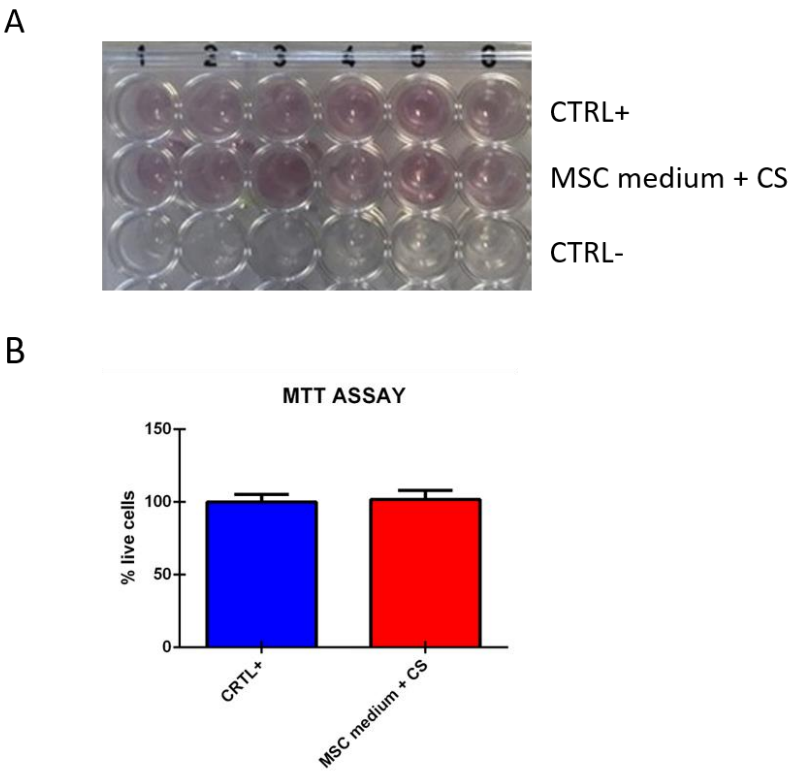

Figure 24: MTT assay. A) MTT assay in positive control condition (CTRL+, purple wells), in MSC medium + CS (purple wells) and in negative control condition (CTRL- white wells). B) The same percentage of live cells was calculated for CTRL+ and MSC medium + CS

DLS to evaluate MV release by MSCs grown within CS

To address MSC activity on CS, the DLS technique was employed to estimate MV release and their respective size. In DLS, when laser light hits particles, it scatters in all directions as long as the particles are small compared to the wavelength (Figure 25 A). The experiment was conducted comparing the content of the supernatant of MSCs grown either within CS or in standard conditions (CTRL+). CS supernatant (in absence of MSCs) was used as negative control (CTRL-). The presence of MVs with a size distribution ranging between 100 and 1000 nm was measured both for CTRL+ (Figure 25 B, red line) and MSCs + CS (Figure 25 B, green line): the observed MV dimensions are compatible with those reported in literature (Rad et al., 2016). Instead CTRL- (Figure 25 B, blue line) showed lower peaks around 10 and 100 nm, indicating the presence of debris. This result suggested that CS did not affect MSC ability to release MVs as indicated by the DLS curves almost overlapping (red and green lines in Figure 25 B).

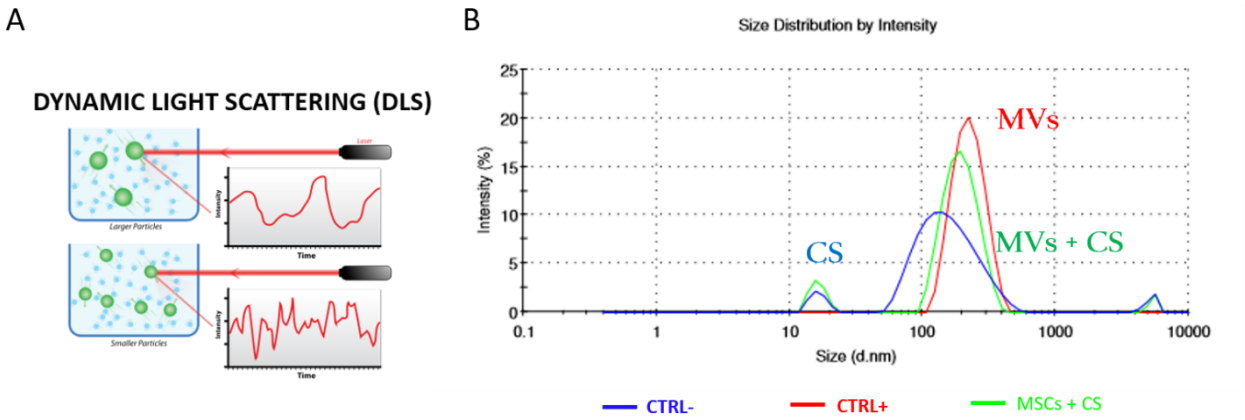

Figure 25: DLS measure. A) scheme of the DLS method measurement from http://www.quantachrome.co.uk/en/particle-size/dynamic-light-scattering.asp#dlsimage. B) the supernatant of MSCs grown alone of with CS revealed MVs presence (red and green lane at 100-1000 nm) compared to CTRL- (blue line) that indicate debris content at ~10 and 100 nm

DCFHA-DA assay to asses MV functionality with CS

In order to confirm that CS does not reduce the paracrine effect of MSCs, we cultured SH-SY5Y cells under oxidative stress (induced by H_2O_2) in presence of supernatant collected from: 1) MSC alone; 2) CS alone; 3) MSCs + CS. As positive control (CTRL+), SH-SY5Y cells were also cultured in their specific medium and similarly stressed with H_2O_2. Then the DCFHA assay was carried out comparing the different conditions. This assay measures the level of oxidative stress expressed as relative fluorescent unit (RFU). The results showed that both MSCs, CS and MSCs +

CS were able to exert an anti-oxidative effect (Figure 26) as shown by a RFU reduction of 58.36% (MSCs), 37.81% (CS) and 65.77% (MSCs + CS) with respect to CTRL+ (cells in stressed condition). These data i) confirm that CS does not affect the paracrine ability of MSCs; and ii) demonstrate that CS alone is able to reduce the cellular oxidative stress.

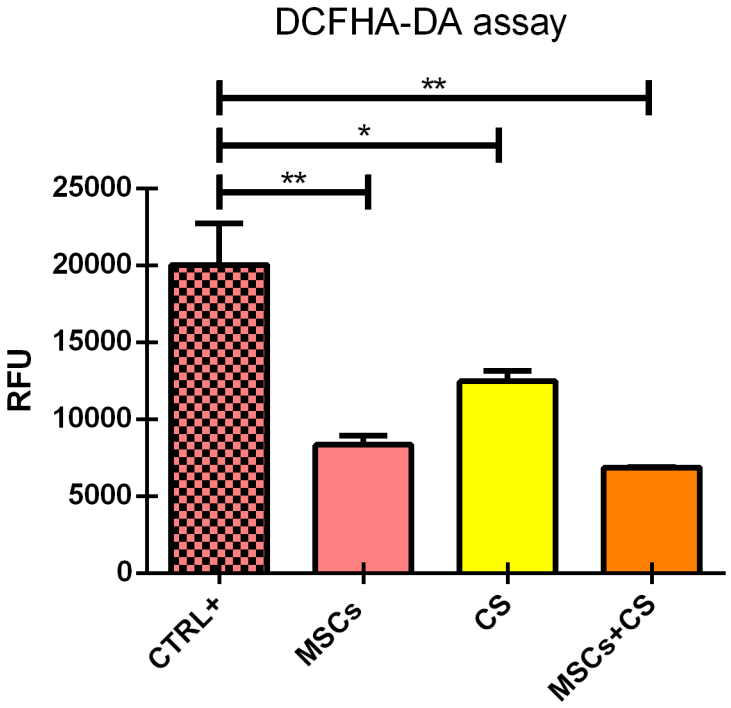

*Figure 26: DCFHA-DA assay. The oxidative stress (expressed as RFU) induced in SH-SY5Y cells by H_2O_2 is reduced by adding MSC, CS and MSC + CS supernatant in comparison to CTRL+ growth condition. Graph: * p-value < 0.05, ** p-value < 0.01, *** p-value < 0.001*

In vivo preliminary results

CS, NP and MSC injection *in vivo*

In order to test *in vivo* stem cell survival in presence of CS and to verify its implantation feasibility, 150,000 EGFP-positive NPs and MSCs were embedded in CS hydrogel and injected immediately after murine SCI transection. After 1 week, consistent with *in vitro* data, no surviving NPs were identified into the spinal parenchyma, while numerous MSCs were visible. As shown in Figure 27, MSCs were found both inside the lesion (as visible in B and, at higher magnification, in J) and surrounding it (F). Although we did not perform an accurate cell count, our suggestion is that the number of survived MSCs was higher than in our previous works (Boido et al., 2014a; Boido et al.,

2014b; Boido et al., 2014c): indeed CS has probably supported MSC survival. Moreover, the astrogliosis (C-G) observed around the lesion is comparable to our previous works.

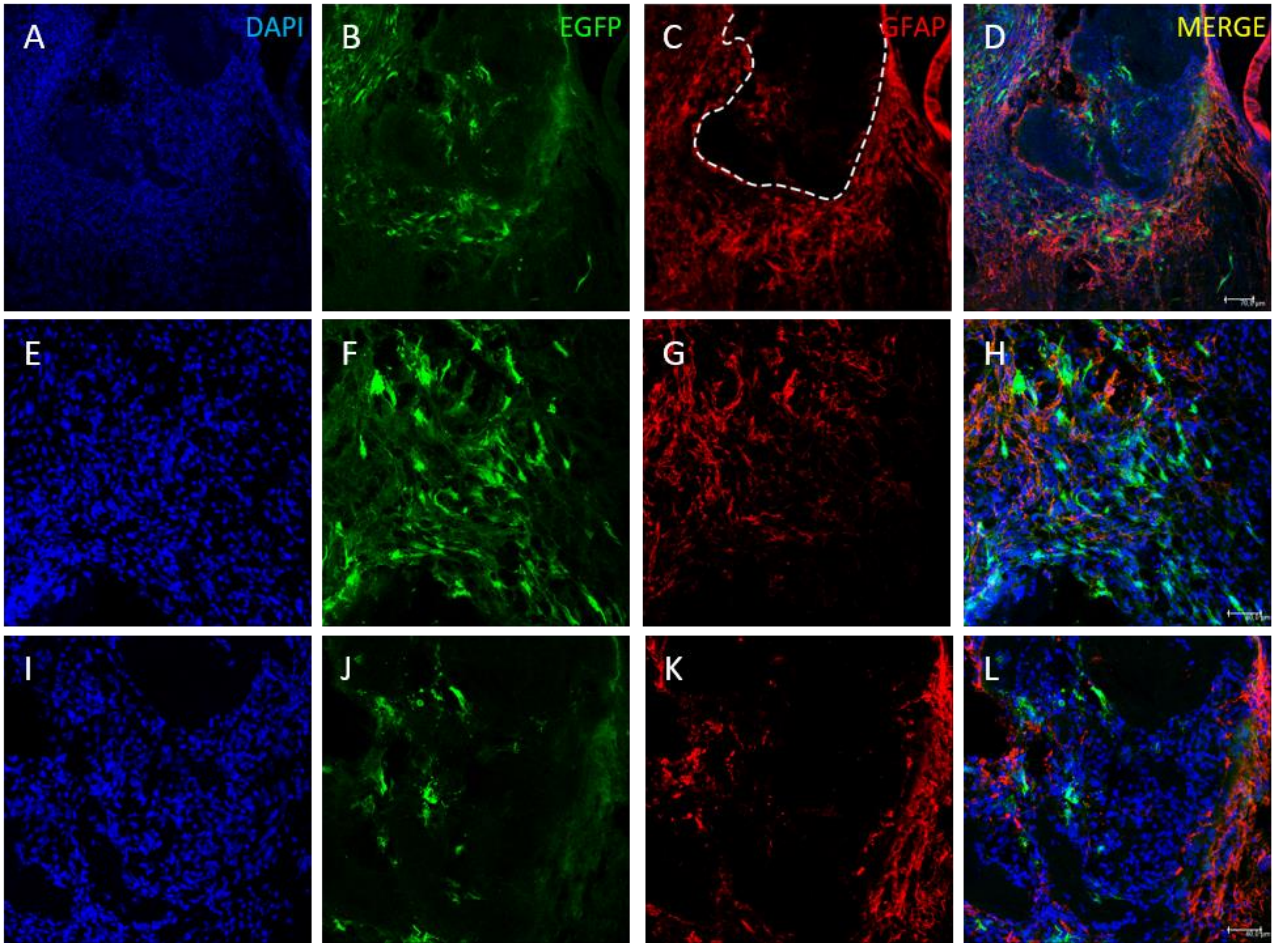

Figure 27: MSC and CS transplantation. In blue DAPI nuclei (A-E-I), in green EGFP-positive MSCs (B-F-J), in red astrocytes forming the glial scar at the lesion site (C-G-K) and the three previous images overlapped (D-H-L). In (A-D) the lesion area at low magnification shows astrocyte distributed around the glial cyst (dashed line in C). At higher magnification MSCs are visible around (F) and inside the lesion (J). Scale bar: (A-D) 70 um, (E-L) 40 um

Cell survival and morphology on nanofibers

Nanofiber sheets (average thickness 2.8 ± 0.6 µm) were specifically realized to mimic ECM. They were produced as both aligned and randomly oriented, functionalized or not with IKVAV peptide in order to test their capacity to allow MSC growth and adhesion.

By Nissl staining, we detected growing MSCs both on functionalized and non-functionalized nanofibers (Figure 28 A-D) at DIV 1, 2 and 5. A better cell elongation was visible for cells plated on aligned nanofibers as shown by nuclei and cell body shape (Figure 28 E-F-G). In order to evaluate cell survival, DAPI-positive MSC nuclei were counted (Figure 28 H). First of all, there was an expected increase in cell proliferating rate from DIV-1 to DIV-5 in all the conditions. Among the analysed nanofibers, the aligned ones better supported the MSC survival (value

comparable to CTRL). Notably, the number of cells grown on functionalized nanofibers was probably underestimated, because of the extreme Nissl intensity due to the intrinsic nanofiber properties (B and D). These results suggest that at least the aligned nanofibers are suitable substrates for cell survival and adhesion/elongation.

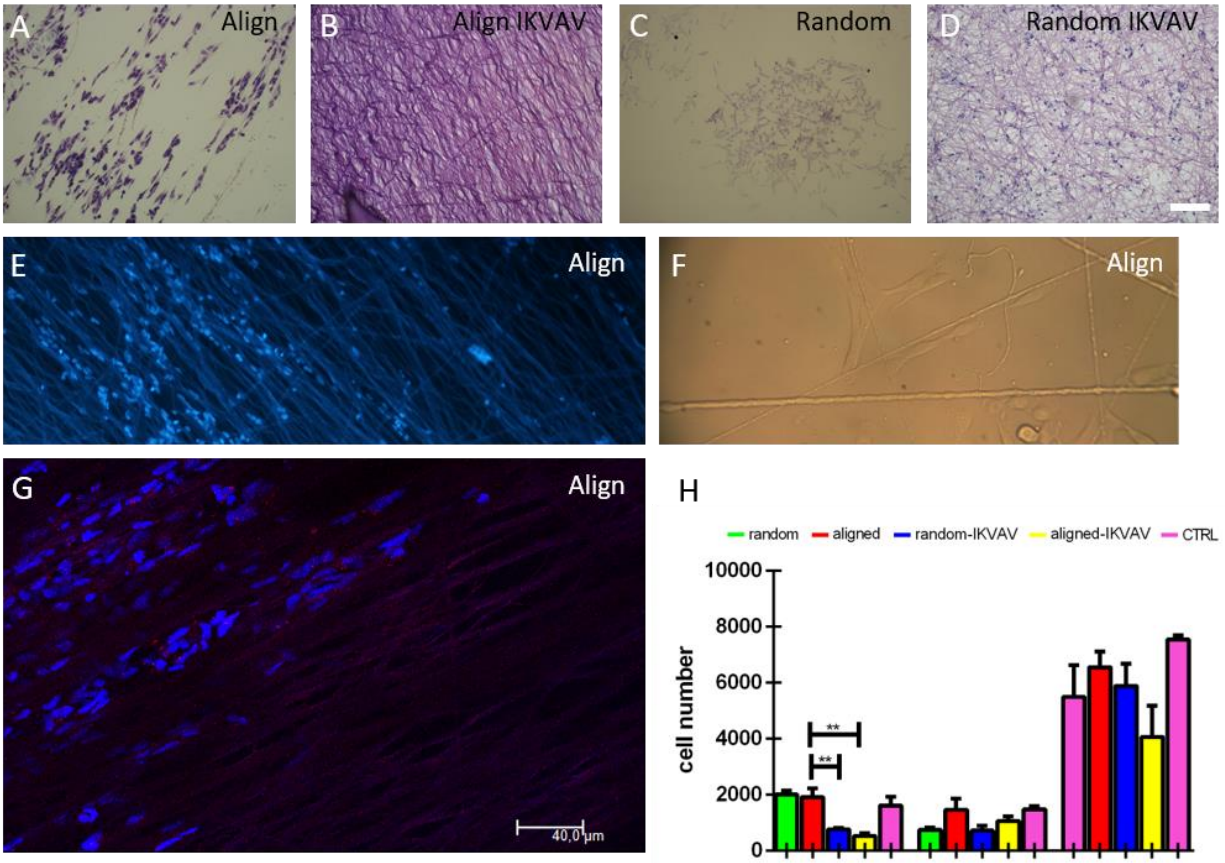

Figure 28: Nanofibers in vitro. MSCs were plated on aligned (A,E-G), aligned-functionalized (B), random (C) and random functionalized (D) nanofibers. On the aligned nanofibers cell elongation is more evident as shown with Nissl staining (A), DAPI (E-G) or in brightfield image (F). Graph shows cell count on single images (H). Scale bars: A-D 100µm, E 70 µm, F 40 µm, G 40 µm

Nanofiber membrane *in vivo*

To evaluate the feasibility of nanofiber membrane implantation *in vivo*, we grafted a square-sized aligned nanofiber sample (Figure 29 A) into the mouse spinal cord immediately after its complete transection. After 1 week, it was possible to identify in the spinal cord the nanofiber sheet thanks to its squared shape, easily recognizable by Nissl staining (Figure 29 B dashed line). No sign of rejection, infection or astrogliosis (Figure 29 C, GFAP immunofluorescence) was observed in proximity of the nanofibers, suggesting a positive integration of the biomaterial into the spinal cord

tissue. Moreover, some host cells with an elongated profile were found lined up following the nanofiber orientation (as previously observed *in vitro*), as shown in Figure 29 D-E.

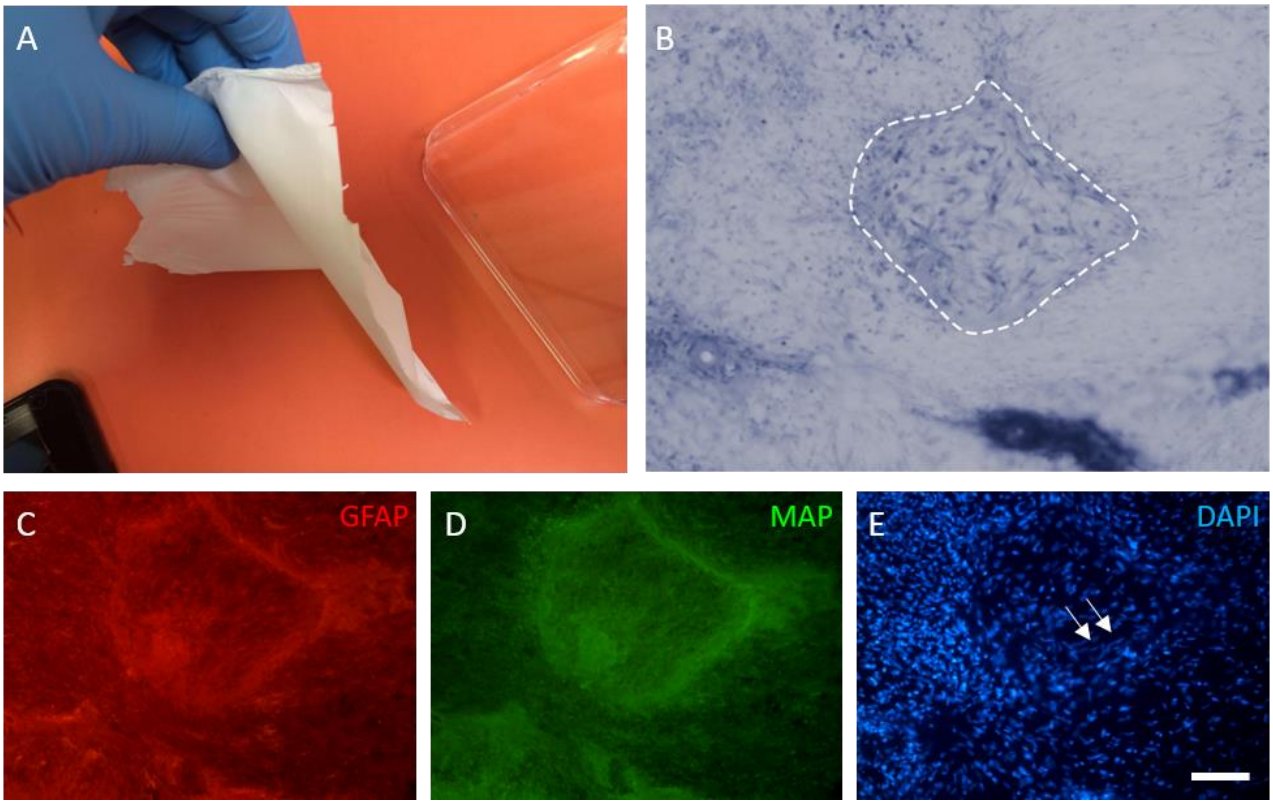

Figure 29: Nanofibers in vivo. (A) Nanofiber sample, (B) Nissl staining allows an easy identification of the square-sized nanofiber membrane into the spinal cord parenchyma (dashed line). (C-E) immunofluorescence reaction for GFAP (C), MAP2 (D) and DAPI (E): elongated host nuclei over the sample are visible (white arrows). Scale bar: 100 um

3.7 DISCUSSION

Combining our expertise on stem cell transplantation in SCI condition and the competences in the biomaterial field of the Ciardelli's group (Politecnico of Torino), we investigated the therapeutic potential of three different innovative biomaterial formulations, namely **inj-bioPU** and **chitosan hydrogels** as tools to vehicle stem cells, and **PU nanofibers** to create a bridge into the injured spinal cord for supporting axon regeneration after trauma. Therefore, we evaluated *in vitro* the biocompatibility of the scaffolds embedded with three types of cells (MSCs, NPs and SH-SY5Y cells), followed by an *in vivo* preliminary evaluation.

MSC and NP graft after SCI

MSC and NP beneficial effects in SCI condition have been extensively studied by several authors (Assinck et al., 2017; Coutts and Keirstead, 2008). Also, in our laboratory, we have demonstrated that MSCs transplanted into the injured murine spinal cord are able to penetrate into the lesion area reducing the lesion volume and improving the functional recovery through a neurotrophic role rather than a cellular substitution (Boido et al., 2014b). On the other hand, NPs can integrate into the host lesioned tissue and differentiate into neurons, as demonstrated by cell positivity for neuronal markers (Boido et al., 2011); moreover they can also secrete neurotrophic factors and immunomodulatory molecules, and consequently reduce the glial cyst and promote SCI functional recovery (Boido et al., 2009; Boido et al., 2011). Moreover, we also demonstrated that the combined graft of MSCs and NPs exerts a synergistic effect both in terms of lesion volume reduction and locomotor functional recovery (Boido et al., 2014a). However, despite the obtained results, the number of survived NPs and MSCs was generally low: indeed, depending on the experimental conditions, the percentage of surviving cells after graft ranged between 1% to 30%. This means that the majority of transplanted cells do not survive after graft, probably due to the adverse conditions present in the spinal cord injury site.

In this context, a therapeutic strategy based on the scaffold use can represent a powerful approach to ameliorate the injured microenvironment and maximize cell survival (Agbay et al., 2016; Kubinová and Syková, 2012). For these reasons, we decided to combine the therapeutic potential of stem cells with the beneficial effects of different biomaterials.

Innovative inj-bioPU hydrogel production

Different polyurethane (PU) hydrogel formulations are now emerging as promising biomaterials to deliver stem cells for the SCI treatment. They can be made of polyethylene glycol (PEG), that *in vitro* has been demonstrated to support bone marrow stromal cell survival and adhesion, and to inhibit free radical production (Comolli et al., 2009; Luo et al., 2002). Since different technical problems related to their production still remain unsolved, an implementation of PU synthesis is required to improve their properties as stem cells delivery system and its possible clinical translationality.

Here we proposed a new biomimetic PU (fabricated in DIMEAS laboratory of Politecnico of Torino, thanks to the collaboration with Dr. Tonda-Turo C and Prof. Ciardelli G.), produced by a mixture of an amphiphilic PEG-based macrodiol, an aliphatic diisocyanate and an aliphatic diamine/diol chain extender (Boffito et al., 2016). With respect to conventional biodegradable polymers (Straley et al., 2010), the inj-bioPU here tested present some additional key features: i) the possibility to control its degradation rate (30-40 days), ii) tailored mechanical properties to better resemble the elastic module of the spinal cord tissue, and iii) the ability to covalently incorporate peptides in the macromolecular chains mimicking the ECM composition in order to enhance its bioactivity and in particular cell adhesion ability. Moreover, we took advantage of an injectable solution that is soluble in aqueous media, (such as physiological solution and culture medium) and that undergoes a sol-gel transition forming a 3D hydrogel at 37° C thanks to its thermosensitive behaviour. This physical transition is a fundamental property because it allows the operator i) to encapsulate cells in polymer aqueous solution and then ii) to inject it with a minimal invasiveness, prior to its in situ jellification. Moreover, thanks to the hydrogel long-term stability in water media at 37° C, it could potentially prolong cell survival until their integration into the host parenchyma.

Inj-bioPU hydrogel *in vitro* testing

Therefore, we exploited all the described biomaterial features to test *in vitro* MSC, NP and SH-SY5Y cell survival into the new inj-bioPU formulation proposed. However, when grown inside the inj-bioPU hydrogels, all type of cells died at DIV-1-2-5 and 7, while when plated near the hydrogel they were able to survive only for few hours.

Indeed PU biocompatibility has been reported both *in vitro* and *in vivo* with contrasting results (Hsieh et al., 2015; Ritfeld et al., 2014). Ritfeld and coll. (2014) reported that the PU-based reverse thermal gel protected bone marrow stromal cells from hydrogen peroxide-mediated death with an

increased cell survival and a decreased apoptosis: however, due to the different formulation, such results are not completely comparable to what we observed. Instead, the cellular debris that we observed inside the hydrogel partially resemble those found by Cole A and Shi R who tested the focal application of a PEG solution directly on isolated spinal cords (Cole and Shi, 2005): in this case the PEG solution induced an irreversible compound action potential reduction in both uninjured and compressed spinal cords indicating its toxicity after a 25 minutes exposure. The authors hypothesized that PEG toxicity could depend on PEG concentration and size, time of exposure and local oxygen and glucose deprivation caused by the solution, even if they were more inclined to possible anatomical compression caused by PEG application.

As concerns our inj-bioPUs, we can exclude an occurring oxygen and glucose deprivation, since, when tested on HaCaT keratinocyte cells, C2C12 muscle cells and human fibroblast cell line the cytocompatibility was > 80% for all the cells (Boffito et al., 2016). Therefore the high cytotoxicity observed can be ascribed to different concomitant aspects, related to cell type in combination with intrinsic hydrogel properties. The inj-bioPU production mainly consists of an acidification step, but if the acidic residuals are not correctly removed, they may be toxic for the cells. We cannot exclude that primary cultures/neurons could be more sensitive compared to other cell types [(as cell lines previously tested;(Boffito et al., 2016)]. These possibilities could explain both the cellular debris inside the hydrogel but also the rapid decrease in cell viability observed near the hydrogel, where the absence of a direct contact with the inj-bioPUs probably delayed cell death. Therefore, this result suggests that further improvement of inj-bioPU production steps are required to generate a material compatible with every cell type.

Innovative formulation of chitosan (CS) hydrogel

While waiting for the optimization of inj-bioPU synthesis, we decided to test another innovative biomaterial formulation based on CS, again realized by Dr. Tonda-Turo C. and Prof. Ciardelli G. (Politecnico of Torino).

CS is already known as a promising biomaterial for tissue engineering both in SCI and in peripheral nerve injury (Gnavi et al., 2013). Indeed, it has been revealed particularly suitable for tissue engineering thanks to its biocompatibility, non-toxicity and biodegradability, with a molecular structure similar to the one of glycosaminoglycans, the main polysaccharides components of the ECM. This feature makes this biomaterial one of the best substitute to fill the gap created by the spinal cord lesion as it can be tailored to well resemble the natural property of the host neural tissue. Several studies have employed CS to test different scaffold formulations like nanofibers, tubes,

channels or conduits in order to guide and promote axon regeneration after SCI (Kim M, Park SR, 2014).

Here we proposed a new CS formulation that combines CS intrinsic property with the main advantage to create a hydrogel solution at physiological pH. Compared to rigid/semi-rigid scaffolds, hydrogels present a high-water content and a viscoelasticity closed to the one of living tissue that can be adjusted to better resemble spinal cord mechanical property. However, the physical and mechanical stability of CS based materials in aqueous solutions is limited and crosslinking agents are required to increase CS performances in a biological environment (Ruini et al., 2015). Therefore, we realized a new formulation that allows to solubilize CS for obtaining a hydrogel at physiological pH. Since solubilization only occurs at acidic pH, we exploited the property of the β-glycerophosphate to maintain the biomaterial in the hydrogel formulation at physiological pH, a necessary condition to create an adequate environment for cell survival. β-glycerophosphate has also the ability to avoid CS precipitation and so the possible release of biomaterial residuals. Moreover, this salt makes the CS hydrogel thermosensitive: at 10° C, it is a solution in which easily encapsulating cells, while at temperature > 25° C it becomes a gel thus ensuring the jellification at physiological pH with low viscosity. Compared to other CS scaffolds, the formulation here used also simplifies CS *in vivo* injection, thus rendering this innovative formulation an optimal tool for SCI treatment *in vivo*.

MSC, NP and SH-SY5Y cell survival and differentiation on CS hydrogel

We showed that both MSCs, NPs and SH-SH5Y cells were able to survive both inside and near the CS hydrogel until 7 days *in vitro*. The ability of β-glicerolophosphate to create a sol-gel scaffold maintaining the physiological pH renders our formulation particularly suitable for cell growth. β-glicerolophosphate has been already used to improve embedded cell survival in different application fields : however, with respect to the other CS formulations that employed β-glicerolophosphate (Cruz-Neves et al., 2017; Dang et al., 2017; Deng et al., 2017), we are able to guarantee the production of a physiological solution perfectly suitable for cell survival compared to the acid hydrogel generally employed. Indeed, even if some cells can survive at low pH in experimental conditions, such kind of solution could be never employed in clinics, thus rendering our formulation also perfectly suitable for future therapeutic applications.

One technical limit we encountered was the CS turbidity that sometimes made difficult cell visualization. Such a problem is typical of the hydrogel formulation, but we easily solved it by cutting the biomaterial in thin sections to obtain well-defined cell images. In this way a cell

counting was possible, revealing that a comparable number of cells was present both in presence of CS and in normal condition. We were also able to find MSCs grown on our CS hydrogel showing a fibroblast like morphology resembling that observed in standard *in vitro* culture (Boido et al., 2014b), confirming that CS does not alter the cell growth.

However, it should be noticed that in our *in vitro* experiments, SH-SY5H cells and MSCs seemed to be more numerous than NPs: such a difference can be explained by a more resistant phenotype of MSCs and SH-SY5Y cells. As neuroblastoma cell line, SH-SY5Y cells are often used for *in vitro* experiments as more resistant compared to primary culture cells. On the other hand, compared to MSCs (that are maintained *in vitro* for at least 2 weeks before hydrogel encapsulation), NPs probably experienced a higher stress when put in contact with CS immediately after cell dissociation. This can explain their lower number compared to MSCs and SH-SY5Y cells *in vitro*, and the similar results later obtained *in vivo*. In any case, even at lower extent, we were able to visualize NPs both inside and near the CS hydrogel as reported in literature for different CS scaffolds [CS membranes, fibers or multifunctional films; (Fang et al., 2010; Skop et al., 2016; Yang et al., 2010a)]. Moreover, NPs also emitted some neuritis, confirming the good CS biocompatibility. Similar results were obtained when rat NSC neurospheres cultured in presence of CS membrane were found to migrate and elongate their neurites, thus suggesting that CS does not prevent NSC initial differentiation (Yang et al., 2010a), as we also observed.

Therefore, since MSCs revealed a cell survival rate higher than NPs in presence of CS, we decided to better investigate CS biocompatibility and properties only with MSCs. Both MTT and calcein assays (common colorimetric assays to verify cell viability) did not reveal any difference between CTRL+ cells (grown without CS) and MSCs grown within CS, thus further consolidating our preliminary observations. Therefore, the CS hydrogel here proposed seems to be an optimal culture condition component that does not alter the normal cell processes.

Based on these observations, we carried out other *in vitro* experiments to verify whether the CS presence could alter the therapeutic efficacy of MSCs.

Assessment of MSC therapeutic efficacy on CS hydrogel

Consistently with the observed higher survival rate of MSCs, we decided to evaluate their activity on CS hydrogel. MSCs, maintaining their stem cell properties, can exert a beneficial role through their neurotrophic activity. Indeed one mechanism of action of MSCs consists in the secretion of bioactive substances such as MVs/exosomes that contain a great variety of biologically active molecules like lipids, proteins, growth factors and miRNAs (Forostyak et al., 2013). MV beneficial

role have been already demonstrated in lethal model of acute kidney injury or ischemic-reperfusion kidney injury, where their release from MSCs exerts a pro-survival effect both *in vitro* and *in vivo* (Bruno et al., 2012; Gatti et al., 2011). Also in SCI studies, the MSC ability at the lesion site to modulate the immune system, prevent apoptosis, promote angiogenesis and proliferation has been attributed to exosome release (Joyce et al., 2010). In agreement with this idea, we evaluated whether the CS presence could alter MV release from MSCs. The DLS analysis revealed the presence of MVs both in the supernatant of normally grown MSCs and in that one collected from MSCs plated into CS hydrogel. This result seems to indicate that CS hydrogel does not affect MSC neurotrophic activity, suggesting CS as a potential vehicle to deliver MSCs, a continuously producing source of trophic factors.

Different types of scaffolds (cryogels, fibers, biomimetic pullulan-collagen hydrogels) have been already demonstrated to sustain the release of growth factors, cytokines, anti-inflammatory and proangiogenic factors, in some cases with different efficiency depending on the biomaterial concentration (Pumberger et al., 2016; Thomas et al., 2014). However, we are the first to demonstrate that the CS hydrogel here proposed supports MSC ability to release MVs.

Moreover, one of the MSC-mediated effects in case of SCI consists in the reduction of cell oxidative stress (Forostyak et al., 2013), partly as a consequence of MV release: therefore we evaluated MV functional activity inside the CS hydrogel. The oxidative stress (induced by H_2O_2) of SH-SY5Y cells grown in a culture medium containing "MSCs + CS" or "MSCs" supernatant was significantly reduced in both conditions compared to CTRL+ (SH-SY5Y in stress condition), suggesting that CS does not alter the possible paracrine therapeutic efficacy of MSCs.

Moreover, even if at lower extent, interestingly in our experiment also the supernatant of CS hydrogel alone was able to reduce the cellular stress, suggesting that CS hydrogel could additionally exert a beneficial effect thanks to its intrinsic properties. Indeed it has been shown that CS can protect adipose-derived MSCs (previously treated with H_2O_2) increasing cell viability both *in vitro* and *in vivo* by reducing ROS species (Liu et al., 2012b). Therefore, CS intrinsic properties should be considered as additional positive effects in combination with the potential of stem cells.

Altogether these results suggest that the CS hydrogel here tested do not negatively influence the activity and functionality of the MVs produced by MSCs, suggesting their possible therapeutic efficacy.

MSC and NP transplantation on CS hydrogel *in vivo*

Considering the encouraging results obtained *in vitro*, we decided to inject MSCs embedded in CS in SCI mouse to preliminarily evaluate their survival *in vivo* and to test the technical feasibility of CS injection. Indeed, it is known that cell encapsulation into biomaterial scaffolds yields additional effects compared to the biomaterials/cells alone (Chen et al., 2011). We observed numerous survived cells both inside and around CS: apparently MSCs were even more abundant than in our previous papers (Boido et al., 2014a; Boido et al., 2014b; Boido et al., 2014c) suggesting that the CS hydrogel here proposed could (even most efficiently) support cell survival in a hostile environment represented by the injury site.

As natural biomaterial, CS has been already demonstrated to be highly biocompatible: after SCI and peripheral nerve injury, different CS scaffold implantation were able to assure MSC survival even for long periods in comparison to other biomaterials or to cell transplantation alone (Chen et al., 2011; Kim et al., 2016; Zhu et al., 2015). Indeed, the surviving cells we observed can be ascribed to CS intrinsic beneficial properties. It has been demonstrated that the *in vivo* increased cell survival of MSCs in the presence of CS is due to its ability to increase the autophagic response and cell metabolic activity (Tseng et al., 2016). Another option is that CS could improve MSC cell survival through ROS scavenging and chemochine recruitment compatible to our *in vitro* observation on SH-SY5Y cells. Also the hydrogel three-dimensional structure could have further contributed to support MSC survival. Indeed, the highly swollen and porous network typical of hydrogel can support the exchange of nutrients with the surrounding tissue (Straley et al., 2010).

Moreover, MSCs were found both around and inside the lesion, suggesting that the CS hydrogel here proposed does not affect the normal cellular behaviour and probably help a better integration into the host tissue. Such a feature seems to be particularly dependent on the CS employed: in fact other CS formulations only support a small number of NPs in the host tissue colonization (Bozkurt et al., 2010).

In vivo CS applications showed contrasting results: after SCI, some authors reported positive effects (Chedly et al., 2017b; Kim et al., 2016), but others refer negative results [no functional improvements; (Bozkurt et al., 2010; Nomura et al., 2008)]. Such discrepancies seem to be related to the intrinsic properties of the scaffold employed. Indeed, assuring a sufficient biomaterial degradation time is a key point to allow both cell survival and scaffold functionality, as demonstrated by the bridging defect observed in SCI patients due to the complete CS disintegration in the post-operative phase (Amr et al., 2014). Among the possible strategies, the physical and mechanical stability of CS formulations can be enhanced by cross-linking agents to the biomaterial

of interest as we proposed here by adding β-glicerophosphate. Indeed another advantage of our CS compound is that it presents a degradation time of 2 months that seems sufficient to efficiently support cell survival and scaffold functionality in the hostile environment of SCI. However further experiments are needed to confirm such hypothesis.

Another essential feature that a good biomaterial should accomplish is to be perfectly integrated inside the host tissue, without triggering an immune reaction. This is particularly important in SCI condition where it should be avoided to exacerbate the inflammatory reaction already triggered by the lesion. Therefore, compared to the synthetic biomaterials, the natural ones represent the best choice to perfectly adapt to the host spinal parenchyma thanks to their physical-chemical properties. Indeed, based on our experience (Boido et al., 2014b), at 7 days after CS injection we did not reveal an increased immune response/inflammation process in proximity to the lesioned area. Despite immune reactions are generally reported for synthetic devices (Kim M, Park SR, 2014), contrasting results have been observed also for natural biomaterials, probably depending on the structure and on the synthesis of the scaffold itself (Bozkurt et al., 2010; Li et al., 2017). Although we did not perform a GFAP quantification to evaluate the inflammation process, it did not seem to be different from our previous experiments (Boido et al., 2014b), indicating the biocompatibility of our formulation.

Therefore, with respect to other CS scaffolds, the demonstrated biocompatibility and integration of the CS formulation here proposed can be exploited in an innovative and particularly suitable manner for SCI treatment. Indeed, i) the biodegradability, ii) the immune tolerance and iii) the capability of maintaining an adequate physiological environment for cell survival makes this CS hydrogel a promising candidate for further analysis.

Properties of a new nanofiber scaffold

As emerging scaffolds in tissue engineering, we also decided to test the biocompatibility of new nanofibers recently generated by our collaborators (Tonda-Turo et al., 2016), with the final aim to implant these scaffolds in combination to the tested hydrogels. Here we would like to exploit the benefits of new nanofiber membranes synthetized starting from different components, poly (ε-caprolactone) diol (PCL) plus 1,2-dichloroethane (DCE), 1,4-diisocyanatobutane and N-Boc serinol (Tonda-Turo et al., 2016). Although two different techniques are documented for nanofiber fabrication, we employed the well-established electrospinning method that allows to produce high surface area-to-volume ratio nanofibers, a feature that contributes to improve cell attachment, proliferation and differentiation. The electrospun nanofibers are fabricated from a liquid solution

that is fed through a capillary tip into a high electric field. In this way, a thin jet is generated and the solution evaporated to form solid nanofibers on a collector (Guo et al., 2014b). Therefore, we obtained a polymer innovative for its flexibility thanks to its synthetic nature that guarantees easy processability and high reproducibility. In order to support and facilitate axon elongation after SCI, we combined the nanofiber geometric character with the intrinsic property of PCL that renders this biomaterial mechanically soft thus mimicking the nature of the spinal cord tissue.

To further facilitate cell adhesion, growth and differentiation, biomimetic biochemical cues were covalently linked to the polymeric chain of PCL nanofibers after scaffold fabrication: this was assured by the functionalization process with the ECM resembling peptide (IKVAV), a component of the novel self-assembling peptide class, already employed to improve nanofiber biocompatibility and cell elongation. Moreover, the 3D structure realized to fully accommodate the whole cell body in all dimensions, was enriched by random and aligned nanofibers synthetization over the scaffold.

Therefore, with respect to other scaffolds type, the innovation of the nanofibers here proposed consists in the combination of geometrical and 3D structure properties with the higher PCL flexibility, required to well fit with the spinal cord tissue.

MSC *in vitro* survival on nanofiber membrane

We firstly tested *in vitro* the biocompatibility of the new nanofiber membranes in presence of MSCs. In comparison to most common synthetic biomaterials, the PCL chosen for the nanofiber synthesis presents numerous advantages including higher biocompatibility, high mechanical strength and flexibility, slow degradation rate, low cost and easy processability. Moreover, in order to improve its hydrophilicity, PCL can be cross-linked with other peptides (such as laminin and collagen) that provide better differentiation and survival properties (Bagher et al., 2016; Silva et al., 2004).

The cells seeded on the nanofibers here proposed were able to grow until 7 days, with a visible increased proliferation during time both on random (functionalized or not) and on aligned (functionalized or not) nanofibers. The good cell rate observed in all the conditions tested suggests the optimal biocompatibility of our formulation. However, surprisingly, the MSC proliferation in presence of functionalized nanofibers was reduced compared to the other conditions: this can be partly explained by the high IKVAV nanofiber affinity for Nissl staining that probably caused an underestimation in cell counting and that did not allow us to appreciate the expected difference between IKVAV and non-functionalized nanofibers. Indeed, it is known that IKVAV peptide not only improves cell viability but also the adherence rate of different cell types (like PC12 cells,

MSCs and NPs) both with respect to flat control scaffolds (Wu et al., 2006; Wu et al., 2010) and to other functionalizing peptides (Bagher et al., 2016; Silva et al., 2013) (Chevallay and Herbage, 2000).

As concerns the nanofiber geometry, we observed that MSCs tend to better grow on aligned nanofibers: indeed on aligned fibers, the cells are able to easily elongate, since they do not meet barriers that are created by the misalignment of the random nanofibers (Prabhakaran et al., 2013). Specific molecular mechanisms seem to be implicated in how cells adapt and interact with nanofibers: it has been demonstrated that the MSC increased elongation on aligned nanofibers is due to an upregulation of focal adhesion kinases that are less expressed when cells are grown on random nanofibers (Andalib et al., 2016). If the kinase expression was silenced, the cell elongation was reverted, suggesting that cells can specifically express preferences based on the biomaterial typology. However, cell orientation on aligned nanofibers is known to be also dependent on the biomaterial geometry and in particular on the fiber diameter. Indeed, it has been reported that a lower Schwann cell proliferation on aligned gelatin fibers compared to the random ones is probably due to the fewer focal adhesion points of the scaffold (Gnavi et al., 2015).

Therefore, the combination of PCL material properties, functionalization and geometric feature of the new nanofibers here proposed make them a valid substrate for efficiently supporting cell growth, and potentially for acting into the lesion cavity as a bridge that can guide the growth/orientation of transplanted cells.

Nanofiber membrane implantation in a SCI mouse

In order to exploit the nanofiber potential, we preliminary tested nanofiber membrane biocompatibility after *in vivo* implantation. The PCL aligned-IKVAV nanofiber membrane here proposed was perfectly integrated into the lesion spinal cord after one week as shown by the host cellular colonization all over the scaffold. These results further confirm the PCL material biocompatibility also *in vivo*, as expected from our results *in vitro*.

Moreover, an essential feature of a new implantable scaffold is its mechanical strength and flexibility. Due to the complex nature of the lesion and partial axon transections often found in the SCI area, the implantation of a rigid scaffold could be surgically complicated and finally detrimental. Indeed, many biomaterial scaffolds are highly rigid and hardly pliable thus affecting the proper placement and adjustment within the injured spinal cord and risking to further compress the tissue. Different biomaterials have been already demonstrated to completely integrate into the host tissue after SCI, even for long periods (Gelain et al., 2011; Nguyen et al., 2017; Palejwala et

al., 2016). However, depending on the biomaterial properties, not all of them can support a proper cell integration and axon growth, as demonstrated by the limited number of nerve fibers found over CS conduits 12 weeks after SCI (Chen et al., 2011). This suggests the geometrical superiority of nanofibers that facilitates its integration into the spinal parenchyma probably thanks to the scaffold alignment resembling the orientation of host axons. Therefore, both the geometrical superiority and the great flexibility of the PCL nanofibers here proposed render them the ideal scaffold to fill the lesion gap, with a minimal invasive implantation. Indeed, one week after the graft, we were able to find host cells elongating over the nanofibers (MAP2 positive cells), thus suggesting that i) its flexibility does not damage the tissue and ii) can promote tissue regeneration.

Notably, after SCI, the combination of a proper guiding scaffold (to orientate axons towards the correct direction) with MSC graft could further promote the regeneration process (Schaub et al., 2016). Moreover, compared to cell transplantation alone, nanofibers present great advantages in guiding the transplanted cells towards a better growth and differentiation. NSCs showed higher differentiation ability (NeuN or MAP2 positive cells) when transplanted *in vivo* on nanofiber scaffolds compared to cell engraftment alone (Ye et al., 2016), also supporting a better functional recovery. Therefore, consistently with our *in vitro* and *in vivo* results, PCL nanofibers features can be exploited to combine the beneficial effect of MSCs implantation with the bridge structure of the nanofibers that creates a favourable environment for tissue regeneration.

Another advantage of nanofibers is that they are generally characterized by high porosity that can be modified to better support neural growth, reduce the number of infiltrating cells and prevent the glial scar formation. Although the immunogenicity is related to the biocompatibility of the material, it is also determined by the geometry and chemical properties of the nanofibers. Therefore, by reducing nanofiber diameter (notably the size of the nanofibers here proposed is 2.8 ± 0.6 μm)), a lower intrinsic immunogenicity than the traditional macroscale scaffolds can be achieved, thereby showing an excellent biocompatibility with the host tissue (Guo et al., 2014a).

To be considered completely biocompatible, biomaterials should not trigger an inflammatory reaction that in turn would be responsible of scaffold rejection and tissue degeneration. Although generally well tolerated, some biomaterials can induce a sustained astrogliosis as demonstrated by abundant reactive astrocytes grown over and at the border of channel scaffolds after *in vivo* implantation in the SCI environment (Bozkurt et al., 2010; Palejwala et al., 2016). Regarding nanofibers, contrasting data are present in literature probably due to the different biomaterial composition and geometry of PCL nanofibers. As demonstrated by Nguyen and coll., PCL-aligned nanofibers did not attract immune cells *in vivo* as indicated by a comparable microglia and astrocyte density between the scaffold and the control group (Nguyen et al., 2017). However, a different PCL

nanofiber formulation has been described to create an intense glial scar that surrounded the scaffold area (Raspa et al., 2016). Therefore, we also analysed the astrocytic response (GFAP positive cells) into the lesion area: the astrogliosis observed was compatible with the inflammatory reaction normally occurring after SCI, and did not seem increased by the scaffold presence thus suggesting the biocompatibility and integration of the new nanofiber membrane here employed. Additionally, Tysseling et al., demonstrated that 24h after SCI, peptide amphiphile-IKVAV nanofibers were even able to reduce astrogliosis and promote axon elongation (Tysseling-Mattiace et al., 2008). Based on these observations, further analyses are needed to also evaluate the potential of our IKVAV-nanofiber membrane in reducing the glial scar formation, thus facilitating the regenerative process.

In conclusion we showed that, with the exception of inj-bio-PUs, the innovative CS and nanofiber formulations here proposed resulted biocompatible for MSC, NP and SH-SY5Y cell growth/integration and well immune tolerated when implanted *in vivo*. Although further analyses are needed to confirm and better characterize CS and nanofiber efficacy *in vivo*, both scaffolds appear promising in the treatment of SCI. Moreover, our final aim will consist in a combined approach, implanting into the injured spinal cord both nanofibers and stem cells embedded into the hydrogel: indeed in this way, we could obtain a double effect deriving by a protective environment (assured by the hydrogel) for MSC survival/neurotrophic activity and by the presence of nanofiber membrane acting as a bridge to promote host axon elongation and guide stem cell orientation.

4 CONCLUSIONS AND FUTURE PERSPECTIVES

The aim of this PhD thesis was to explore new potential therapeutic strategies applicable for SCI. Despite injured neurons try to regenerate after SCI, their attempts fail because of a non-permissive regrowth environment, thus leading to the functional sensorimotor deficits affecting the quality of life of millions people. Several therapeutic interventions, from cell replacing to gene therapy, are under investigation, to date without a definitive solution. Therefore, the big challenge of action regeneration failure encourages the investigation of innovative strategies to support and promote this process. Here we proposed two different and original experimental approaches in order i) to better understand the intrinsic potential of axon regeneration and ii) to facilitate it with the help of technological devices.

miRNAs are recognized as one of the most powerful inner regulatory system whose manipulation can be exploited as a strategy to revert SCI pathological mechanisms partly due to their dysregulation. Indeed, some strategies that specifically target one single miRNA or a specific set of miRNAs have been already revealed as successful approaches to promote functional recovery after SCI. Although the list of miRNAs functionally involved in axonal regrowth is long in literature, here we aimed at identifying miRNAs whose precocious dysregulation after SCI could be targeted to reactivate/increase the intrinsic axon regeneration potential. By analysing the CSMN mirRNA dysregulation, we identified one promising miRNA candidate, miR-7b-3p, whose upregulation after SCI seems directly related to the trauma. To confirm this, we will further investigate its role in regeneration and neuroprotection in an *in vitro* model of axotomy. In addition, we are also going to validate the predicted targets of this miRNA in order to elucidate the reason of its overexpression after SCI. Despite the manipulation of one single miRNA cannot be considered the most effective therapeutic strategy, our results will also allow to better understand miRNA mechanisms of action and add new elements to the miRNA complex networks. Therefore, in this context, miR-7b-3p should be considered a new possible target for SCI therapy.

An alternative promising strategy to promote axon regeneration is the employment of biomimetic materials. In SCI, the beneficial effects of several biomaterial devices have been already described, each one with its specific advantages and defects mainly dependent on the feature of the biomaterial composition and its geometry. However, their clinical application is still limited due to several technical problems mainly related to the biomaterial production. Here we tested innovative biomaterial formulations, that we finally intend to use in combination with stem cells, in order to exploit their respective properties and to boost their therapeutic effects. The innovative formulation

of the CS hydrogel here tested allows to embed stem cells into a solution at physiological pH, an essential condition to allow a long-lasting cell survival in the hostile SCI environment. Thanks to this feature, our encouraging experimental results gets this formulation closer to a future clinical application with respect to the acidic hydrogels and the rigid scaffolds generally employed in SCI studies. Moreover, since biomaterial mechanical strength is an essential feature for scaffold clinical application, we also exploited PCL to create soft nanofibers that better resemble the native structure of spinal cord. Its high biocompatibility and its good immune tolerance make this scaffold perfectly suitable for future clinical application. Indeed nanofibers present the great advantage to guide the regenerating axons towards the correct direction thanks to their aligned geometry and small diameter.

Therefore, consistently with the good *in vitro* results obtained we are now consolidating the preliminary *in vivo* results both for the CS hydrogel and for the aligned-nanofibers with the aim to combine their implantation with the stem cell graft into the injured spinal cord.

In conclusion, although at different extent, both miRNAs and biomaterial scaffolds are now emerging as new potential strategies for SCI application. A better comprehension of miRNAs dysregulation after SCI and a continuously improvement in biomaterial properties and composition are essential features to allow their translationality for a future clinical application.

ACKNOWLEDGEMENTS

First of all I want to thank my tutor, Professor Alessandro Vercelli, for welcoming me in his research team and making these projects possible. Thank you for supporting me in an active and independent research that made me growth as a person and as a “scientist”.

I also would like to thank Dr. Marina Boido who took me under her supervision from my master degree and taught me how research should be faced. Thank you for your patience and your contribution to my research.

Then I would like to thank all my colleagues for their significant contributions to this research. First of all, thank to Elena S. and Gaia B., who passionately showed me the big and new world of molecular biology. Thanks to all the students, especially Soraya who actively contributed to the data presented.

Then I’m grateful to Dr. Darrell Green, Dr. Irina Mohorianu, Professor Tamas Dalmay, Dr. Meritixcell Pons, Professor Davide De Pietri Tonellli, Dr. Chiara Tonda-Turo and Professor Gianluca Ciardelli who collaborated to these projects with their great experience.

Thank all for guiding me in this challenging experience.

BIBLIOGRAPHY

Abematsu, M., Tsujimura, K., Yamano, M., Saito, M., Kohno, K., Kohyama, J., Namihira, M., Komiya, S. and Nakashima, K. (2010). Neurons derived from transplanted neural stem cells restore disrupted neuronal circuitry in a mouse model of spinal cord injury. *J. Clin. Invest.* **120**, 3255–66.

Agbay, A., Edgar, J. M., Robinson, M., Styan, T., Wilson, K., Schroll, J., Ko, J., Khadem Mohtaram, N., Jun, M. B.-G. and Willerth, S. M. (2016). Biomaterial Strategies for Delivering Stem Cells as a Treatment for Spinal Cord Injury. *Cells Tissues Organs* **202**, 42–51.

Ahmed, S. (2009). The culture of neural stem cells. *J. Cell. Biochem.* **106**, 1–6.

Ahuja, C. S., Wilson, J. R., Nori, S., Kotter, M. R. N., Druschel, C., Curt, A. and Fehlings, M. G. (2017). Traumatic spinal cord injury. *Nat. Rev. Dis. Prim.* **3**, 17018.

Amr, S. M., Gouda, A., Koptan, W. T., Galal, A. A., Abdel-Fattah, D. S., Rashed, L. A., Atta, H. M. and Abdel-Aziz, M. T. (2014). Bridging defects in chronic spinal cord injury using peripheral nerve grafts combined with a chitosan-laminin scaffold and enhancing regeneration through them by co-transplantation with bone-marrow-derived mesenchymal stem cells: Case series of 14 patient. *J. Spinal Cord Med.* **37**, 54–71.

Andalib, M. N., Lee, J. S., Ha, L., Dzenis, Y. and Lim, J. Y. (2016). Focal adhesion kinase regulation in stem cell alignment and spreading on nanofibers. *Biochem. Biophys. Res. Commun.* **473**, 920–925.

Anderson, T. E. (1982). A controlled pneumatic technique for experimental spinal cord contusion. *J. Neurosci. Methods* **6**, 327–33.

Ankeny, D. P., McTigue, D. M. and Jakeman, L. B. (2004). Bone marrow transplants provide tissue protection and directional guidance for axons after contusive spinal cord injury in rats. *Exp. Neurol.* **190**, 17–31.

Ansorena, E., De Berdt, P., Ucakar, B., Simón-Yarza, T., Jacobs, D., Schakman, O., Jankovski, A., Deumens, R., Blanco-Prieto, M. J., Préat, V., et al. (2013). Injectable alginate hydrogel loaded with GDNF promotes functional recovery in a hemisection model of spinal cord injury. *Int. J. Pharm.* **455**, 148–158.

Arlotta, P., Molyneaux, B. J., Chen, J., Inoue, J., Kominami, R. and Macklis, J. D. (2005). Neuronal Subtype-Specific Genes that Control Corticospinal Motor Neuron Development In Vivo. *Neuron* **45**, 207–221.

Assinck, P., Duncan, G. J., Hilton, B. J., Plemel, J. R. and Tetzlaff, W. (2017). Cell transplantation therapy for spinal cord injury. *Nat. Neurosci.* **20**, 637–647.

Awad, B. I., Carmody, M. A. and Steinmetz, M. P. (2015). Potential Role of Growth Factors in the Management of Spinal Cord Injury. *World Neurosurg.* **83**, 120–131.

Azbill, R. D., Mu, X. and Springer, J. E. (2000). Riluzole increases high-affinity glutamate uptake in rat spinal cord synaptosomes. *Brain Res.* **871**, 175–80.

Bagher, Z., Azami, M., Ebrahimi-Barough, S., Mirzadeh, H., Solouk, A., Soleimani, M., Ai, J., Nourani, M. R. and Joghataei, M. T. (2016). Differentiation of Wharton's Jelly-Derived

Mesenchymal Stem Cells into Motor Neuron-Like Cells on Three-Dimensional Collagen-Grafted Nanofibers. *Mol. Neurobiol.* **53**, 2397–2408.

Bakshi, A., Barshinger, A. L., Swanger, S. A., Madhavani, V., Shumsky, J. S., Neuhuber, B. and Fischer, I. (2006). Lumbar puncture delivery of bone marrow stromal cells in spinal cord contusion: a novel method for minimally invasive cell transplantation. *J. Neurotrauma* **23**, 55–65.

Barca-Mayo, O. and De Pietri Tonelli, D. (2014). Convergent microRNA actions coordinate neocortical development. *Cell. Mol. Life Sci.* **71**, 2975–2995.

Bartel, D. P. (2004). MicroRNAs: genomics, biogenesis, mechanism, and function. *Cell* **116**, 281–97.

Becker, D., Sadowsky, C. L. and McDonald, J. W. (2003). Restoring function after spinal cord injury. *Neurologist* **9**, 1–15.

Beckers, M., Mohorianu, I., Stocks, M., Applegate, C., Dalmay, T. and Moulton, V. (2017). Comprehensive processing of high-throughput small RNA sequencing data including quality checking, normalization, and differential expression analysis using the UEA sRNA Workbench. *RNA* **23**, 823–835.

Bélanger, M., Drew, T., Provencher, J. and Rossignol, S. (1996). A comparison of treadmill locomotion in adult cats before and after spinal transection. *J. Neurophysiol.* **76**, 471–91.

Bhalala, O. G., Pan, L., Sahni, V., McGuire, T. L., Gruner, K., Tourtellotte, W. G. and Kessler, J. A. (2012). microRNA-21 regulates astrocytic response following spinal cord injury. *J. Neurosci.* **32**, 17935–47.

Blesch, A. and Tuszynski, M. H. (2003). Cellular GDNF delivery promotes growth of motor and dorsal column sensory axons after partial and complete spinal cord transections and induces remyelination. *J. Comp. Neurol.* **467**, 403–17.

Blow, M. J., Grocock, R. J., van Dongen, S., Enright, A. J., Dicks, E., Futreal, P. A., Wooster, R. and Stratton, M. R. (2006). RNA editing of human microRNAs. *Genome Biol.* **7**, R27.

Boffito, M. polyurethane-based thermosensitive hydrogels as drug release and tissue engineering platforms: design and in vitro characterization, Gioffredi, E., Chiono, V., Calzone, S., Ranzato, E., Martinotti, S. and Ciardelli, G. (2016). Novel polyurethane-based thermosensitive hydrogels as drug release and tissue engineering platforms: design and *in vitro* characterization. *Polym. Int.* **65**, 756–769.

Boido, M., Rupa, R., Garbossa, D., Fontanella, M., Ducati, A. and Vercelli, A. (2009). Embryonic and adult stem cells promote raphespinal axon outgrowth and improve functional outcome following spinal hemisection in mice. *Eur. J. Neurosci.* **30**, 833–46.

Boido, M., Garbossa, D. and Vercelli, A. (2011). Early graft of neural precursors in spinal cord compression reduces glial cyst and improves function. *J. Neurosurg. Spine* **15**, 97–106.

Boido, M., Niapour, A., Hossein, S., De Amicis Elena, Matilde, G. and Vercelli, A. (2014a). "Combined Treatment by Cotransplantation of Mesenchymal Stem Cells and Neural Progenitors with Exercise and Enriched Environment Housing in Mouse Spinal Cord Injury," Advances in Stem Combined Treatment by Cotransplantation of Mesenchymal Stem C. **2014**,.

Boido, M., Garbossa, D., Fontanella, M., Ducati, A. and Vercelli, A. (2014b). Mesenchymal Stem Cell Transplantation Reduces Glial Cyst and Improves Functional Outcome After Spinal

Cord Compression. *World Neurosurg.* **81**, 183–190.

Boido, M., Piras, A., Valsecchi, V., Spigolon, G., Mareschi, K., Ferrero, I., Vizzini, A., Temi, S., Mazzini, L., Fagioli, F., et al. (2014c). Human mesenchymal stromal cell transplantation modulates neuroinflammatory milieu in a mouse model of amyotrophic lateral sclerosis. *Cytotherapy* **16**, 1059–1072.

Bonner, J. F., Connors, T. M., Silverman, W. F., Kowalski, D. P., Lemay, M. A. and Fischer, I. (2011). Grafted Neural Progenitors Integrate and Restore Synaptic Connectivity across the Injured Spinal Cord. *J. Neurosci.* **31**, 4675–4686.

Bouyer, L. J. (2005). Animal models for studying potential training strategies in persons with spinal cord injury. *J. Neurol. Phys. Ther.* **29**, 117–25.

Bozkurt, G., Mothe, A. J., Zahir, T., Kim, H., Shoichet, M. S. and Tator, C. H. (2010). Chitosan Channels Containing Spinal Cord-Derived Stem/Progenitor Cells for Repair of Subacute Spinal Cord Injury in the Rat. *Neurosurgery* **67**, 1733–1744.

Bracken, M. B., Shepard, M. J., Collins, W. F., Holford, T. R., Baskin, D. S., Eisenberg, H. M., Flamm, E., Leo-Summers, L., Maroon, J. C., Marshall, L. F., et al. (1992). Methylprednisolone or naloxone treatment after acute spinal cord injury: 1-year follow-up data. *J. Neurosurg.* **76**, 23–31.

Bradbury, E. J. and McMahon, S. B. (2006). Spinal cord repair strategies: why do they work? *Nat. Rev. Neurosci.* **7**, 644–653.

Bregman, B. S., Coumans, J.-V., Dai, H. N., Kuhn, P. L., Lynskey, J., McAtee, M. and Sandhu, F. (2002). Chapter 18 Transplants and neurotrophic factors increase regeneration and recovery of function after spinal cord injury.pp. 257–273.

Brock, J. H., Rosenzweig, E. S., Blesch, A., Moseanko, R., Havton, L. A., Edgerton, V. R. and Tuszynski, M. H. (2010). Local and remote growth factor effects after primate spinal cord injury. *J. Neurosci.* **30**, 9728–37.

Bruno, S., Grange, C., Collino, F., Deregibus, M. C., Cantaluppi, V., Biancone, L., Tetta, C. and Camussi, G. (2012). Microvesicles Derived from Mesenchymal Stem Cells Enhance Survival in a Lethal Model of Acute Kidney Injury. *PLoS One* **7**, e33115.

Buller, B., Liu, X., Wang, X., Zhang, R. L., Zhang, L., Hozeska-Solgot, A., Chopp, M. and Zhang, Z. G. (2010). MicroRNA-21 protects neurons from ischemic death. *FEBS J.* **277**, 4299–4307.

Cafferty, W. B. J., Duffy, P., Huebner, E. and Strittmatter, S. M. (2010). MAG and OMgp synergize with Nogo-A to restrict axonal growth and neurological recovery after spinal cord trauma. *J. Neurosci.* **30**, 6825–37.

Caron, I., Rossi, F., Papa, S., Aloe, R., Sculco, M., Mauri, E., Sacchetti, A., Erba, E., Panini, N., Parazzi, V., et al. (2016). A new three dimensional biomimetic hydrogel to deliver factors secreted by human mesenchymal stem cells in spinal cord injury. *Biomaterials* **75**, 135–147.

Casha, S., Yu, W. R. and Fehlings, M. G. (2005). FAS deficiency reduces apoptosis, spares axons and improves function after spinal cord injury. *Exp. Neurol.* **196**, 390–400.

Casha, S., Zygun, D., McGowan, M. D., Bains, I., Yong, V. W. and Hurlbert, R. J. (2012). Results of a phase II placebo-controlled randomized trial of minocycline in acute spinal cord injury. *Brain* **135**, 1224–36.

Catapano, L. A., Arlotta, P., Cage, T. A. and Macklis, J. D. (2004). Stage-specific and opposing roles of BDNF, NT-3 and bFGF in differentiation of purified callosal projection neurons toward cellular repair of complex circuitry. *Eur. J. Neurosci.* **19**, 2421–2434.

Chadborn, N. H., Ahmed, A. I., Holt, M. R., Prinjha, R., Dunn, G. A., Jones, G. E. and Eickholt, B. J. (2006). PTEN couples Sema3A signalling to growth cone collapse. *J. Cell Sci.* **119**,.

Chakrabarti, M., Banik, N. L. and Ray, S. K. (2014). MiR-7-1 potentiated estrogen receptor agonists for functional neuroprotection in VSC4.1 motoneurons. *Neuroscience* **256**, 322–33.

Chedly, J., Soares, S., Montembault, A., von Boxberg, Y., Veron-Ravaille, M., Mouffle, C., Benassy, M.-N., Taxi, J., David, L. and Nothias, F. (2017a). Physical chitosan microhydrogels as scaffolds for spinal cord injury restoration and axon regeneration. *Biomaterials* **138**, 91–107.

Chedly, J., Soares, S., Montembault, A., von Boxberg, Y., Veron-Ravaille, M., Mouffle, C., Benassy, M.-N., Taxi, J., David, L. and Nothias, F. (2017b). Physical chitosan microhydrogels as scaffolds for spinal cord injury restoration and axon regeneration. *Biomaterials* **138**, 91–107.

Chen, J., Li, Y., Katakowski, M., Chen, X., Wang, L., Lu, D., Lu, M., Gautam, S. C. and Chopp, M. (2003). Intravenous bone marrow stromal cell therapy reduces apoptosis and promotes endogenous cell proliferation after stroke in female rat. *J. Neurosci. Res.* **73**, 778–86.

Chen, J., Leong, S.-Y. and Schachner, M. (2005). Differential expression of cell fate determinants in neurons and glial cells of adult mouse spinal cord after compression injury. *Eur. J. Neurosci.* **22**, 1895–1906.

Chen, H., Shalom-Feuerstein, R., Riley, J., Zhang, S.-D., Tucci, P., Agostini, M., Aberdam, D., Knight, R. A., Genchi, G., Nicotera, P., et al. (2010). miR-7 and miR-214 are specifically expressed during neuroblastoma differentiation, cortical development and embryonic stem cells differentiation, and control neurite outgrowth in vitro. *Biochem. Biophys. Res. Commun.* **394**, 921–927.

Chen, X., Yang, Y., Yao, J., Lin, W., Li, Y., Chen, Y., Gao, Y., Yang, Y., Gu, X. and Wang, X. (2011). Bone marrow stromal cells-loaded chitosan conduits promote repair of complete transection injury in rat spinal cord. *J. Mater. Sci. Mater. Med.* **22**, 2347–2356.

Chevallay, B. and Herbage, D. (2000). Collagen-based biomaterials as 3D scaffold for cell cultures: applications for tissue engineering and gene therapy. *Med. Biol. Eng. Comput.* **38**, 211–8.

Chotivichit, A., Ruangchainikom, M., Chiewvit, P., Wongkajornsilp, A. and Sujirattanawimol, K. (2015). Chronic spinal cord injury treated with transplanted autologous bone marrow-derived mesenchymal stem cells tracked by magnetic resonance imaging: a case report. *J. Med. Case Rep.* **9**, 79.

Cifuentes, D., Xue, H., Taylor, D. W., Patnode, H., Mishima, Y., Cheloufi, S., Ma, E., Mane, S., Hannon, G. J., Lawson, N. D., et al. (2010). A novel miRNA processing pathway independent of Dicer requires Argonaute2 catalytic activity. *Science* **328**, 1694–8.

Cole, A. and Shi, R. (2005). Prolonged focal application of polyethylene glycol induces conduction block in guinea pig spinal cord white matter. *Toxicol. Vitr.* **19**, 215–220.

Comolli, N., Neuhuber, B., Fischer, I. and Lowman, A. (2009). In vitro analysis of PNIPAAm–

PEG, a novel, injectable scaffold for spinal cord repair. *Acta Biomater.* **5**, 1046–1055.

Corti, S., Locatelli, F., Papadimitriou, D., Strazzer, S., Bonato, S. and Comi, G. P. (2005). Nuclear reprogramming and adult stem cell potential. *Histol. Histopathol.* **20**, 977–86.

Coutts, M. and Keirstead, H. S. (2008). Stem cells for the treatment of spinal cord injury. *Exp. Neurol.* **209**, 368–377.

Crain, B. J., Tran, S. D. and Mezey, E. (2005). Transplanted human bone marrow cells generate new brain cells. *J. Neurol. Sci.* **233**, 121–123.

Cregg, J. M., DePaul, M. A., Filous, A. R., Lang, B. T., Tran, A. and Silver, J. (2014). Functional regeneration beyond the glial scar. *Exp. Neurol.* **253**, 197–207.

Cruz-Neves, S., Shirosaki, Y., Miyazaki, T. and Hayakawa, S. (2017). Characterization and degradation study of chitosan-siloxane hybrid microspheres synthesized using a microfluidic approach. *Mater. Sci. Eng. C* **81**, 571–579.

Cui, C., Xu, G., Qiu, J. and Fan, X. (2015). Up-regulation of miR-26a promotes neurite outgrowth and ameliorates apoptosis by inhibiting PTEN in bupivacaine injured mouse dorsal root ganglia. *Cell Biol. Int.* **39**, 933–942.

Curtis, R., Green, D., Lindsay, R. M. and Wilkin, G. P. (1993). Up-regulation of GAP-43 and growth of axons in rat spinal cord after compression injury. *J. Neurocytol.* **22**, 51–64.

Cuzzocrea, S., Genovese, T., Mazzon, E., Crisafulli, C., Di Paola, R., Muià, C., Collin, M., Esposito, E., Bramanti, P. and Thiemermann, C. (2006). Glycogen Synthase Kinase-3beta Inhibition Reduces Secondary Damage in Experimental Spinal Cord Trauma. *J. Pharmacol. Exp. Ther.* **318**, 79–89.

da Silva Meirelles, L., Chagastelles, P. C. and Nardi, N. B. (2006). Mesenchymal stem cells reside in virtually all post-natal organs and tissues. *J. Cell Sci.* **119**, 2204–13.

Dajas-Bailador, F., Bonev, B., Garcez, P., Stanley, P., Guillemot, F. and Papalopulu, N. (2012). microRNA-9 regulates axon extension and branching by targeting Map1b in mouse cortical neurons. *Nat. Neurosci.* **15**, 697–699.

Dang, Q., Liu, K., Zhang, Z., Liu, C., Liu, X., Xin, Y., Cheng, X., Xu, T., Cha, D. and Fan, B. (2017). Fabrication and evaluation of thermosensitive chitosan/collagen/α, β-glycerophosphate hydrogels for tissue regeneration. *Carbohydr. Polym.* **167**, 145–157.

Danilov, C. A. and Steward, O. (2015). Conditional genetic deletion of PTEN after a spinal cord injury enhances regenerative growth of CST axons and motor function recovery in mice. *Exp. Neurol.* **266**, 147–160.

de Chevigny, A., Coré, N., Follert, P., Gaudin, M., Barbry, P., Béclin, C. and Cremer, H. (2012). miR-7a regulation of Pax6 controls spatial origin of forebrain dopaminergic neurons. *Nat. Neurosci.* **15**, 1120–6.

Del Río, J. A., González-Billault, C., Ureña, J. M., Jiménez, E. M., Barallobre, M. J., Pascual, M., Pujadas, L., Simó, S., La Torre, A., Wandosell, F., et al. (2004). MAP1B Is Required for Netrin 1 Signaling in Neuronal Migration and Axonal Guidance. *Curr. Biol.* **14**, 840–850.

Deng, A., Kang, X., Zhang, J., Yang, Y. and Yang, S. (2017). Enhanced gelation of chitosan/β-sodium glycerophosphate thermosensitive hydrogel with sodium bicarbonate and biocompatibility evaluated. *Mater. Sci. Eng. C* **78**, 1147–1154.

Devaux, S., Cizkova, D., Mallah, K., Karnoub, M.-A., Laouby, Z., Kobeissy, F., Blasko, J.,

Nataf, S., Pays, L., Meriaux, C., et al. (2017). RhoA inhibitor treatment at acute phase of spinal cord injury may induce neurite outgrowth and synaptogenesis. *Mol. Cell. Proteomics* mcp.M116.064881.

Di Giovanni, S., Faden, A. I., Yakovlev, A., Duke-Cohan, J. S., Finn, T., Thouin, M., Knoblach, S., De Biase, A., Bregman, B. S. and Hoffman, E. P. (2005). Neuronal plasticity after spinal cord injury: identification of a gene cluster driving neurite outgrowth. *FASEB J.* **19**, 153–4.

DiTella, M. C., Feiguin, F., Carri, N., Kosik, K. S. and Cáceres, A. (1996). MAP-1B/TAU functional redundancy during laminin-enhanced axonal growth. *J. Cell Sci.* **109 (Pt 2)**, 467–77.

Dotti, C. G., Sullivan, C. A. and Banker, G. A. (1988). The establishment of polarity by hippocampal neurons in culture. *J. Neurosci.* **8**, 1454–68.

Doxakis, E. (2010). Post-transcriptional regulation of alpha-synuclein expression by mir-7 and mir-153. *J. Biol. Chem.* **285**, 12726–34.

Dumont, R. J., Okonkwo, D. O., Verma, S., Hurlbert, R. J., Boulos, P. T., Ellegala, D. B. and Dumont, a S. (2001). Acute spinal cord injury, part I: pathophysiologic mechanisms. *Clin. Neuropharmacol.* **24**, 254–64.

Dweep, H., Sticht, C., Pandey, P. and Gretz, N. (2011). miRWalk – Database: Prediction of possible miRNA binding sites by "walking" the genes of three genomes. *J. Biomed. Inform.* **44**, 839–847.

Emery, D. L., Royo, N. C., Fischer, I., Saatman, K. E. and McIntosh, T. K. (2003). Plasticity following injury to the adult central nervous system: is recapitulation of a developmental state worth promoting? *J. Neurotrauma* **20**, 1271–92.

Englund, U., Bjorklund, A., Wictorin, K., Lindvall, O. and Kokaia, M. (2002). Grafted neural stem cells develop into functional pyramidal neurons and integrate into host cortical circuitry. *Proc. Natl. Acad. Sci. U. S. A.* **99**, 17089–94.

Eriksson, C., Björklund, A. and Wictorin, K. (2003). Neuronal differentiation following transplantation of expanded mouse neurosphere cultures derived from different embryonic forebrain regions. *Exp. Neurol.* **184**, 615–35.

Fan, Y., Siklenka, K., Arora, S. K., Ribeiro, P., Kimmins, S., Xia, J., E.Y., C., A.G., H., T., I. and L., B. (2016). miRNet - dissecting miRNA-target interactions and functional associations through network-based visual analysis. *Nucleic Acids Res.* **44**, W135–W141.

Fang, P., Gao, Q., Liu, W.-J., Qi, X.-X., Li, G.-B., Zhang, J., Li, Z.-H., Sun, J.-L., Sun, J.-H. and Gao, Y.-M. (2010). Survival and differentiation of neuroepithelial stem cells on chitosan bicomponent fibers. *Chin. J. Physiol.* **53**, 208–14.

Fehlings, M. G. and Perrin, R. G. (2006). The Timing of Surgical Intervention in the Treatment of Spinal Cord Injury: A Systematic Review of Recent Clinical Evidence. *Spine (Phila. Pa. 1976).* **31**, S28–S35.

Fernández-Martos, C. M., González-Fernández, C., González, P., Maqueda, A., Arenas, E. and Rodríguez, F. J. (2011). Differential Expression of Wnts after Spinal Cord Contusion Injury in Adult Rats. *PLoS One* **6**, e27000.

Fertuzinhos, S., Li, M., Kawasawa, Y. I., Ivic, V., Franjic, D., Singh, D., Crair, M. and Šestan, N. (2014). Laminar and Temporal Expression Dynamics of Coding and Noncoding RNAs in

the Mouse Neocortex. *Cell Rep.* **6**, 938–950.

Filippov, V., Solovyev, V., Filippova, M. and Gill, S. S. (2000). A novel type of RNase III family proteins in eukaryotes. *Gene* **245**, 213–21.

Forostyak, S., Jendelova, P. and Sykova, E. (2013). The role of mesenchymal stromal cells in spinal cord injury, regenerative medicine and possible clinical applications. *Biochimie* **95**, 2257–70.

Freund, P., Wheeler-Kingshott, C. A., Nagy, Z., Gorgoraptis, N., Weiskopf, N., Friston, K., Thompson, A. J. and Hutton, C. (2012). Axonal integrity predicts cortical reorganisation following cervical injury. *J. Neurol. Neurosurg. Psychiatry* **83**, 629–37.

Friedenstein, A. J., Gorskaja, J. F. and Kulagina, N. N. (1976). Fibroblast precursors in normal and irradiated mouse hematopoietic organs. *Exp. Hematol.* **4**, 267–74.

Gao, M., Lu, P., Bednark, B., Lynam, D., Conner, J. M., Sakamoto, J. and Tuszynski, M. H. (2013). Templated agarose scaffolds for the support of motor axon regeneration into sites of complete spinal cord transection. *Biomaterials* **34**, 1529–1536.

Garbossa, D., Boido, M., Fontanella, M., Fronda, C., Ducati, A. and Vercelli, A. (2012). Recent therapeutic strategies for spinal cord injury treatment: possible role of stem cells. *Neurosurg. Rev.* **35**, 293–311; discussion 311.

Gasperini, L., Mano, J. F. and Reis, R. L. (2014). Natural polymers for the microencapsulation of cells. *J. R. Soc. Interface* **11**, 20140817–20140817.

Gatti, S., Bruno, S., Deregibus, M. C., Sordi, A., Cantaluppi, V., Tetta, C. and Camussi, G. (2011). Microvesicles derived from human adult mesenchymal stem cells protect against ischaemia-reperfusion-induced acute and chronic kidney injury. *Nephrol. Dial. Transplant.* **26**, 1474–1483.

Gelain, F., Panseri, S., Antonini, S., Cunha, C., Donega, M., Lowery, J., Taraballi, F., Cerri, G., Montagna, M., Baldissera, F., et al. (2011). Transplantation of nanostructured composite scaffolds results in the regeneration of chronically injured spinal cords. *ACS Nano* **5**, 227–36.

Gensel, J. C. and Zhang, B. (2015). Macrophage activation and its role in repair and pathology after spinal cord injury. *Brain Res.* **1619**, 1–11.

Ghibaudi, M., Boido, M. and Vercelli, A. (2017). Functional integration of complex miRNA networks in central and peripheral lesion and axonal regeneration. *Prog. Neurobiol.*

Gnavi, S., Barwig, C., Freier, T., Haastert-Talini, K., Grothe, C. and Geuna, S. (2013). The use of chitosan-based scaffolds to enhance regeneration in the nervous system. *Int. Rev. Neurobiol.* **109**, 1–62.

Gnavi, S., Fornasari, B., Tonda-Turo, C., Laurano, R., Zanetti, M., Ciardelli, G. and Geuna, S. (2015). The Effect of Electrospun Gelatin Fibers Alignment on Schwann Cell and Axon Behavior and Organization in the Perspective of Artificial Nerve Design. *Int. J. Mol. Sci.* **16**, 12925–12942.

Goold, R. G. and Gordon-Weeks, P. R. (2005). The MAP kinase pathway is upstream of the activation of GSK3β that enables it to phosphorylate MAP1B and contributes to the stimulation of axon growth. *Mol. Cell. Neurosci.* **28**, 524–534.

Goraltchouk, A., Scanga, V., Morshead, C. M. and Shoichet, M. S. (2006). Incorporation of protein-eluting microspheres into biodegradable nerve guidance channels for controlled

release. *J. Control. Release* **110**, 400–7.

Green, H. F. and Nolan, Y. M. (2012). Unlocking mechanisms in interleukin-1β-induced changes in hippocampal neurogenesis—a role for GSK-3β and TLX. *Transl. Psychiatry* **2**, e194.

Gros, T., Sakamoto, J. S., Blesch, A., Havton, L. A. and Tuszynski, M. H. (2010). Regeneration of long-tract axons through sites of spinal cord injury using templated agarose scaffolds. *Biomaterials* **31**, 6719–6729.

Grous, L. C., Vernengo, J., Jin, Y., Himes, B. T., Shumsky, J. S., Fischer, I. and Lowman, A. (2013). Implications of poly(*N* -isopropylacrylamide)- *g*- poly(ethylene glycol) with codissolved brain-derived neurotrophic factor injectable scaffold on motor function recovery rate following cervical dorsolateral funiculotomy in the rat. *J. Neurosurg. Spine* **18**, 641–652.

Gruner, J. A. (1992). A Monitored Contusion Model of Spinal Cord Injury in the Rat. *J. Neurotrauma* **9**, 123–128.

Gu, X., Meng, S., Liu, S., Jia, C., Fang, Y., Li, S., Fu, C., Song, Q., Lin, L. and Wang, X. (2014). miR-124 Represses ROCK1 Expression to Promote Neurite Elongation Through Activation of the PI3K/Akt Signal Pathway. *J. Mol. Neurosci.* **52**, 156–165.

Guo, J.-S., Qian, C.-H., Ling, E.-A. and Zeng, Y.-S. (2014a). Nanofiber scaffolds for treatment of spinal cord injury. *Curr. Med. Chem.* **21**, 4282–9.

Guo, J.-S., Qian, C.-H., Ling, E.-A. and Zeng, Y.-S. (2014b). Nanofiber scaffolds for treatment of spinal cord injury. *Curr. Med. Chem.* **21**, 4282–9.

Ha, M. and Kim, V. N. (2014). Regulation of microRNA biogenesis. *Nat. Rev. Mol. Cell Biol.* **15**, 509–524.

Habgood, M. D., Bye, N., Dziegielewska, K. M., Ek, C. J., Lane, M. A., Potter, A., Morganti-Kossmann, C. and Saunders, N. R. (2007). Changes in blood-brain barrier permeability to large and small molecules following traumatic brain injury in mice. *Eur. J. Neurosci.* **25**, 231–238.

Hains, B. C., Black, J. A. and Waxman, S. G. (2003). Primary cortical motor neurons undergo apoptosis after axotomizing spinal cord injury. *J. Comp. Neurol.* **462**, 328–341.

Hammond, S. M. (2015). An overview of microRNAs. *Adv. Drug Deliv. Rev.* **87**, 3–14.

Han, J., Lee, Y., Yeom, K.-H., Kim, Y.-K., Jin, H. and Kim, V. N. (2004). The Drosha-DGCR8 complex in primary microRNA processing. *Genes Dev.* **18**, 3016–3027.

Han, D., Wu, C., Xiong, Q., Zhou, L. and Tian, Y. (2015). Anti-inflammatory Mechanism of Bone Marrow Mesenchymal Stem Cell Transplantation in Rat Model of Spinal Cord Injury. *Cell Biochem. Biophys.* **71**, 1341–1347.

Heo, I., Ha, M., Lim, J., Yoon, M.-J., Park, J.-E., Kwon, S. C., Chang, H. and Kim, V. N. (2012). Mono-uridylation of pre-microRNA as a key step in the biogenesis of group II let-7 microRNAs. *Cell* **151**, 521–32.

Hicks, A. L., Adams, M. M., Martin Ginis, K., Giangregorio, L., Latimer, A., Phillips, S. M. and McCartney, N. (2005). Long-term body-weight-supported treadmill training and subsequent follow-up in persons with chronic SCI: effects on functional walking ability and measures of subjective well-being. *Spinal Cord* **43**, 291–298.

Himes, B. T., Neuhuber, B., Coleman, C., Kushner, R., Swanger, S. A., Kopen, G. C., Wagner, J., Shumsky, J. S. and Fischer, I. (2006). Recovery of Function Following Grafting of

Human Bone Marrow-Derived Stromal Cells into the Injured Spinal Cord. *Neurorehabil. Neural Repair* **20**, 278–296.

Hofstetter, C. P., Schwarz, E. J., Hess, D., Widenfalk, J., El Manira, A., Prockop, D. J. and Olson, L. (2002). Marrow stromal cells form guiding strands in the injured spinal cord and promote recovery. *Proc. Natl. Acad. Sci. U. S. A.* **99**, 2199–204.

Hofstetter, C. P., Holmström, N. A. V, Lilja, J. A., Schweinhardt, P., Hao, J., Spenger, C., Wiesenfeld-Hallin, Z., Kurpad, S. N., Frisén, J. and Olson, L. (2005). Allodynia limits the usefulness of intraspinal neural stem cell grafts; directed differentiation improves outcome. *Nat. Neurosci.* **8**, 346–53.

Horn, K. P., Busch, S. A., Hawthorne, A. L., van Rooijen, N. and Silver, J. (2008). Another barrier to regeneration in the CNS: activated macrophages induce extensive retraction of dystrophic axons through direct physical interactions. *J. Neurosci.* **28**, 9330–41.

Horsham, J. L., Ganda, C., Kalinowski, F. C., Brown, R. A. M., Epis, M. R. and Leedman, P. J. (2015). MicroRNA-7: A miRNA with expanding roles in development and disease. *Int. J. Biochem. Cell Biol.* **69**, 215–224.

Hosseini, S. M., Sharafkhah, A., Koohi-Hosseinabadi, O. and Semsar-Kazerooni, M. (2016). Transplantation of Neural Stem Cells Cultured in Alginate Scaffold for Spinal Cord Injury in Rats. *Asian Spine J.* **10**, 611.

Houweling, D. A., van Asseldonk, J. T., Lankhorst, A. J., Hamers, F. P., Martin, D., Bär, P. R. and Joosten, E. A. (1998a). Local application of collagen containing brain-derived neurotrophic factor decreases the loss of function after spinal cord injury in the adult rat. *Neurosci. Lett.* **251**, 193–6.

Houweling, D. A., Lankhorst, A. J., Gispen, W. H., Bär, P. R. and Joosten, E. A. (1998b). Collagen containing neurotrophin-3 (NT-3) attracts regrowing injured corticospinal axons in the adult rat spinal cord and promotes partial functional recovery. *Exp. Neurol.* **153**, 49–59.

Hsieh, F.-Y., Lin, H.-H. and Hsu, S. (2015). 3D bioprinting of neural stem cell-laden thermoresponsive biodegradable polyurethane hydrogel and potential in central nervous system repair. *Biomaterials* **71**, 48–57.

Hu, J.-Z., Huang, J.-H., Zeng, L., Wang, G., Cao, M. and Lu, H.-B. (2013). Anti-Apoptotic Effect of MicroRNA-21 after Contusion Spinal Cord Injury in Rats. *J. Neurotrauma* **30**, 1349–1360.

Hur, E.-M. and Zhou, F.-Q. (2010). GSK3 signalling in neural development. *Nat. Rev. Neurosci.* **11**, 539–551.

Hur, J. W., Cho, T.-H., Park, D.-H., Lee, J.-B., Park, J.-Y. and Chung, Y.-G. (2016). Intrathecal transplantation of autologous adipose-derived mesenchymal stem cells for treating spinal cord injury: A human trial. *J. Spinal Cord Med.* **39**, 655–664.

Hurtado, A., Cregg, J. M., Wang, H. B., Wendell, D. F., Oudega, M., Gilbert, R. J. and McDonald, J. W. (2011). Robust CNS regeneration after complete spinal cord transection using aligned poly-l-lactic acid microfibers. *Biomaterials* **32**, 6068–6079.

Hwang, D. H., Kim, H. M., Kang, Y. M., Joo, I. S., Cho, C.-S., Yoon, B.-W., Kim, S. U. and Kim, B. G. (2011). Combination of multifaceted strategies to maximize the therapeutic benefits of neural stem cell transplantation for spinal cord repair. *Cell Transplant.* **20**, 1361–79.

in 't Anker, P. S., Noort, W. A., Scherjon, S. A., Kleijburg-van der Keur, C., Kruisselbrink, A. B., van Bezooijen, R. L., Beekhuizen, W., Willemze, R., Kanhai, H. H. H. and Fibbe, W. E. (2003). Mesenchymal stem cells in human second-trimester bone marrow, liver, lung, and spleen exhibit a similar immunophenotype but a heterogeneous multilineage differentiation potential. *Haematologica* **88**, 845–52.

Jee, M. K., Jung, J. S., Im, Y. Bin, Jung, S. J. and Kang, S. K. (2012). Silencing of miR20a is crucial for Ngn1-mediated neuroprotection in injured spinal cord. *Hum. Gene Ther.* **23**, 508–20.

Jiang, H., Guo, W., Liang, X. and Rao, Y. (2005). Both the Establishment and the Maintenance of Neuronal Polarity Require Active Mechanisms. *Cell* **120**, 123–135.

Jiang, J.-J., Liu, C.-M., Zhang, B.-Y., Wang, X.-W., Zhang, M., Saijilafu, Zhang, S.-R., Hall, P., Hu, Y.-W. and Zhou, F.-Q. (2015). MicroRNA-26a supports mammalian axon regeneration in vivo by suppressing GSK3β expression. *Cell Death Dis.* **6**, e1865.

Jo, D. H., Kim, J. H., Cho, C. S., Cho, Y.-L., Jun, H. O., Yu, Y. S., Min, J.-K. and Kim, J. H. (2014). STAT3 inhibition suppresses proliferation of retinoblastoma through down-regulation of positive feedback loop of STAT3/miR-17-92 clusters. *Oncotarget* **5**, 11513–11525.

Johnson, R., Noble, W., Tartaglia, G. G. and Buckley, N. J. (2012). Neurodegeneration as an RNA disorder. *Prog. Neurobiol.* **99**, 293–315.

Joyce, N., Annett, G., Wirthlin, L., Olson, S., Bauer, G. and Nolta, J. A. (2010). Mesenchymal stem cells for the treatment of neurodegenerative disease. *Regen. Med.* **5**, 933–946.

Karimi-Abdolrezaee, S., Eftekharpour, E., Wang, J., Morshead, C. M. and Fehlings, M. G. (2006). Delayed transplantation of adult neural precursor cells promotes remyelination and functional neurological recovery after spinal cord injury. *J. Neurosci.* **26**, 3377–89.

Kawahara, Y., Megraw, M., Kreider, E., Iizasa, H., Valente, L., Hatzigeorgiou, A. G. and Nishikura, K. (2008). Frequency and fate of microRNA editing in human brain. *Nucleic Acids Res.* **36**, 5270–80.

Ketting, R. F., Fischer, S. E., Bernstein, E., Sijen, T., Hannon, G. J. and Plasterk, R. H. (2001). Dicer functions in RNA interference and in synthesis of small RNA involved in developmental timing in C. elegans. *Genes Dev.* **15**, 2654–2659.

Khvorova, A., Reynolds, A. and Jayasena, S. D. (2003). Functional siRNAs and miRNAs exhibit strand bias. *Cell* **115**, 209–16.

Kigerl, K. A., Gensel, J. C., Ankeny, D. P., Alexander, J. K., Donnelly, D. J. and Popovich, P. G. (2009). Identification of Two Distinct Macrophage Subsets with Divergent Effects Causing either Neurotoxicity or Regeneration in the Injured Mouse Spinal Cord. *J. Neurosci.* **29**, 13435–13444.

Kim, V. N. (2004). MicroRNA precursors in motion: exportin-5 mediates their nuclear export. *Trends Cell Biol.* **14**, 156–9.

Kim, G. M., Xu, J., Xu, J., Song, S. K., Yan, P., Ku, G., Xu, X. M. and Hsu, C. Y. (2001). Tumor necrosis factor receptor deletion reduces nuclear factor-kappaB activation, cellular inhibitor of apoptosis protein 2 expression, and functional recovery after traumatic spinal cord injury. *J. Neurosci.* **21**, 6617–25.

Kim, M., Park, S. R. and Choi, B. H. (2014). Biomaterial scaffolds used for the regeneration of spinal cord injury (SCI). *Histol. Histopathol.* **29**, 1395–408.

Kim, Y. C., Kim, Y. H., Kim, J. W. and Ha, K. Y. (2016). Transplantation of Mesenchymal Stem Cells for Acute Spinal Cord Injury in Rats: Comparative Study between Intralesional Injection and Scaffold Based Transplantation. *J. Korean Med. Sci.* **31**, 1373–82.

Kim M, Park SR, C. B. (2014). Biomaterial scaffolds used for the regeneration of spinal cord injury (SCI). - PubMed - NCBI. *Histol Histopathol*.

King, V. R., Phillips, J. B., Hunt-Grubbe, H., Brown, R. and Priestley, J. V (2006). Characterization of non-neuronal elements within fibronectin mats implanted into the damaged adult rat spinal cord. *Biomaterials* **27**, 485–96.

Knight, S. W. and Bass, B. L. (2001). A Role for the RNase III Enzyme DCR-1 in RNA Interference and Germ Line Development in Caenorhabditis elegans. *Science (80-.).* **293**, 2269–2271.

Koda, M., Hashimoto, M., Murakami, M., Yoshinaga, K., Ikeda, O., Yamazaki, M., Koshizuka, S., Kamada, T., Moriya, H., Shirasawa, H., et al. (2004). Adenovirus vector-mediated in vivo gene transfer of brain-derived neurotrophic factor (BDNF) promotes rubrospinal axonal regeneration and functional recovery after complete transection of the adult rat spinal cord. *J. Neurotrauma* **21**, 329–37.

Kong, X.-B., Tang, Q.-Y., Chen, X.-Y., Tu, Y., Sun, S.-Z. and Sun, Z.-L. (2017). Polyethylene glycol as a promising synthetic material for repair of spinal cord injury. *Neural Regen. Res.* **12**, 1003–1008.

Koseki, H., Donegá, M., Lam, B. Y., Petrova, V., van Erp, S., Yeo, G. S., Kwok, J. C., ffrench-Constant, C., Eva, R. and Fawcett, J. W. (2017). Selective rab11 transport and the intrinsic regenerative ability of CNS axons. *Elife* **6**,.

Kozomara, A. and Griffiths-Jones, S. (2014). miRBase: annotating high confidence microRNAs using deep sequencing data. *Nucleic Acids Res.* **42**, D68-73.

Kubinová, Š. and Syková, E. (2012). Biomaterials combined with cell therapy for treatment of spinal cord injury. *Regen. Med.* **7**, 207–224.

Kushchayev, S. V., Giers, M. B., Hom Eng, D., Martirosyan, N. L., Eschbacher, J. M., Mortazavi, M. M., Theodore, N., Panitch, A. and Preul, M. C. (2016). Hyaluronic acid scaffold has a neuroprotective effect in hemisection spinal cord injury. *J. Neurosurg. Spine* **25**, 114–124.

Kwon, B. K., Oxland, T. R. and Tetzlaff, W. (2002). Animal models used in spinal cord regeneration research. *Spine (Phila. Pa. 1976).* **27**, 1504–10.

KWON, B., Tetzlaff, W., Grauer, J. N., Beiner, J. and Vaccaro, A. R. (2004). Pathophysiology and pharmacologic treatment of acute spinal cord injury*1. *Spine J.* **4**, 451–464.

Lai, K.-O. and Ip, N. Y. (2013). Structural plasticity of dendritic spines: The underlying mechanisms and its dysregulation in brain disorders. *Biochim. Biophys. Acta - Mol. Basis Dis.* **1832**, 2257–2263.

Lavine, S. D., Hofman, F. M. and Zlokovic, B. V. (1998). Circulating Antibody against Tumor Necrosis Factor–Alpha Protects Rat Brain from Reperfusion Injury. *J. Cereb. Blood Flow Metab.* **18**, 52–58.

Lee, B. (2004). Injury in the spinal cord may produce cell death in the brain. *Brain Res.* **1020**, 37–44.

Lee, R. C. and Ambros, V. (2001). An extensive class of small RNAs in Caenorhabditis elegans. *Science* **294**, 862–4.

Lee, K. Y. and Mooney, D. J. (2012). Alginate: properties and biomedical applications. *Prog. Polym. Sci.* **37**, 106.

Lee, R. C., Feinbaum, R. L. and Ambros, V. (1993). The C. elegans heterochronic gene lin-4 encodes small RNAs with antisense complementarity to lin-14. *Cell* **75**, 843–854.

Lee, Y., Kim, M., Han, J., Yeom, K.-H., Lee, S., Baek, S. H. and Kim, V. N. (2004). MicroRNA genes are transcribed by RNA polymerase II. *EMBO J.* **23**, 4051–4060.

Lee, H., McKeon, R. J. and Bellamkonda, R. V (2010). Sustained delivery of thermostabilized chABC enhances axonal sprouting and functional recovery after spinal cord injury. *Proc. Natl. Acad. Sci. U. S. A.* **107**, 3340–5.

Lescaudron, L., Unni, D. and Dunbar, G. L. (2003). Autologous adult bone marrow stem cell transplantation in an animal model of huntington's disease: behavioral and morphological outcomes. *Int. J. Neurosci.* **113**, 945–56.

Li, B. and Sun, H. (2013). MiR-26a promotes neurite outgrowth by repressing PTEN expression. *Mol. Med. Rep.* **8**, 676–80.

Li, Y., Chen, J., Wang, L., Zhang, L., Lu, M. and Chopp, M. (2001). Intracerebral transplantation of bone marrow stromal cells in a 1-methyl-4-phenyl-1,2,3,6-tetrahydropyridine mouse model of Parkinson's disease. *Neurosci. Lett.* **316**, 67–70.

Li, X., Liu, X., Cui, L., Brunson, C., Zhao, W., Bhat, N. R., Zhang, N. and Wen, X. (2013a). Engineering an in situ crosslinkable hydrogel for enhanced remyelination. *FASEB J.* **27**, 1127–36.

Li, H. Y., Führmann, T., Zhou, Y. and Dalton, P. D. (2013b). Host reaction to poly(2-hydroxyethyl methacrylate) scaffolds in a small spinal cord injury model. *J. Mater. Sci. Mater. Med.* **24**, 2001–2011.

Li, D.-W., Lei, X., He, F.-L., He, J., Liu, Y.-L., Ye, Y.-J., Deng, X., Duan, E. and Yin, D.-C. (2017). Silk fibroin/chitosan scaffold with tunable properties and low inflammatory response assists the differentiation of bone marrow mesenchymal stem cells. *Int. J. Biol. Macromol.*

Liu, N.-K., Wang, X.-F., Lu, Q.-B. and Xu, X.-M. (2009). Altered microRNA expression following traumatic spinal cord injury. *Exp. Neurol.* **219**, 424–9.

Liu, G., Detloff, M. R., Miller, K. N., Santi, L. and Houlé, J. D. (2012a). Exercise modulates microRNAs that affect the PTEN/mTOR pathway in rats after spinal cord injury. *Exp. Neurol.* **233**, 447–456.

Liu, Z., Wang, H., Wang, Y., Lin, Q., Yao, A., Cao, F., Li, D., Zhou, J., Duan, C., Du, Z., et al. (2012b). The influence of chitosan hydrogel on stem cell engraftment, survival and homing in the ischemic myocardial microenvironment. *Biomaterials* **33**, 3093–3106.

Liu, Z.-H., Yip, P. K., Adams, L., Davies, M., Lee, J. W., Michael, G. J., Priestley, J. V. and Michael-Titus, A. T. (2015). A Single Bolus of Docosahexaenoic Acid Promotes Neuroplastic Changes in the Innervation of Spinal Cord Interneurons and Motor Neurons and Improves Functional Recovery after Spinal Cord Injury. *J. Neurosci.* **35**, 12733–12752.

LJ, B. (2005). Animal models for studying potential training strategies in persons with spinal cord injury. *J. Neurol. Phys. Ther.* **29**, 117–125 9p.

Lu, P., Wang, Y., Graham, L., McHale, K., Gao, M., Wu, D., Brock, J., Blesch, A., Rosenzweig, E. S., Havton, L. A., et al. (2012). Long-Distance Growth and Connectivity of Neural Stem Cells after Severe Spinal Cord Injury. *Cell* **150**, 1264–1273.

Lu, X. C., Zheng, J. Y., Tang, L. J., Huang, B. S., Li, K., Tao, Y., Yu, W., Zhu, R. L., Li, S. and Li, L. X. (2015). MiR-133b Promotes Neurite Outgrowth by Targeting RhoA Expression. *Cell. Physiol. Biochem.* **35**, 246–258.

Luo, J. and Shi, R. (2004). Diffusive oxidative stress following acute spinal cord injury in guinea pigs and its inhibition by polyethylene glycol. *Neurosci. Lett.* **359**, 167–170.

Luo, J., Borgens, R. and Shi, R. (2002). Polyethylene glycol immediately repairs neuronal membranes and inhibits free radical production after acute spinal cord injury. *J. Neurochem.* **83**, 471–80.

Mandalfino, P., Rice, G., Smith, A., Klein, J. L., Rystedt, L. and Ebers, G. C. (2000). Bone marrow transplantation in multiple sclerosis. *J. Neurol.* **247**, 691–5.

Mayer-Proschel, M., Kalyani, A. J., Mujtaba, T. and Rao, M. S. (1997). Isolation of lineage-restricted neuronal precursors from multipotent neuroepithelial stem cells. *Neuron* **19**, 773–85.

Mazzini, L., Mareschi, K., Ferrero, I., Vassallo, E., Oliveri, G., Nasuelli, N., Oggioni, G. D., Testa, L. and Fagioli, F. (2008). Stem cell treatment in Amyotrophic Lateral Sclerosis. *J. Neurol. Sci.* **265**, 78–83.

McTigue, D. M., Wei, P. and Stokes, B. T. (2001). Proliferation of NG2-positive cells and altered oligodendrocyte numbers in the contused rat spinal cord. *J. Neurosci.* **21**, 3392–400.

Mendonça, M. V., Larocca, T., de Freitas Souza, B., Villarreal, C., Silva, L. F., Matos, A., Novaes, M., Bahia, C. M., de Oliveira Melo Martinez, A., Kaneto, C., et al. (2014). Safety and neurological assessments after autologous transplantation of bone marrow mesenchymal stem cells in subjects with chronic spinal cord injury. *Stem Cell Res. Ther.* **5**, 126.

Miller, L. E. and Herbert, W. (2016). Health and economic benefits of physical activity for patients with spinal cord injury. *Clin. Outcomes Res.* **Volume 8**, 551–558.

Mocchetti, I., Rabin, S. J., Colangelo, A. M., Whittemore, S. R. and Wrathall, J. R. (1996). Increased basic fibroblast growth factor expression following contusive spinal cord injury. *Exp. Neurol.* **141**, 154–64.

Mohorianu, I., Schwach, F., Jing, R., Lopez-Gomollon, S., Moxon, S., Szittya, G., Sorefan, K., Moulton, V. and Dalmay, T. (2011). Profiling of short RNAs during fleshy fruit development reveals stage-specific sRNAome expression patterns. *Plant J.* **67**, 232–246.

Montenegro-Venegas, C., Tortosa, E., Rosso, S., Peretti, D., Bollati, F., Bisbal, M., Jausoro, I., Avila, J., Caceres, A. and Gonzalez-Billault, C. (2010). MAP1B Regulates Axonal Development by Modulating Rho-GTPase Rac1 Activity. *Mol. Biol. Cell* **21**, 3518–3528.

Mortazavi, A., Williams, B. A., McCue, K., Schaeffer, L. and Wold, B. (2008). Mapping and quantifying mammalian transcriptomes by RNA-Seq. *Nat. Methods* **5**, 621–628.

Mothe, A. J. and Tator, C. H. (2012). Advances in stem cell therapy for spinal cord injury. *J. Clin. Invest.* **122**, 3824–3834.

Mullany, L. E., Wolff, R. K. and Slattery, M. L. (2015). Effectiveness and Usability of Bioinformatics Tools to Analyze Pathways Associated with miRNA Expression. *Cancer Inform.* **14**, 121–30.

Nakajima, H., Uchida, K., Guerrero, A. R., Watanabe, S., Sugita, D., Takeura, N., Yoshida, A., Long, G., Wright, K. T., Johnson, W. E. B., et al. (2012). Transplantation of Mesenchymal Stem Cells Promotes an Alternative Pathway of Macrophage Activation and Functional Recovery after Spinal Cord Injury. *J. Neurotrauma* **29**, 1614–1625.

Nakanishi, K., Nakasa, T., Tanaka, N., Ishikawa, M., Yamada, K., Yamasaki, K., Kamei, N., Izumi, B., Adachi, N., Miyaki, S., et al. (2010). Responses of microRNAs 124a and 223 following spinal cord injury in mice. *Spinal Cord* **48**, 192–196.

Namiki, J., Kojima, A. and Tator, C. H. (2000). Effect of brain-derived neurotrophic factor, nerve growth factor, and neurotrophin-3 on functional recovery and regeneration after spinal cord injury in adult rats. *J. Neurotrauma* **17**, 1219–31.

Nguyen, L. H., Gao, M., Lin, J., Wu, W., Wang, J. and Chew, S. Y. (2017). Three-dimensional aligned nanofibers-hydrogel scaffold for controlled non-viral drug/gene delivery to direct axon regeneration in spinal cord injury treatment. *Sci. Rep.* **7**, 42212.

Nielson, J. L., Sears-Kraxberger, I., Strong, M. K., Wong, J. K., Willenberg, R. and Steward, O. (2010). Unexpected Survival of Neurons of Origin of the Pyramidal Tract after Spinal Cord Injury. *J. Neurosci.* **30**, 11516–11528.

Nieto-Diaz, M., Esteban, F. J., Reigada, D., Muñoz-Galdeano, T., Yunta, M., Caballero-López, M., Navarro-Ruiz, R., Del Águila, A. and Maza, R. M. (2014). MicroRNA dysregulation in spinal cord injury: causes, consequences and therapeutics. *Front. Cell. Neurosci.* **8**, 53.

Ning, B., Gao, L., Liu, R.-H., Liu, Y., Zhang, N.-S. and Chen, Z.-Y. (2014). microRNAs in spinal cord injury: potential roles and therapeutic implications. *Int. J. Biol. Sci.* **10**, 997–1006.

Nix, P. and Bastiani, M. (2013). Neuroscience. Heterochronic genes turn back the clock in old neurons. *Science* **340**, 282–3.

Nógrádi, A., Szabó, A., Pintér, S. and Vrbová, G. (2007). Delayed riluzole treatment is able to rescue injured rat spinal motoneurons. *Neuroscience* **144**, 431–438.

Nomura, H., Zahir, T., Kim, H., Katayama, Y., Kulbatski, I., Morshead, C. M., Shoichet, M. S. and Tator, C. H. (2008). Extramedullary chitosan channels promote survival of transplanted neural stem and progenitor cells and create a tissue bridge after complete spinal cord transection. *Tissue Eng. Part A* **14**, 649–65.

Novikova, L. N., Pettersson, J., Brohlin, M., Wiberg, M. and Novikov, L. N. (2008). Biodegradable poly-beta-hydroxybutyrate scaffold seeded with Schwann cells to promote spinal cord repair. *Biomaterials* **29**, 1198–206.

Ohta, M., Suzuki, Y., Noda, T., Ejiri, Y., Dezawa, M., Kataoka, K., Chou, H., Ishikawa, N., Matsumoto, N., Iwashita, Y., et al. (2004). Bone marrow stromal cells infused into the cerebrospinal fluid promote functional recovery of the injured rat spinal cord with reduced cavity formation. *Exp. Neurol.* **187**, 266–78.

Okamura, K., Hagen, J. W., Duan, H., Tyler, D. M. and Lai, E. C. (2007). The mirtron pathway generates microRNA-class regulatory RNAs in Drosophila. *Cell* **130**, 89–100.

Okutan, O., Solaroglu, I., Beskonakli, E. and Taskin, Y. (2007). Recombinant human erythropoietin decreases myeloperoxidase and caspase-3 activity and improves early functional results after spinal cord injury in rats. *J. Clin. Neurosci.* **14**, 364–8.

Ortiz, L. A., Dutreil, M., Fattman, C., Pandey, A. C., Torres, G., Go, K. and Phinney, D. G.

(2007). Interleukin 1 receptor antagonist mediates the antiinflammatory and antifibrotic effect of mesenchymal stem cells during lung injury. *Proc. Natl. Acad. Sci. U. S. A.* **104**, 11002–7.

Oudega, M. and Perez, M. A. (2012). Corticospinal reorganization after spinal cord injury. *J. Physiol.* **590**, 3647–63.

Oudega, M., Gautier, S. E., Chapon, P., Fragoso, M., Bates, M. L., Parel, J. M. and Bunge, M. B. (2001). Axonal regeneration into Schwann cell grafts within resorbable poly(alpha-hydroxyacid) guidance channels in the adult rat spinal cord. *Biomaterials* **22**, 1125–36.

Palejwala, A. H., Fridley, J. S., Mata, J. A., Samuel, E. L. G., Luerssen, T. G., Perlaky, L., Kent, T. A., Tour, J. M. and Jea, A. (2016). Biocompatibility of reduced graphene oxide nanoscaffolds following acute spinal cord injury in rats. *Surg. Neurol. Int.* **7**, 75.

Palmer, T. D., Takahashi, J. and Gage, F. H. (1997). The adult rat hippocampus contains primordial neural stem cells. *Mol. Cell. Neurosci.* **8**, 389–404.

Park, K. K., Liu, K., Hu, Y., Kanter, J. L. and He, Z. (2010). PTEN/mTOR and axon regeneration. *Exp. Neurol.* **223**, 45–50.

Parr, A. M., Kulbatski, I., Zahir, T., Wang, X., Yue, C., Keating, A. and Tator, C. H. (2008). Transplanted adult spinal cord-derived neural stem/progenitor cells promote early functional recovery after rat spinal cord injury. *Neuroscience* **155**, 760–70.

Patel, M., Vandevord, P. J., Matthew, H., Wu, B., Desilva, S. and Wooley, P. H. (2006). Video-Gait Analysis of Functional Recovery of Nerve Repaired with Chitosan Nerve Guides. *Tissue Eng.* **12**, 3189–3199.

Patist, C. M., Mulder, M. B., Gautier, S. E., Maquet, V., Jérôme, R. and Oudega, M. (2004). Freeze-dried poly(D,L-lactic acid) macroporous guidance scaffolds impregnated with brain-derived neurotrophic factor in the transected adult rat thoracic spinal cord. *Biomaterials* **25**, 1569–82.

Pearson, A. G., Gray, C. W., Pearson, J. F., Greenwood, J. M., During, M. J. and Dragunow, M. (2003). ATF3 enhances c-Jun-mediated neurite sprouting. *Brain Res. Mol. Brain Res.* **120**, 38–45.

Pineau, I. and Lacroix, S. (2007). Proinflammatory cytokine synthesis in the injured mouse spinal cord: Multiphasic expression pattern and identification of the cell types involved. *J. Comp. Neurol.* **500**, 267–285.

Pittenger, M. F., Mackay, A. M., Beck, S. C., Jaiswal, R. K., Douglas, R., Mosca, J. D., Moorman, M. A., Simonetti, D. W., Craig, S. and Marshak, D. R. (1999). Multilineage potential of adult human mesenchymal stem cells. *Science* **284**, 143–7.

Pollock, A., Bian, S., Zhang, C., Chen, Z. and Sun, T. (2014). Growth of the developing cerebral cortex is controlled by microRNA-7 through the p53 pathway. *Cell Rep.* **7**, 1184–96.

Pons-Espinal, M., de Luca, E., Marzi, M. J., Beckervordersandforth, R., Armirotti, A., Nicassio, F., Fabel, K., Kempermann, G. and De Pietri Tonelli, D. (2017). Synergic Functions of miRNAs Determine Neuronal Fate of Adult Neural Stem Cells. *Stem Cell Reports* **8**, 1046–1061.

Prabhakaran, M. P., Vatankhah, E. and Ramakrishna, S. (2013). Electrospun aligned PHBV/collagen nanofibers as substrates for nerve tissue engineering. *Biotechnol. Bioeng.* **110**, 2775–84.

Prüfer, K., Stenzel, U., Dannemann, M., Green, R. E., Lachmann, M. and Kelso, J. (2008). PatMaN: rapid alignment of short sequences to large databases. *Bioinformatics* **24**, 1530–1.

Pumberger, M., Qazi, T. H., Ehrentraut, M. C., Textor, M., Kueper, J., Stoltenburg-Didinger, G., Winkler, T., von Roth, P., Reinke, S., Borselli, C., et al. (2016). Synthetic niche to modulate regenerative potential of MSCs and enhance skeletal muscle regeneration. *Biomaterials* **99**, 95–108.

Puschmann, T. B., de Pablo, Y., Zandén, C., Liu, J. and Pekny, M. (2014). A Novel Method for Three-Dimensional Culture of Central Nervous System Neurons. *Tissue Eng. Part C Methods* **20**, 485–492.

Qiao, L.-Y. and Vizzard, M. A. (2005). Spinal cord injury-induced expression of TrkA, TrkB, phosphorylated CREB, and c-Jun in rat lumbosacral dorsal root ganglia. *J. Comp. Neurol.* **482**, 142–154.

Qiu, J., Cai, D., Dai, H., McAtee, M., Hoffman, P. N., Bregman, B. S. and Filbin, M. T. (2002). Spinal axon regeneration induced by elevation of cyclic AMP. *Neuron* **34**, 895–903.

Rad, F., Pourfathollah, A. A., Yari, F., Mohammadi, S. and Kheirandish, M. (2016). Microvesicles preparation from mesenchymal stem cells. *Med. J. Islam. Repub. Iran* **30**, 398.

Raspa, A., Marchini, A., Pugliese, R., Mauri, M., Maleki, M., Vasita, R. and Gelain, F. (2016). A biocompatibility study of new nanofibrous scaffolds for nervous system regeneration. *Nanoscale* **8**, 253–265.

Repici, M., Chen, X., Morel, M.-P., Doulazmi, M., Sclip, A., Cannaya, V., Veglianese, P., Kraftsik, R., Mariani, J., Borsello, T., et al. (2012). Specific inhibition of the JNK pathway promotes locomotor recovery and neuroprotection after mouse spinal cord injury. *Neurobiol. Dis.* **46**, 710–21.

Ribeiro, T. B., Duarte, A. S. S., Longhini, A. L. F., Pradella, F., Farias, A. S., Luzo, A. C. M., Oliveira, A. L. R. and Olalla Saad, S. T. (2015). Neuroprotection and immunomodulation by xenografted human mesenchymal stem cells following spinal cord ventral root avulsion. *Sci. Rep.* **5**, 16167.

Ribeiro-Samy, S., Silva, N. A., Correlo, V. M., Fraga, J. S., Pinto, L., Teixeira-Castro, A., Leite-Almeida, H., Almeida, A., Gimble, J. M., Sousa, N., et al. (2013). Development and characterization of a PHB-HV-based 3D scaffold for a tissue engineering and cell-therapy combinatorial approach for spinal cord injury regeneration. *Macromol. Biosci.* **13**, 1576–92.

Ritfeld, G. J., Rauck, B. M., Novosat, T. L., Park, D., Patel, P., Roos, R. A. C., Wang, Y. and Oudega, M. (2014). The effect of a polyurethane-based reverse thermal gel on bone marrow stromal cell transplant survival and spinal cord repair. *Biomaterials* **35**, 1924–1931.

Rodgers, E. E. and Theibert, A. B. Functions of PI 3-kinase in development of the nervous system. *Int. J. Dev. Neurosci.* **20**, 187–97.

Roncon, P., Soukupovà, M., Binaschi, A., Falcicchia, C., Zucchini, S., Ferracin, M., Langley, S. R., Petretto, E., Johnson, M. R., Marucci, G., et al. (2015). MicroRNA profiles in hippocampal granule cells and plasma of rats with pilocarpine-induced epilepsy – comparison with human epileptic samples. *Sci. Rep.* **5**, 14143.

Rosales-Cortés, M., Peregrina-Sandoval, J., Bañuelos-Pineda, J., Sarabia-Estrada, R., Gómez-Rodiles, C. C., Albarrán-Rodríguez, E., Zaitseva, G. P. and Pita-López, M. L. (2003). Immunological study of a chitosan prosthesis in the sciatic nerve regeneration of the

axotomized dog. *J. Biomater. Appl.* **18**, 15–23.

Ruini, F., Tonda-Turo, C., Chiono, V. and Ciardelli, G. (2015). Chitosan membranes for tissue engineering: comparison of different crosslinkers. *Biomed. Mater.* **10**, 65002.

Rusk, N. (2008). When microRNAs activate translation. *Nat. Methods* **5**, 122–123.

Sadowsky, C., Volshteyn, O., Schultz, L. and McDonald, J. W. (2002). Spinal cord injury. *Disabil. Rehabil.* **24**, 680–7.

Saijilafu, Hur, E.-M., Liu, C.-M., Jiao, Z., Xu, W.-L. and Zhou, F.-Q. (2013). PI3K-GSK3 signalling regulates mammalian axon regeneration by inducing the expression of Smad1. *Nat. Commun.* **4**, 2690.

Sakakibara, A. and Hatanaka, Y. (2015). Neuronal polarization in the developing cerebral cortex. *Front. Neurosci.* **9**, 116.

Sanchez-Ramos, J., Song, S., Cardozo-Pelaez, F., Hazzi, C., Stedeford, T., Willing, A., Freeman, T. B., Saporta, S., Janssen, W., Patel, N., et al. (2000). Adult Bone Marrow Stromal Cells Differentiate into Neural Cells in Vitro. *Exp. Neurol.* **164**, 247–256.

Schaub, N. J., Johnson, C. D., Cooper, B. and Gilbert, R. J. (2016). Electrospun Fibers for Spinal Cord Injury Research and Regeneration. *J. Neurotrauma* **33**, 1405–15.

Scheffler, B., Walton, N. M., Lin, D. D., Goetz, A. K., Enikolopov, G., Roper, S. N. and Steindler, D. A. (2005). Phenotypic and functional characterization of adult brain neuropoiesis. *Proc. Natl. Acad. Sci. U. S. A.* **102**, 9353–8.

Shi, J., Marinovich, A. and Barres, B. A. (1998). Purification and characterization of adult oligodendrocyte precursor cells from the rat optic nerve. *J. Neurosci.* **18**, 4627–36.

Silva, G. A., Czeisler, C., Niece, K. L., Beniash, E., Harrington, D. A., Kessler, J. A. and Stupp, S. I. (2004). Selective Differentiation of Neural Progenitor Cells by High-Epitope Density Nanofibers. *Science (80-.).* **303**, 1352–1355.

Silva, N. A., Sousa, R. A., Fraga, J. S., Fontes, M., Leite-Almeida, H., Cerqueira, R., Almeida, A., Sousa, N., Reis, R. L. and Salgado, A. J. (2013). Benefits of Spine Stabilization with Biodegradable Scaffolds in Spinal Cord Injured Rats. *Tissue Eng. Part C Methods* **19**, 101–108.

Skop, N. B., Calderon, F., Cho, C. H., Gandhi, C. D. and Levison, S. W. (2016). Optimizing a multifunctional microsphere scaffold to improve neural precursor cell transplantation for traumatic brain injury repair. *J. Tissue Eng. Regen. Med.* **10**, E419–E432.

Sorefan, K., Pais, H., Hall, A. E., Kozomara, A., Griffiths-Jones, S., Moulton, V. and Dalmay, T. (2012). Reducing ligation bias of small RNAs in libraries for next generation sequencing. *Silence* **3**, 4.

Stevanato, L. and Sinden, J. D. (2014). The effects of microRNAs on human neural stem cell differentiation in two- and three-dimensional cultures. *Stem Cell Res. Ther.* **5**, 49.

Stirling, D. P., Khodarahmi, K., Liu, J., McPhail, L. T., McBride, C. B., Steeves, J. D., Ramer, M. S. and Tetzlaff, W. (2004). Minocycline treatment reduces delayed oligodendrocyte death, attenuates axonal dieback, and improves functional outcome after spinal cord injury. *J. Neurosci.* **24**, 2182–90.

Straley, K. S., Foo, C. W. P. and Heilshorn, S. C. (2010). Biomaterial design strategies for the treatment of spinal cord injuries. *J. Neurotrauma* **27**, 1–19.

Sun, X., Zhou, Z., Fink, D. J. and Mata, M. (2013). HspB1 silences translation of PDZ-RhoGEF by enhancing miR-20a and miR-128 expression to promote neurite extension. *Mol. Cell. Neurosci.* **57**, 111–119.

Suzuki, H., Kanchiku, T., Imajo, Y., Yoshida, Y., Nishida, N., Gondo, T., Yoshii, S. and Taguchi, T. (2015). Artificial collagen-filament scaffold promotes axon regeneration and long tract reconstruction in a rat model of spinal cord transection. *Med. Mol. Morphol.* **48**, 214–24.

Tapia, V. S., Herrera-Rojas, M. and Larrain, J. (2017). JAK-STAT pathway activation in response to spinal cord injury in regenerative and non-regenerative stages of Xenopus laevis. *Regen. (Oxford, England)* **4**, 21–35.

Terada, N., Hamazaki, T., Oka, M., Hoki, M., Mastalerz, D. M., Nakano, Y., Meyer, E. M., Morel, L., Petersen, B. E. and Scott, E. W. (2002). Bone marrow cells adopt the phenotype of other cells by spontaneous cell fusion. *Nature* **416**, 542–545.

Terraf, P., Kouhsari, S. M., Ai, J. and Babaloo, H. (2017). Tissue-Engineered Regeneration of Hemisected Spinal Cord Using Human Endometrial Stem Cells, Poly ε-Caprolactone Scaffolds, and Crocin as a Neuroprotective Agent. *Mol. Neurobiol.* **54**, 5657–5667.

Theis, T., Yoo, M., Park, C. S., Chen, J., Kügler, S., Gibbs, K. M. and Schachner, M. (2016). Lentiviral Delivery of miR-133b Improves Functional Recovery After Spinal Cord Injury in Mice. *Mol. Neurobiol.*

Thomas, D., Fontana, G., Chen, X., Sanz-Nogués, C., Zeugolis, D. I., Dockery, P., O'Brien, T. and Pandit, A. (2014). A shape-controlled tuneable microgel platform to modulate angiogenic paracrine responses in stem cells. *Biomaterials* **35**, 8757–66.

Tonda-Turo, C., Boffito, M., Cassino, C., Gentile, P. and Ciardelli, G. (2016). Biomimetic polyurethane – Based fibrous scaffolds. *Mater. Lett.* **167**, 9–12.

Tonda-Turo, C., Ruini, F., Ramella, M., Boccafoschi, F., Gentile, P., Gioffredi, E., Falvo D'Urso Labate, G. and Ciardelli, G. (2017a). Non-covalently crosslinked chitosan nanofibrous mats prepared by electrospinning as substrates for soft tissue regeneration. *Carbohydr. Polym.* **162**, 82–92.

Tonda-Turo, C., Ruini, F., Ramella, M., Boccafoschi, F., Gentile, P., Gioffredi, E., Falvo D'Urso Labate, G. and Ciardelli, G. (2017b). Non-covalently crosslinked chitosan nanofibrous mats prepared by electrospinning as substrates for soft tissue regeneration. *Carbohydr. Polym.* **162**, 82–92.

Tsai, E. C., Dalton, P. D., Shoichet, M. S. and Tator, C. H. (2004). Synthetic hydrogel guidance channels facilitate regeneration of adult rat brainstem motor axons after complete spinal cord transection. *J. Neurotrauma* **21**, 789–804.

Tseng, T.-C., Hsieh, F.-Y. and Hsu, S. (2016). Increased cell survival of cells exposed to superparamagnetic iron oxide nanoparticles through biomaterial substrate-induced autophagy. *Biomater. Sci.* **4**, 670–677.

Tysseling-Mattiace, V. M., Sahni, V., Niece, K. L., Birch, D., Czeisler, C., Fehlings, M. G., Stupp, S. I. and Kessler, J. A. (2008). Self-Assembling Nanofibers Inhibit Glial Scar Formation and Promote Axon Elongation after Spinal Cord Injury. *J. Neurosci.* **28**, 3814–3823.

Tzeng, S. F., Cheng, H., Lee, Y. S., Wu, J. P., Hoffer, B. J. and Kuo, J. S. (2001). Expression of neural cell adhesion molecule in spinal cords following a complete transection. *Life Sci.* **68**,

1005–12.

Uchida, N., Buck, D. W., He, D., Reitsma, M. J., Masek, M., Phan, T. V., Tsukamoto, A. S., Gage, F. H. and Weissman, I. L. (2000). Direct isolation of human central nervous system stem cells. *Proc. Natl. Acad. Sci.* **97**, 14720–14725.

Urdzíková, L. M., Růžička, J., LaBagnara, M., Kárová, K., Kubinová, Š., Jiráková, K., Murali, R., Syková, E., Jhanwar-Uniyal, M. and Jendelová, P. (2014). Human mesenchymal stem cells modulate inflammatory cytokines after spinal cord injury in rat. *Int. J. Mol. Sci.* **15**, 11275–93.

Vaquero, J., Zurita, M., Rico, M. A., Bonilla, C., Aguayo, C., Montilla, J., Bustamante, S., Carballido, J., Marin, E., Martinez, F., et al. (2016). An approach to personalized cell therapy in chronic complete paraplegia: The Puerta de Hierro phase I/II clinical trial. *Cytotherapy* **18**, 1025–36.

Vaucheret, H., Vazquez, F., Crété, P. and Bartel, D. P. (2004). The action of ARGONAUTE1 in the miRNA pathway and its regulation by the miRNA pathway are crucial for plant development. *Genes Dev.* **18**, 1187–1197.

Vercelli, A. and Boido, M. (2015). Chapter 15 – Spinal Cord Injury. In *Neurobiology of Brain Disorders*, pp. 207–218.

Vercelli, A., Repici, M., Garbossa, D. and Grimaldi, A. (2000). Recent techniques for tracing pathways in the central nervous system of developing and adult mammals. *Brain Res. Bull.* **51**, 11–28.

Vercelli, A., Mereuta, O. M., Garbossa, D., Muraca, G., Mareschi, K., Rustichelli, D., Ferrero, I., Mazzini, L., Madon, E. and Fagioli, F. (2008). Human mesenchymal stem cell transplantation extends survival, improves motor performance and decreases neuroinflammation in mouse model of amyotrophic lateral sclerosis. *Neurobiol. Dis.* **31**, 395–405.

Vo, N., Klein, M. E., Varlamova, O., Keller, D. M., Yamamoto, T., Goodman, R. H. and Impey, S. (2005). A cAMP-response element binding protein-induced microRNA regulates neuronal morphogenesis. *Proc. Natl. Acad. Sci. U. S. A.* **102**, 16426–31.

Wang, T., Yuan, W., Liu, Y., Zhang, Y., Wang, Z., Chen, X., Feng, S., Xiu, Y. and Li, W. (2015a). miR-142-3p is a Potential Therapeutic Target for Sensory Function Recovery of Spinal Cord Injury. *Med. Sci. Monit.* **21**, 2553–6.

Wang, J., Wang, J., Lu, P., Cai, Y., Wang, Y., Hong, L., Ren, H., Heng, B. C., Liu, H., Zhou, J., et al. (2015b). Local delivery of FTY720 in PCL membrane improves SCI functional recovery by reducing reactive astrogliosis. *Biomaterials* **62**, 76–87.

Wang, C., Sun, C., Hu, Z., Huo, X., Yang, Y., Liu, X., Botchway, B. O. A., Davies, H. and Fang, M. (2017a). Improved Neural Regeneration with Olfactory Ensheathing Cell Inoculated PLGA Scaffolds in Spinal Cord Injury Adult Rats. *Neurosignals* **25**, 1–14.

Wang, W. M., Lu, G., Su, X. W., Lyu, H. and Poon, W. S. (2017b). MicroRNA-182 Regulates Neurite Outgrowth Involving the PTEN/AKT Pathway. *Front. Cell. Neurosci.* **11**, 96.

Wannier, T., Schmidlin, E., Bloch, J. and Rouiller, E. M. (2005). A Unilateral Section of the Corticospinal Tract at Cervical Level in Primate Does Not Lead to Measurable Cell Loss in Motor Cortex. *J. Neurotrauma* **22**, 703–717.

Watson, C., Paxinos, G., Kayalioglu, G. and Christopher & Dana Reeve Foundation. (2009).

The spinal cord : a Christopher and Dana Reeve Foundation text and atlas. Elsevier/Academic Press.

Wen, Y., Yu, S., Wu, Y., Ju, R., Wang, H., Liu, Y., Wang, Y. and Xu, Q. (2016). Spinal cord injury repair by implantation of structured hyaluronic acid scaffold with PLGA microspheres in the rat. *Cell Tissue Res.* **364**, 17–28.

Wu, D. and Murashov, A. K. (2013). MicroRNA-431 regulates axon regeneration in mature sensory neurons by targeting the Wnt antagonist Kremen1. *Front. Mol. Neurosci.* **6**, 35.

Wu, S., Suzuki, Y., Ejiri, Y., Noda, T., Bai, H., Kitada, M., Kataoka, K., Ohta, M., Chou, H. and Ide, C. (2003). Bone marrow stromal cells enhance differentiation of cocultured neurosphere cells and promote regeneration of injured spinal cord. *J. Neurosci. Res.* **72**, 343–51.

Wu, Y., Zheng, Q., Du, J., Song, Y., Wu, B. and Guo, X. (2006). Self-assembled IKVAV peptide nanofibers promote adherence of PC12 cells. *J. Huazhong Univ. Sci. Technolog. Med. Sci.* **26**, 594–6.

Wu, B., Zheng, Q., Wu, Y., Guo, X. and Zou, Z. (2010). Effect of IKVAV peptide nanofiber on proliferation, adhesion and differentiation into neurocytes of bone marrow stromal cells. *J. Huazhong Univ. Sci. Technolog. Med. Sci.* **30**, 178–82.

Wurmser, A. E., Nakashima, K., Summers, R. G., Toni, N., D'Amour, K. A., Lie, D. C. and Gage, F. H. (2004). Cell fusion-independent differentiation of neural stem cells to the endothelial lineage. *Nature* **430**, 350–6.

Xie, M., Li, M., Vilborg, A., Lee, N., Shu, M.-D., Yartseva, V., Šestan, N. and Steitz, J. A. (2013). Mammalian 5'-capped microRNA precursors that generate a single microRNA. *Cell* **155**, 1568–80.

Xie, J., Jin, B., Li, D.-W., Shen, B., Gong, N., Zhang, T.-Z. and Dong, P. (2015). Effect of laminin-binding BDNF on induction of recurrent laryngeal nerve regeneration by miR-222 activation of mTOR signal pathway. *Am. J. Transl. Res.* **7**, 1071–80.

Xin, H., Li, Y., Buller, B., Katakowski, M., Zhang, Y., Wang, X., Shang, X., Zhang, Z. G. and Chopp, M. (2012). Exosome-Mediated Transfer of miR-133b from Multipotent Mesenchymal Stromal Cells to Neural Cells Contributes to Neurite Outgrowth. *Stem Cells* **30**, 1556–1564.

Xu, P., Billmeier, M., Mohorianu, I., Green, D., Fraser, W. D. and Dalmay, T. (2015). An improved protocol for small RNA library construction using High Definition adapters. *Methods Next Gener. Seq.* **2**,.

Yandava, B. D., Billinghurst, L. L. and Snyder, E. Y. (1999). "Global" cell replacement is feasible via neural stem cell transplantation: evidence from the dysmyelinated shiverer mouse brain. *Proc. Natl. Acad. Sci. U. S. A.* **96**, 7029–34.

Yang, Y., De Laporte, L., Rives, C. B., Jang, J.-H., Lin, W.-C., Shull, K. R. and Shea, L. D. (2005). Neurotrophin releasing single and multiple lumen nerve conduits. *J. Control. Release* **104**, 433–46.

Yang, W., Chendrimada, T. P., Wang, Q., Higuchi, M., Seeburg, P. H., Shiekhattar, R. and Nishikura, K. (2006). Modulation of microRNA processing and expression through RNA editing by ADAR deaminases. *Nat. Struct. Mol. Biol.* **13**, 13–21.

Yang, Z., Mo, L., Duan, H. and Li, X. (2010a). Effects of chitosan/collagen substrates on the behavior of rat neural stem cells. *Sci. China Life Sci.* **53**, 215–222.

Yang, J.-S., Maurin, T., Robine, N., Rasmussen, K. D., Jeffrey, K. L., Chandwani, R., Papapetrou, E. P., Sadelain, M., O'Carroll, D. and Lai, E. C. (2010b). Conserved vertebrate mir-451 provides a platform for Dicer-independent, Ago2-mediated microRNA biogenesis. *Proc. Natl. Acad. Sci.* **107**, 15163–15168.

Yasvoina, M. V, Genç, B., Jara, J. H., Sheets, P. L., Quinlan, K. A., Milosevic, A., Shepherd, G. M. G., Heckman, C. J. and Özdinler, P. H. (2013). eGFP expression under UCHL1 promoter genetically labels corticospinal motor neurons and a subpopulation of degeneration-resistant spinal motor neurons in an ALS mouse model. *J. Neurosci.* **33**, 7890–904.

Yazihan, N., Uzuner, K., Salman, B., Vural, M., Koken, T. and Arslantas, A. (2008). Erythropoietin improves oxidative stress following spinal cord trauma in rats. *Injury* **39**, 1408–13.

Ye, J., Qin, Y., Wu, Y., Wang, P., Tang, Y., Huang, L., Ma, M., Zeng, Y. and Shen, H. (2016). Using primate neural stem cells cultured in self-assembling peptide nanofiber scaffolds to repair injured spinal cords in rats. *Spinal Cord* **54**, 933–941.

Yoshimura, T., Kawano, Y., Arimura, N., Kawabata, S., Kikuchi, A. and Kaibuchi, K. (2005). GSK-3β Regulates Phosphorylation of CRMP-2 and Neuronal Polarity. *Cell* **120**, 137–149.

Yu, W. R., Liu, T., Fehlings, T. K. and Fehlings, M. G. (2009). Involvement of mitochondrial signaling pathways in the mechanism of Fas-mediated apoptosis after spinal cord injury. *Eur. J. Neurosci.* **29**, 114–31.

Yu, Y.-M., Gibbs, K. M., Davila, J., Campbell, N., Sung, S., Todorova, T. I., Otsuka, S., Sabaawy, H. E., Hart, R. P. and Schachner, M. (2011). MicroRNA miR-133b is essential for functional recovery after spinal cord injury in adult zebrafish. *Eur. J. Neurosci.* **33**, 1587–1597.

Yunta, M., Nieto-Díaz, M., Esteban, F. J., Caballero-López, M., Navarro-Ruíz, R., Reigada, D., Pita-Thomas, D. W., Águila, Á. del, Muñoz-Galdeano, T. and Maza, R. M. (2012). MicroRNA Dysregulation in the Spinal Cord following Traumatic Injury. *PLoS One* **7**, e34534.

Zhang, Y., Bo, X., Schoepfer, R., Holtmaat, A. J. D. G., Verhaagen, J., Emson, P. C., Lieberman, A. R. and Anderson, P. N. (2005). Growth-associated protein GAP-43 and L1 act synergistically to promote regenerative growth of Purkinje cell axons in vivo. *Proc. Natl. Acad. Sci. U. S. A.* **102**, 14883–8.

Zhang, Y., Ueno, Y., Liu, X. S., Buller, B., Wang, X., Chopp, M. and Zhang, Z. G. (2013a). The MicroRNA-17-92 cluster enhances axonal outgrowth in embryonic cortical neurons. *J. Neurosci.* **33**, 6885–94.

Zhang, Z., Pinto, A. M., Wan, L., Wang, W., Berg, M. G., Oliva, I., Singh, L. N., Dengler, C., Wei, Z. and Dreyfuss, G. (2013b). Dysregulation of synaptogenesis genes antecedes motor neuron pathology in spinal muscular atrophy. *Proc. Natl. Acad. Sci. U. S. A.* **110**, 19348–53.

Zhang, N., Fang, M., Chen, H., Gou, F. and Ding, M. (2014). Evaluation of spinal cord injury animal models. *Neural Regen. Res.* **9**, 2008–12.

Zhang, J., Sun, X.-Y. and Zhang, L.-Y. (2015). MicroRNA-7/Shank3 axis involved in schizophrenia pathogenesis. *J. Clin. Neurosci.* **22**, 1254–7.

Zhou, F.-Q. and Snider, W. D. (2006). Intracellular control of developmental and regenerative axon growth. *Philos. Trans. R. Soc. B Biol. Sci.* **361**, 1575–1592.

Zhou, L., Baumgartner, B. J., Hill-Felberg, S. J., McGowen, L. R. and Shine, H. D. (2003). Neurotrophin-3 expressed in situ induces axonal plasticity in the adult injured spinal cord. *J. Neurosci.* **23**, 1424–31.

Zhou, S., Shen, D., Wang, Y., Gong, L., Tang, X., Yu, B., Gu, X. and Ding, F. (2012). microRNA-222 Targeting PTEN Promotes Neurite Outgrowth from Adult Dorsal Root Ganglion Neurons following Sciatic Nerve Transection. *PLoS One* **7**, e44768.

Zhu, L., Liu, T., Cai, J., Ma, J. and Chen, A. (2015). Repair and regeneration of lumbosacral nerve defects in rats with chitosan conduits containing bone marrow mesenchymal stem cells. *Injury* **46**, 2156–2163.

Ziu, M., Fletcher, L., Savage, J. G., Jimenez, D. F., Digicaylioglu, M. and Bartanusz, V. (2014). Spatial and temporal expression levels of specific microRNAs in a spinal cord injury mouse model and their relationship to the duration of compression. *Spine J.* **14**, 353–60.

Ziv, Y., Avidan, H., Pluchino, S., Martino, G. and Schwartz, M. (2006). Synergy between immune cells and adult neural stem/progenitor cells promotes functional recovery from spinal cord injury. *Proc. Natl. Acad. Sci. U. S. A.* **103**, 13174–9.

Zou, H., Ho, C., Wong, K. and Tessier-Lavigne, M. (2009). Axotomy-induced Smad1 activation promotes axonal growth in adult sensory neurons. *J. Neurosci.* **29**, 7116–23.

Zou, Y., Chiu, H., Zinovyeva, A., Ambros, V., Chuang, C.-F. and Chang, C. (2013). Developmental decline in neuronal regeneration by the progressive change of two intrinsic timers. *Science* **340**, 372–6.

Zou, H., Ding, Y., Wang, K., Xiong, E., Peng, W., Du, F., Zhang, Z., Liu, J. and Gong, A. (2015a). MicroRNA-29A/PTEN pathway modulates neurite outgrowth in PC12 cells. *Neuroscience* **291**, 289–300.

Zou, H., Ding, Y., Shi, W., Xu, X., Gong, A., Zhang, Z. and Liu, J. (2015b). MicroRNA-29c/PTEN Pathway is Involved in Mice Brain Development and Modulates Neurite Outgrowth in PC12 Cells. *Cell. Mol. Neurobiol.* **35**, 313–322.

Zuber, M., Zia, F., Zia, K. M., Tabasum, S., Salman, M. and Sultan, N. (2015). Collagen based polyurethanes—A review of recent advances and perspective. *Int. J. Biol. Macromol.* **80**, 366–74.

PERSONAL INFORMATION

ABSTRACTS AND ORAL PRESENTATIONS

POSTER: **Ghibaudi Matilde**, Boido Marina, Niapour Ali, Salehi Hossein, De Amicis Elena and Vercelli Alessandro "Effects of cell therapy, exercise and enriched environment on a murine model of spinal cord injury", FENS congress, Milan, July 5-9, 2014

ORAL PRESENTATION: **Ghibaudi Matilde**, Boido Marina, Green Darrell, Mohorianu Irina, Tropiano Marta, Rovito Daniela, Dalmay Tamas and Vercelli Alessandro "microRNA expression profiling in a mouse spinal cord injury model", Big Roles for small RNAs conference, June 29, Norwich, University of East Anglia (UK), 2016

POSTER: **Ghibaudi Matilde**, Boido Marina, Green Darrell, Mohorianu Irina, Rovito Daniela, Garbossa Diego, Dalmay Tamas, Vercelli Alessandro "microRNA expression profiling in a mouse spinal cord injury model", Neuroscience congress, San Diego, November 12-16, 2016

ORAL PRESENTATION AND POSTER: **Ghibaudi Matilde**, Boido Marina, Green Darrell, Mohorianu Irina, Berto Gaia, Pourshayesteh Soraya, Garbossa Diego, Dalmay Tamas and Vercelli Alessandro "MicroRNA expression profiling in a mouse spinal cord injury model", ISCORE 2017, November 3-4, Barcelona, Spain, 2017

ORAL PRESENTATION: **Ghibaudi Matilde**, Boido Marina, Green Darrell, Mohorianu Irina, Berto Gaia, Pourshayesteh Soraya, Garbossa Diego, Dalmay Tamas and Vercelli Alessandro "MicroRNA expression profiling in a mouse spinal cord injury model", Neurospine workshop, November 16, Milan, Italy, 2017

ATTENDED COURSES

Functional Neuroimaging, 14-15-16-17-18 July 2014, Turin

Writing course, 10-11-12 July 2014, Turin

Neural Development and Neurodevelopmental disorders-NENS Course 22-26 September 2014, Turin

Allen Institute for Brain Science-Infromational overwiev and training workshop, 3 October 2014, Turin

Stem cells in Neuroscience, 24-28 November 2014, Lausanne, Switzerland

Neurobiology I-Cellular and molecular organization of the nervous system, June 21-July22, Turin

Biostatistics, June-July 2015, Turin

Spinal cord Injury,12-19 September, 2015 Bressanone, Italy

The aging brain: Cellular Mechanisms Interfacing Human Pathology, 28 September-2 October, 2015, Turin

Neurobiology II-Functional organization of neural system, September 15-December 15, Turin

Single cell analysis overwiev, challenges and solutions, webinar, Qiagen, November 18, 2015

Engenireed Biomaterials and Biomedical Devices in the regenerative medicine of the Nervous System, November 19-20, 2015, Turin

Bibliography, March 2016, Turin

Biostatistics, May-June 2016, Turin, 2016

Scientific english B1-B2, March-June 2016, 2016 Turin

MEETINGS

FENS congress, Milan, July 5-9 2014

Neuroscience congress, San Diego, November 12-16 2016

ISCORE 2017, Barcelona, November 3-4 2017

Neurospine workshop, Milan, November 16 2017

INVITED SEMINARS

"microRNA expression profiling in a mouse spinal cord injury model", Big Roles for small RNAs conference, 29 June 2016, Norwich, University of East Anglia, UK

"microRNA expression profiling in a mouse spinal cord injury model", Neurospine workshop, November 16, Milan, Italy, 2017

AWARDS AND SCHOLARSHIP

2014 – **today** PhD scholarship granted by GIROTONDO ONLUS

2014 "Optime Awards", Riconoscimento al merito nello studio, Unione Industriale, Turin

2014 FENS-IBRO STIPEND AWARDED to attend the course "Stem cells in Neuroscience, Lausanne, Switzerland

2017 "Call for Creative Communities", Open Incet, Turin

LIST OF PUBLICATIONS

ARTICLES ON PEER REVIEWED JOURNALS

"Combined treatment by cotrasplantation of mesenchymal stem cells and neural progenitors with exercise and enriched environment housing in mouse spinal cord injury", Advances in Stem Cells, Boido Marina, Niapour Ali, Salehi Hossein, De Amicis Elena, **Ghibaudi Matilde** and Alessandro Vercelli, 2014

"Functional integration of complex miRNA networks in central and peripheral lesion and axonal regeneration", Progress in Neurobiology, **Ghibaudi Matilde**, Boido Marina and Vercelli Alessandro, 2017